# *Escherichia coli's* literal link to infection: Exploring mutagenesis of the FimH adhesin to allosterically "lock" in low-affinity

Victoria Blythe Rodriguez

A dissertation

submitted in partial fulfillment of the

requirements for the degree of

Doctor of Philosophy

University of Washington

2012

Reading Committee:

Wendy Thomas, Chair

Evgeni Sokurenko

James Bryers

Program Authorized to Offer Degree:

Bioengineering

University of Washington

**Abstract**

*Escherichia coli's* literal link to infection:
Exploring mutagenesis of the FimH adhesin to allosterically "lock" in low-affinity

Victoria Blythe Rodriguez

Chair of the Supervisory Committee:
Associate Professor Wendy Thomas
Department of Bioengineering

Expressed by most commensal and uropathogenic *Escherichia coli* (*E.coli*), the protein FimH mediates adhesion via catch-bonds to ligand mannose and has become a significant antigen for antiadhesive therapies targeted at urinary tract infections (UTIs). A possible barrier to therapies is that the FimH crystal structure shows a substantial allosteric conformational change between a low and high-affinity state and it is uncertain which regions contribute to the change. Additionally, previous work strongly suggests that the FimH ligand-binding lectin domain's (LD's) stability depends on its interaction with the fimbrial-anchoring pilin domain (PD). This may explain evidence of antibodies raised against the isolated LD biasing the high-affinity state and allosterically *enhancing* FimH adhesion to urothelial cells. My thesis is devoted to the investigation of a "locked" low-affinity FimH for future antiadhesive therapies.

First, we used RosettaDesign and human insight to synthesize 10 point mutants in 4 regions that we predicted would stabilize either state. By measuring the binding to mannosyl substrates and preferred conformation with a high-affinity-binding monoclonal antibody (MAb), we demonstrated that each region investigated was part of the FimH allosteric pathway. Second,

one particular low-affinity variant, V27C-L34C or “locked-low”, was characterized in new forms that physically altered the PD’s interaction with the LD in order to assess the LD’s independence. Locked-low may be unlocked to increase binding via reducing agent dithiothreitol (DTT). Under native conditions (without soluble ligand and DTT), our investigation discovered that locked-low pili containing an altered PD, FocH, and its isolated LD were unrecognized by high-affinity-binding MAbs and weakly bound mannosyl substrates. Our study strongly suggests the native LD may independently stabilize a low-affinity state. This is also the first LD isolate that switches states via DTT to be useful in future biophysical characterization. Third, we generated mouse-MAbs from the LD isolate and preliminary data indicate these MAbs significantly ($p < 0.05$) reduce the adhesion of wildtype FimH-expressing *E.coli* to urothelial cells *in vitro*. This work will aide future development of novel antiadhesive therapies designed to inhibit the adhesion of uropathogenic *E.coli*.

## Table of Contents

# List of Figures

## Acknowledgements

This work acknowledges the serendipity of timing. The collaboration between the Sokurenko and Thomas lab, the publications revealing high impact information about the FimH catch-bond, and the specialized students/scientists at the University of Washington created a perfect storm for my research.

*Dr. Evgeni Sokurenko Laboratory* I wish to acknowledge the research scientists of the Sokurenko lab. Dr. Veronika Tchesnokova taught me basic microbiological techniques when I initially entered the laboratory. Dr. Pavel Aprikian also contributed heavily to the design of and advisement on all protein purification techniques described within this document. Dr. Dagmara Kisiela contributed to the advisement and participated in execution of the monoclonal antibody studies at the latter stages of my research. All throughout my studies in the Sokurenko lab, Dr. Tchesnokova, Dr. Aprikian, and Dr. Kisiela provided exhaustive advice on how to improve my techniques and gave ample knowledge that expedited my research findings. Dr. Evgeni Sokurenko, especially, can in one sentence precisely dictate exactly what experiment is necessary to understand FimH or answer a question haunting one for months. It is a rare gift. Additionally, the research environment in the Sokurenko lab always kept me at attention for the next funny incident or story; they are a rich group of characters that always kept me shaking with laughter.

*Dr. Wendy Thomas Laboratory* I wish to acknowledge the diverse team of students and research scientists in the Thomas lab. Dr. Olga Yakovenko taught me my first flow-chamber experiment and I would like to consider her the flow-chamber whisperer. She has an amazing

talent for understanding the eccentricities of the flow-chamber set-up. Dr. Becky Whitfield, too, is a flow-chamber whisperer and also an absolute necessary friend in ensuring I got to the gym and laboratory in the wee hours of every morning. I would still have a year left of research if it were not for her get-up-and-go attitude! Dr. Matt Whitfield advised on and executed the atomic force microscopy experiments, from which I gleaned terrific data on the mechanism of my mutations that I wouldn't have observed with traditional experiments. The Thomas lab is by far the best graduate research environment with a passion for a balanced lifestyle that I will practice and preach.

*Talented Students* Dr. Kristy Katzenmeyer is a brilliant researcher and sage well beyond her years who has left the Department of Bioengineering to establish herself at the US Food and Drug Administration. She and I entered graduate school together and I am inspired by her technical skill, mentorship, organization, and resourceful nature. She is a leader that needs to be recognized and has become my best friend. Ph.D. candidate, Neil Umbreit, is a part of the Department of Biochemistry and a former Molecular Biophysics Training Grant trainee that I had the pleasure of interacting with during my tenure as a trainee myself. He and I were the only graduate students who had similar research as part of the trainee cohort. I was always nervous to present to the other trainees as I knew that Neil would ask the most challenging questions concerning the protein structure or biomechanics of my FimH mutants. He pushes how I think about my research and I cannot wait to see him finish his own Ph.D.

*Mentors* There are many women mentors who have encouraged me to become the woman that I am today with or without their knowing. My mother, Ava, is my first mentor by not only

setting an example of how to be a mom, but encouraging the development of skills not traditionally considered to be “what women are good at”: Science, Technology, Engineering, and Mathematics. She is a woman who was often the only person of her sex in Math courses and at positions in IBM, she had the tough part of ensuring that I can succeed as a woman. Mrs. Pat Mokry was the first person who introduced me to the wonderful world of Physiology and Anatomy in high school. She always added a little extra information or discussions to each class that eventually inspired me to consider Science as a career. Dr. Ann Saterbak, Professor in the Practice of Bioengineering Education and Associate Chair of Undergraduate Affairs at Rice University, was my toughest professor at Rice as well as my biggest supporter of achieving equal treatment when I required additional aide due to my learning disability. Dr. Suzie Pun, Associate Professor of Bioengineering at the University of Washington, is the one who pushed me the most of all by denying what I thought was mine: a Ph.D. Without her tough-love, I would not know my own resourcefulness, mental strength, and poise in the face of adversity. Dr. Carmen Sidbury, former Assistant Dean in the College of Engineering at the University of Washington, believed in my ability as a Ph.D. so much as to provide me with needed funding to complete my Master’s degree in Bioengineering. I hope that one day, I can pay it forward. Dr. Eve Riskin, Professor of Electrical Engineering and Associate Dean for Academic Affairs, stepped in as my advisor once Dr. Sidbury left and opened my world to actively participate as a leader in PEERs (Promoting Equity in Engineering Relationships). She also became a terrific addition as my acting Graduate Student Representative. And finally, Dr. Wendy Thomas, Associate Professor of Bioengineering, is my principle investigator. She is a woman who believes in my ability to achieve.

## Dedication

To my twin sister, Ashley, who is my true companion. We were thrown together on this journey and with her never do I grow weary, never do I grow old.

To my father, Phil, who stood outside a college in Boston when I was 11 years old and said "If you want to go here for school, you can. You can go anywhere you want, and we will support you."

To my mother, Ava, my first mentor, who replied to my nervousness about a Math class in high school: "I'm great at Math. You will be, too." She is the woman who replied to my concerns about my first Calculus class at Rice University with, "I loved Calculus. You will, too." My best grades in my entire educational career have come from those words of encouragement; my best subject was and is Mathematics.

To my principal investigator, Dr. Wendy Thomas, who simply believes in me. She fills the spaces in my mind with inspiration.

To the graduate student who has opened this thesis to peruse what might be inside, to the graduate student who may be struggling in his/her research, to the graduate student who has been told that he/she does not have the potential to be a Ph.D. To that I say:

"I am the face of those graduate students. I became a Ph.D. You can be a Ph.D., too."

# Chapter I Introduction

## Problem statement

Urinary tract infections (UTIs) have an immense impact on human health, medical staff's workload, as well as the economy. Cases of infection account for an estimated 8.3 million visits to the doctor in the United States alone with an annual cost approximation of $2.3 billion in 2010 (adjusted for inflation) (Foxman 2002; 2005; Foxman 2010). A study conducted in 2000 of nosocomial acquired UTIs estimated an added $676 to a patient's hospital bill (equivalent to $ 842 in 2010) along with an extra night's stay in the hospital (Saint 2000; Foxman 2010), totaling 1 million extra days per year. Additionally, 40% of all hospital acquired infections are traced to catheter-associated UTIs (Foxman 2010).

When considering the ramifications of the disease, uncomplicated UTIs (normal genitourinary tract and no instrumentation) in nonobstructive individuals and nonpregnant adult females are considered benign with no long-term medical consequences (Foxman 2002). Conversely, pregnant females as well as pediatric patients are at considerable risk. Pyelonephritis, premature delivery, and fetal mortality may affect the former while there is impaired renal function and end-stage renal disease in association with the latter (Foxman 2002). Although still not well understood, two in every five women will develop a UTI during their lifetime while men are less commonly affected (Foxman 2002; 2005). The risk of reoccurrence in women increases to 20% after the first, 30% after the second, and 80% after the third infection (2005). General risk factors associated with the disease include a variety of unisexual circumstances

such as obstructions to the flow of urine, use of catheters, diabetes, immunosuppressive disorders, urinary tract abnormalities, genetic history, behaviors which increase exposure, and many others (2005).

The urinary tract is involved in the process of forming and excreting urine and consists of the kidneys, ureters, bladder, and urethra. Urinary tract infections are defined as the infiltration of a microbial pathogen within parts of the urinary tract and are the most prevalent bacterial infection. The name of the infection relates to the site where the infection has occurred: cystitis (bladder), pyelonephritis (kidneys), and urine (bacteriuria) (Foxman 2002). The most common bacteria associated with infection are uropathogenic strains of *Escherichia coli* (*E.coli*) (Foxman 2010). Uropathogenic *E.coli* (UPEC) are unlike the strains of *E.coli* regularly inhabiting the gastrointestinal tract of healthy individuals. Strains of UPEC have adapted in such a way as to allow for access and colonization of the urinary tract while escaping the surveillance of the immune system. Antimicrobial drugs used to treat UTIs are becoming increasingly less effective due to an increase in drug resistant *E.coli* (Karlowsky, Kelly et al. 2002; Zhanel, Hisanaga et al. 2005; Schito, Naber et al. 2009). A drawback of conventional antibiotic treatment is destruction of beneficial flora within the gut and has been recently argued as equivalent to placebo in resolving uncomplicated UTIs (Foxman 2002). Recently, research efforts have been focused on preventing bacterial adhesion and therefore colonization in the urinary tract through the use of antiadhesive therapies such as ligand-like inhibitors or vaccines. Several studies using FimH to immunize various animal models were successful in protection against an *E.coli* infection (Langermann, Palaszynski et al. 1997; Langermann, Mollby et al. 2000), but there is no evidence

of an FDA approved vaccine on the market. The lack of an available UTI therapy motivates continual research of the disease mechanism of UPEC and its potential interaction with a vaccine prior to the development of an effective therapy.

## Solution

The majority of UTIs are often initiated by the colonization of *E.coli* bacteria and 90% of these express a particular fimbrial appendage, or pili, known as common or type 1 fimbriae. At the tip of each pili is a 30 kDa adhesin, FimH, that is composed of a lectin or mannose-binding domain, and a pilin domain that anchors FimH to the fimbriae. FimH binds to mannosyl and oligomannosyl residues on the surface of uroepithelial cells, intestinal epithelial cells, red blood cells, neutrophils, and yeast (Sokurenko, Chesnokova et al. 1997). Through increased tensile mechanical force along its structure such as during urination, the FimH protein increases its affinity for the mannosylated surface of the urinary tract. This phenomenon is a "catch-bond" and it is a mechanism that facilitates initial colonization leading to a UTI. Similar catch-bond systems include leukocytes patrolling vessel walls for inflammation or myosin/actin interaction during muscle contraction (Finger, Puri et al. 1996; Guo and Guilford 2006).

The FimH protein's catch-bond is characterized by weak binding (fast dissociation rate) and strong binding (slow dissociation rate) known as the low- and high-affinity state, respectively. An allosteric mechanism for FimH's switch from low- to high-affinity was proposed and experimentally confirmed under force (Aprikian, Tchesnokova et al. 2007) as well as in the presence of a monoclonal antibody, which recognizes an epitope far from the binding pocket

(Tchesnokova, Aprikian et al. 2008). Most recently, the structure of the high-affinity state (Choudhury, Thompson et al. 1999) and the low-affinity state (Le Trong, Aprikian et al. 2010) exhibit two distinct conformations and demonstrate that mechanical activation results from a force-induced allosteric conformational change.

It may be hypothesized that the lack of a commercial vaccine is directly related to FimH's two distinct conformations. Indeed, Tchesnokova et al., points out that although antibody therapy development is an alternative to antibiotic treatment of bacterial infections, the antibodies raised against FimH may only be targeted to its low- or high-affinity conformational states (Tchesnokova, Aprikian et al. 2011). Tchesnokova et al., later showed that antibodies raised against the FimH lectin domain are biased solely to epitopes of the high-affinity state, are able to allosterically *enhance* FimH adhesion, and may easily be shed if the low-affinity conformation is favored (Tchesnokova, Aprikian et al. 2011). An alternative strategy for preventing bacterial adhesion is thus to develop allosteric inhibitors or antibodies that stabilize the low-affinity state. To our knowledge, an allosteric antiadhesive that targets the low-affinity state of FimH has never been reported. Characterization of the low-affinity conformation may provide the means to develop a successful allosteric inhibitor or antibody.

**Hypothesis**

The FimH protein is allosterically driven by multiple regions within its lectin domain. We can use these regions to investigate the possibility of synthesizing an allosterically "locked" low-affinity variant along with its isolated lectin domain. This would deepen our understanding of

allosterically driven catch-bond behavior as well as aide in the development of antiadhesive therapies targeted at UTI causing *E.coli*.

**Summary of thesis achievements**

1. We used RosettaDesign and human insight to synthesize 10 mutations in 4 regions that we predicted would allosterically stabilize the low or high-affinity conformation of FimH. By measuring the binding to mannosyl substrates and preferred conformation with a high-affinity-binding monoclonal antibody (MAb), we demonstrated that each region investigated was part of the FimH allosteric pathway. Additionally, each region may be mutated to sustain a low-affinity variant.
2. One particular low-affinity variant, mutant V27C-L34C or "locked-low", was characterized in new forms that physically altered the pilin domain's interaction with the lectin domain in order to assess the lectin domain's independence. Mutant "locked-low" may be unlocked to increase binding via reducing agent dithiothreitol (DTT). Under native conditions (without ligand and DTT in solution), our investigation discovered that locked-low pili containing an altered pilin domain, FocH, and its isolated LD were unrecognized by high-affinity-binding MAbs and weakly bound to mannosyl substrates. Our study strongly suggests that under native conditions, LD interaction with the pilin domain is not required to stabilize a low-affinity state. This is also the first native low-affinity isolated LD and the first isolated LD capable of switching states via DTT.
3. Mouse-monoclonal antibodies were generated from the locked-low isolated LD. Both MAb10 and MAb926 significantly inhibit the binding of wildtype K12-expressing *E.coli* and high-affinity A188D-expressing *E.coli* ($p < 0.05$) to a mannosyl substrate. Additionally, preliminary data indicate these MAbs significantly ($p < 0.05$) reduce the adhesion of wildtype K12-expressing *E.coli* to urothelial cells *in vitro*.

# Chapter II Background

## What is a catch bond?

*The proof is all around us*

Dembo et al., in 1988 first coined the term "catch bond" in a theoretically based study to distinguish receptor-ligand interactions that strengthened under force to those that dissociate (Dembo, Torney et al. 1988). Although there was already a wealth of supporting evidence for the existence of catch bonds in naturally occurring adhesins, it was not until 2002 when Thomas et al., experimentally demonstrated and suggested this phenomenon is force induced. Some of the adhesins proposed to participate in catch bonds with a ligand include selectins involved in leukocyte-stabilized rolling across inflamed/activated endothelial cells or activated platelets (Finger, Puri et al. 1996; Thomas 2008). There are various types of selectins involved in this process that may be exposed on leukocytes (L-selectin), platelets (P-selectin), and endothelial cells (P- and E-selectin). The ligand binding all of these selectins is the sugar molecule sulfate sialyl-Lewis x within the glycoprotein PSGL-1, mentioned previously. Another catch-bond interaction involves the motor protein myosin's binding to the cytoskeletal protein actin which drives muscle contraction (Guo and Guilford 2006). Platelets have also been proposed to have shear-enhanced binding to blood protein von Willebrand factor as a way to initialize clot formation to injured endothelium (Goto, Ikeda et al. 1998). Finally, adhesins at the tips of fimbriae coating *E.coli* have been hypothesized to mediate the necessary first step in the disease process of forming a UTI infection to epithelial cells lining the urinary tract. Indeed, the

catch bond as a mechanism of force-induced adhesion to mannosyl surfaces has been demonstrated under flow and in single-molecule binding experiments (Thomas, Trintchina et al. 2002; Thomas, Forero et al. 2006; Yakovenko, Sharma et al. 2008). Our current understanding of how this mighty receptor-ligand interaction works follows in the next several sections.

*Basis of adhesion between proteins: noncovalent forces*

Adhesion at the cellular level is a process by which a pair or complex of proteins interact and bind via noncovalent bonds. Noncovalent bonds encompass hydrogen bonding between neutral groups or peptides, repulsive/attractive ionic interactions, hydrophobic interactions, and van der Waals interactions. In general, proteins collide constantly at the cellular level due to random thermal movement and create noncovalent bonds between each other during this process. Unless the interacting surfaces have complimentary surfaces, individual noncovalent bonds are too weak to associate the two proteins for long (Alberts B 2002). Yet, when the colliding surfaces due match as in a receptor for its ligand, numerous noncovalent bonds can be combined together to lower and stabilize the free energy of a receptor-ligand interaction to an astounding degree. That is, if there is a binding reaction between a ligand (L) and its receptor (R), there is an association ($k_{on}$) and disassociation constant ($k_{off}$) related to the reaction:

$$L + R \rightleftharpoons LR$$

Eventually, the interaction will achieve an equilibrium status represented by the equilibrium constant ($K_{eq}$):

$$\frac{[\mathrm{LR}]}{[\mathrm{L}][R]} = \frac{k_{on}}{k_{off}} = \mathrm{K}_{eq}$$

where the brackets represent the molar concentration of each component. It is understandable that the higher the equilibrium constant, the higher the stability of the interaction versus the separation of receptor and ligand. The equilibrium constant $K_{eq}$ varies exponentially with the Gibbs free energy (ΔG) or stability of any biochemical interaction with the general equation (Alberts B 2002; Nelson and Cox 2005):

$$\mathrm{K}_{eq} = e^{-\Delta \mathrm{G}/\boldsymbol{R}\mathrm{T}}$$

where ***R*** (not R as in receptor) is the gas constant (8.315 J/mol*K) and T is absolute temperature (298 K). Note that a large and negative ΔG value indicates a favorable interaction. This equation makes it understandable why a large and negative ΔG or the ΔG associated with combining several noncovalent bonds between two interfacing macromolecules is enough to profoundly increase $K_{eq}$ and thereby the association of receptor and ligand.

*Adhesive proteins form two classes of bonds: slip vs. catch bonds*

When tensile-mechanical force is applied to a ligand-receptor interaction, the bond is increasingly likely to dissociate and has been experimentally represented using atomic force microscopy (AFM), optical tweezers, biomembrane force probe (BFP), or in flow chamber (Marshall, Long et al. 2003; Thomas 2008). This is an intuitive expectation and a representation of the exponential decline in lifetime as a function of force is represented in Figure 1A (Thomas,

Vogel et al. 2008). The bond representing this behavior in response to force is known as a slip bond and the effect of the rate constant of the individual interaction breaking on a molecular scale, *k*, has been theoretically and experimentally determined (Bell 1978; Shapiro and Qian 1997; Evans 2001; Marshall, Long et al. 2003):

$$k(f) = k_0 \cdot e^{f \cdot \frac{\Delta x}{k_b T}}$$

Where $k_0$ is the rate constant of unbinding (like $k_{off}$ previously) without an applied external force, $f$ is the applied force, $\Delta x$ is the distance of interaction that changes as a result of the transition, $T$ is temperature, and $k_b$ is the Boltzmann constant or unit energy at $T$. Boltzmann constant is related to the gas constant, $\boldsymbol{R}$, by $k_b = \boldsymbol{R}/N_A$ where $N_A$ is Avogadro constant. The reason for the switch is that the Boltzmann constant is used here as we are discussing interactions on the molecular scale rather than the molar scale as in the previous section.

If constant force is applied on multiple bonds over a period of time, the fraction of bonds surviving will decrease linearly on the log scale (Thomas 2008; Thomas, Vogel et al. 2008)(Figure 1A). The inset in Figure 1A emphasizes the equation drawn above in which increasing force on the bond interaction increases the rate *k* of unbinding thereby decreasing the individual bond lifetime.

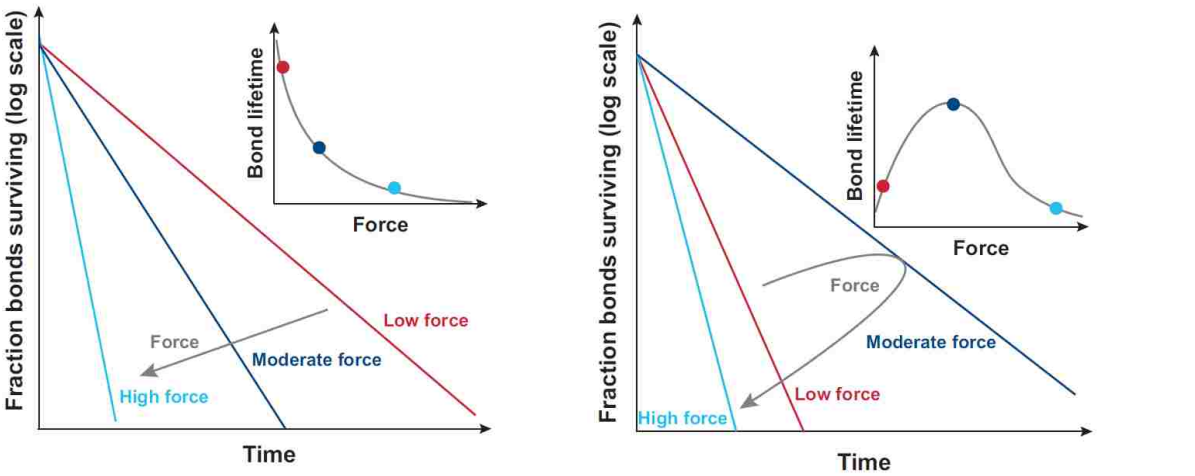


Most receptor-ligand interactions dissociate under force or high flow conditions. However, a minority of biological interactions actually increase association under increasing tensile mechanical force along the axis of interaction. This phenomenon is known as a "catch bond" (Dembo, Torney et al. 1988). Catch bonds display a nonintuitive response to force in that the bond lifetime increases with force up to a threshold (critical force) and then subsides into a representation equal to a slip bond (Figure 1B). This was first experimentally proven at the single-molecule level using atomic force microscopy (AFM) examining the leukocyte adhesion protein P-selectin and its interaction with its ligand P-selectin glycoprotein ligand-1 (PSGL-1) (Marshall, Long et al. 2003). The dissociation rate remained constant during the application of constant force to separate P-selectin and its ligand, just like a slip-bond (Thomas 2008). Yet, when constant force was applied and the time necessary for the bond to rupture were graphed as a function of force, the dissociation rate constant declined with ever increasing force up to a

peak rupture force. A representation of selectins response in Figure 1B emphasizes the fraction of bond survival increase at the critical force (moderate force) while distinguishing lower survival at low and high forces alike (Thomas, Vogel et al. 2008). This result confirmed the existence of a catch bond.

Understanding this quality about a catch bond leads us back to the idea of energy stability gained when a ligand interacts with its receptor. At a particular range of high forces for a catch bond, the dissociation rate constant is too low for the pair to separate. Instead, it may be considered to be at a trough of a bond energy landscape. To add more complexity to defining catch bonds, it is understandable that the naturally occurring catch bonds mentioned previously all display different structures and therefore defined by different models/energy landscapes. Several models include the one-state/two-pathway model as in selectins (Pereverzev, Prezhdo et al. 2005) and myosin (Guo and Guilford 2006) displayed in Figure 1B, the sliding/rebinding model also suggested for selectins (Lou, Yago et al. 2006; Lou and Zhu 2007), and the model that currently describes FimH interacting with mannose: the two-state allosteric model (Thomas, Forero et al. 2006; Pereverzev, Prezhdo et al. 2011). A defined energy landscape and model for FimH is discussed in the next section.

*The two-state allosteric catch-bond mathematical model for FimH*

Thomas et al, derived the basis of the two-state allosteric model while observing the pause lifetimes of FimH containing *E.coli* rolling along a mannosylated surface at various fluid flow-

rates (producing a drag force on FimH to be detailed in the section “parallel-plate flow chamber” later on in this chapter) (Thomas, Forero et al. 2006). The use of the latest knowledge in FimH crystal structure (Le Trong, Aprikian et al. 2010) along with constantly updating experimental data (Yakovenko, Sharma et al. 2008; Yakovenko, Tchesnokova et al. 2011) have allowed for additional enhancements (Whitfield, Ghose et al. 2010; Pereverzev, Prezhdo et al. 2011) (for one of the updates see “fimbrial structure and function” in the next section), but the original model will suffice in developing a basis for understanding FimH’s two low-energy conformational states.

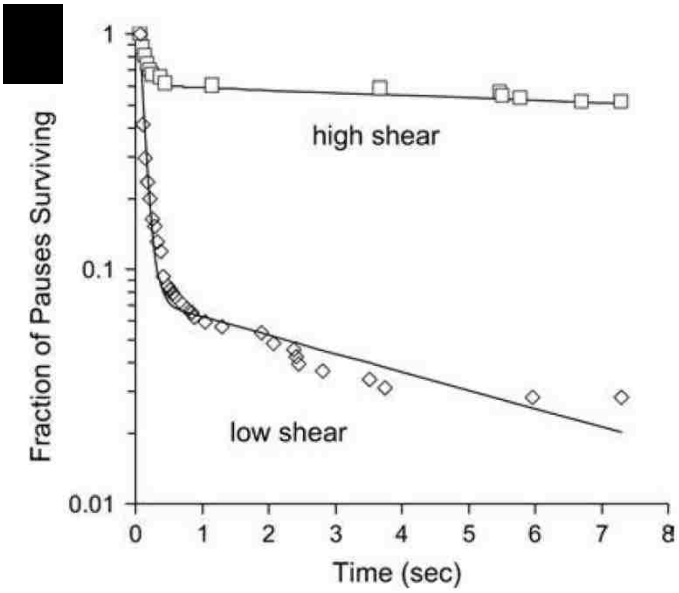


By mapping the fraction of survival of the *E.coli* on the surface at particular flow rates, which impart low to high wall shear stresses, a double exponential decay emerges at any shear stress (Figure 2). That is there are two distinct behaviors represented by the *E.coli* under study. Within each shear examined, the *E.coli* paused for very short periods of time and in turn, the same *E.coli* paused significantly longer periods of time as demonstrated by the sharp inflections for each curve of Figure 2. The two types of pauses could not be explained by multiple bond formation (Thomas, Forero et al. 2006;

Pereverzev, Prezhdo et al. 2011), rather two separate low-energy FimH conformations represented by a stable strong bond (for long pauses) and a stable, yet slightly weaker bond (for short pauses).

The weak bond and strong bond were each delegated as state 1 and state 2, respectively, with

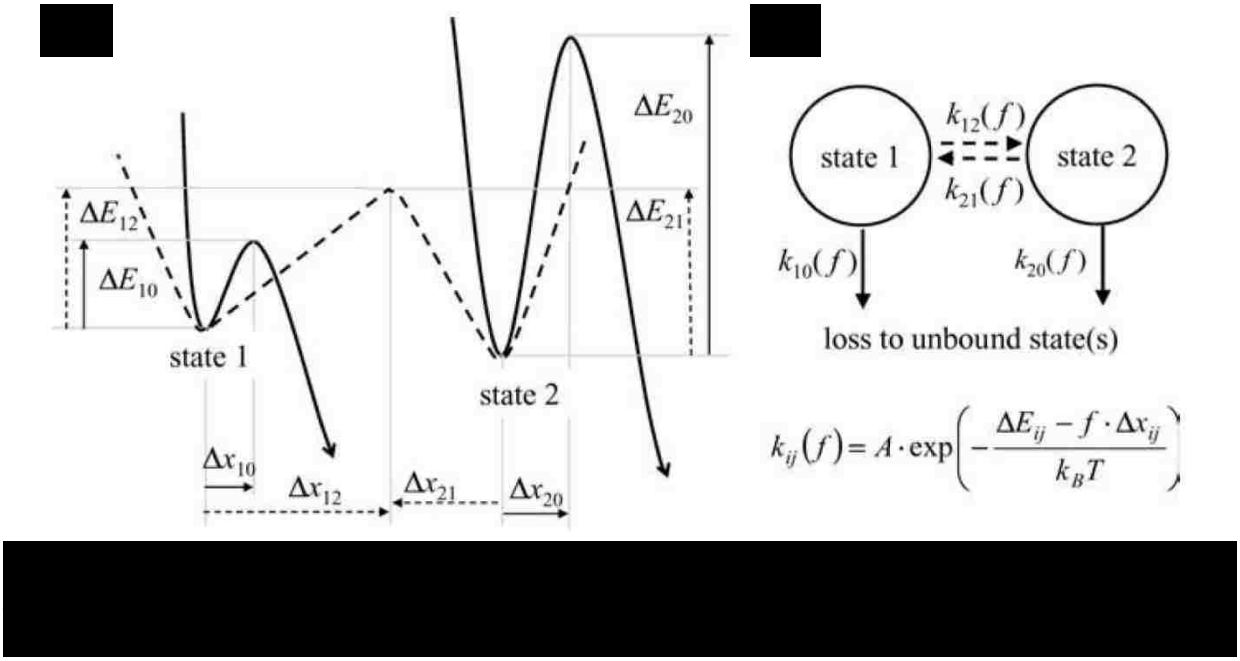


a molecular-scale energy diagram (A) and schematic (B) represented by Thomas et al in Figure 3. The dashed lines indicate the allosteric transition in between state 1 and 2 while the solid lines indicate the unbinding from state 1 and 2. For simplicity, let's consider state transitions in the absence of force first. The energy required for FimH to transform conformations from state to state or even unbind (represented by "0") have an exponential effect on the transition rate $k_{ij}$ where *i* and *j* represent the original (1 or 2) and final states (1 or 2), respectively:

$$k_{ij}^{0} \propto e^{-\frac{\Delta E_{ij}}{k_b T}} \rightarrow k_{ij}^{0} = Ae^{-\frac{\Delta E_{ij}}{k_b T}}$$

where $\Delta E_{ij}$ represents the energy barrier on the molecular scale between the transition (Figure 3A), $T$ is temperature, $k_b$ is the Boltzmann constant or unit energy at $T$ as previously defined ($k_b = \boldsymbol{R}/N_A$ where $N_A$ is Avogadro constant), and $A$ is attempt frequency. Knowing that the bond lifetime is enhanced in state 2, decreasing the reversion to state 1 (2 → 1) or unbinding (2 → 0), the transition energy $\Delta E_{21}$ or $\Delta E_{20}$ is larger than $\Delta E_{12}$ or $\Delta E_{10,}$ respectively.

When tensile mechanical force, $f$, is applied to FimH, force affects $k_{ij}$ in a similar manner as a slip bond shown previously, in which we discovered $k(f) = k_0 \cdot e^{f \cdot \frac{\Delta x}{k_b T}}$:

$$k_{ij}(f) = Ae^{-\frac{(\Delta E_{ij} - f\Delta x)}{k_b T}} = k_{ij}^0 \cdot e^{f \cdot \frac{\Delta x_{ij}}{k_b T}}$$

Considering the energy diagram in Figure 3A, force decreases the energy barrier by the amount $f \cdot \Delta x_{ij}$ for all transitions. Like before, this equation simply emphasizes how force exponentially affects rate $k_{ij}$.

Using the schematic of the two-state model in Figure 3B, a differential equation for the probability ($B_i$) of occupancy in a given state may be represented as a function of time:

$$d\frac{B_1(t)}{dt} = k_{21} \times B_2(t) - (k_{10} + k_{12}) \times B_1(t)$$

$$d\frac{B_2(t)}{dt} = k_{12} \times B_1(t) - (k_{20} + k_{21}) \times B_2(t)$$

The simple equation of $B_1(t) + B_2(t) = B(t)$ to determine the complete lifetime was solved by Thomas et al., using the above ordinary differential equations and initial conditions according to

the general flow chamber experiment (Thomas, Forero et al. 2006). The reader is encouraged to seek the solution to the equation, but it is not necessary to understand the solution while reading this dissertation. What should be taken away from this exercise is that the bond survival predicts the double exponential decay observed in flow chamber experiments as a function of time.

In conclusion, understanding the basic equations governing the allosteric switch in between states provides a perspective on how changing the energy barrier of either state may profoundly affect transitions in the two-state allosteric model. *A low-affinity mutant FimH would hypothetically have a preference for state 1 bond formations. In this work, it is of interest to enhance the energetic stability of state 1 (create a deeper trough with large and negative ΔE) to in turn decrease the rate of transition to state 2 (increasing $\Delta E_{12}$); perhaps eliminating the transition all together under typical physiological circumstances.*

## Type 1 fimbriated *E.coli*

Type 1 fimbriated *E. coli* form catch bonds with terminal mannosyl residues on the surface of uroepithelial cells, intestinal epithelial cells, red blood cells, neutrophils, and yeast (Sokurenko, Chesnokova et al. 1997). The adhesive protein allowing for catch bond formation is known as FimH and is located at the tips of each fimbria, which coat the surfaces of both commensal and uropathogenic strains of *E.coli* (UPEC). In addition to allowing for adhesion to these cell types, FimH is the essential component during the synthesis of pili. The next section and subsections

review the structural components of fimbriae along with FimH and relates each structural feature back to the adhesive behavior explored in the previous section.

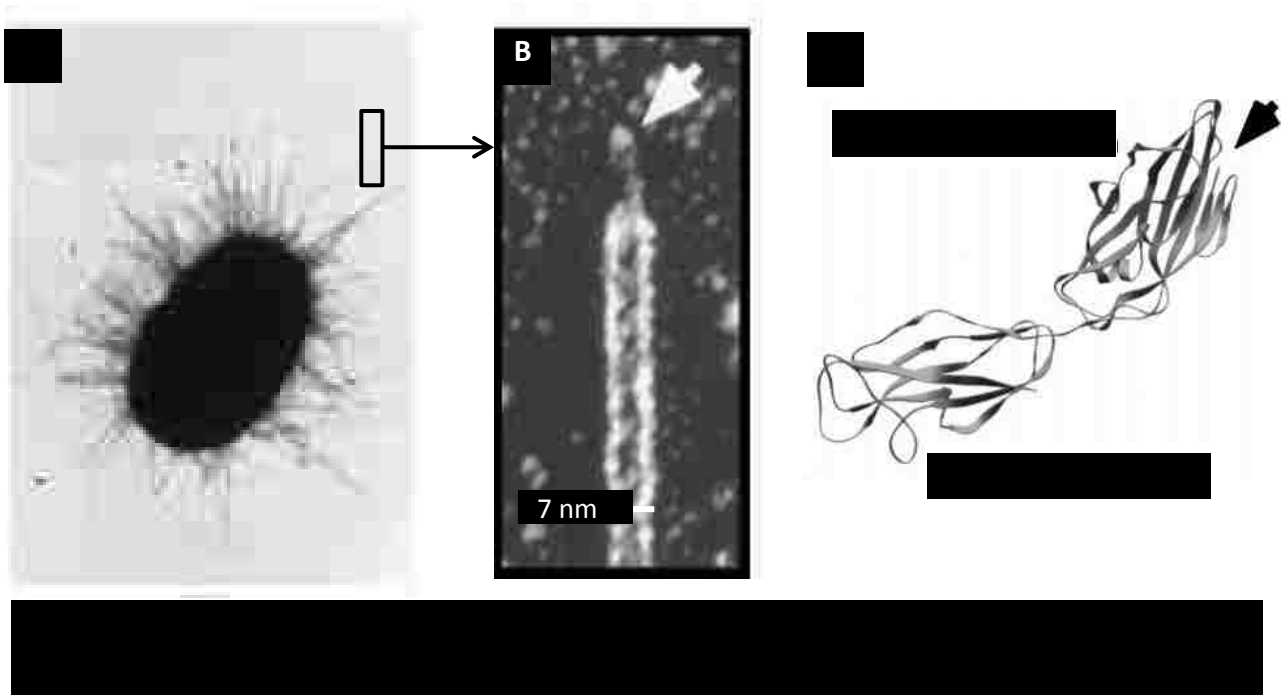


*Fimbrial structure and function*

Bacteria are coated with fimbrial appendages that are 7 nm wide and can extend up to several microns in length. Figure 4 provides an overview of the orientation of *E.coli* with its multitude of hairy fimbrial appendages (Sokurenko, Chesnokova et al. 1997; Mulvey, Schilling et al. 2000). It was estimated using electron micrographs on type 1 fimbriae expressing *E.coli* that recombinant strains from various wild type backgrounds did not have a distinct difference between the average sizes and expression levels of fimbriae, which were 501-602 nm long and

contained 171-200 fimbriae (Sokurenko, Courtney et al. 1995). Fimbriae are coiled right-handed helical rods containing linked FimA subunits structurally anchored by β-strand donation between adjacent FimA neighbors. There are approximately over 1,000 FimA subunits within one coil and at the tip of each there exists an extension known as the fibrillum (Hahn, Wild et al. 2002). The fibrillum contains two minor structural subunits, FimF and FimG, as well as the adhesin FimH (Krogfelt, Bergmans et al. 1990; Munera, Palomino et al. 2008; Waksman and Hultgren 2009) (Figure 4B and C, and Figure 5).

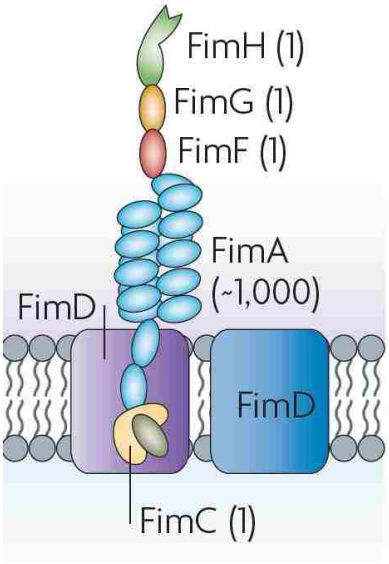


Interestingly, FimH is required for FimA expression or pilus biogenesis. Briefly, a conserved chaperone-usher pathway has evolved to secrete several kinds of structures exposed on the surface of Gram-negative bacteria (Sauer, Remaut et al. 2004). The process involves chaperone protein FimC that binds and stabilizes fimbrial subunits recently transported to the periplasm. The outer-membrane usher protein, FimD, recognizes the complexes (FimC-FimH, FimC-FimF, etc.), recruits them in proper order, assists FimC dissociation, assists in polymerization, and then expels the newly synthesized structure using a hydrophilic pore through to the extracellular space (Saulino, Bullitt et al. 2000; Vetsch, Puorger et al. 2004; Remaut, Rose et al. 2006; Vetsch, Erilov et al. 2006; Munera, Palomino et al. 2008).

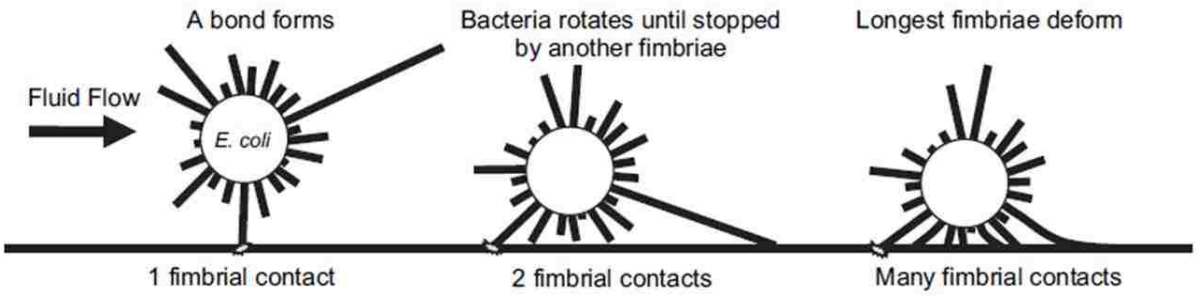


It has been recently demonstrated using simulations of fimbriated *E.coli* that the act of rolling, indicative of weak bond formations (state 1), is highly dependent on the mechanics of fimbrial interaction with the underlying surface (Whitfield, Ghose et al. 2010). Based on the simulation results, Whitfield et al., proposed fimbrial deformation (bending and buckling) as a way to increase the contact of FimH to a mannosylated surface and that catch bonds are not required for the rolling action of *E.coli* (Figure 6). The involvement of each fimbriae does not change the two-state catch-bond model previously described for FimH, but the simulations used the model to develop the current theory and the reader is encouraged to examine the simulations along with the progression of the model (Whitfield, Ghose et al. 2010). In essence, the catch-bond mechanism causes the observed stationary adhesion (not rolling) while fimbrial deformation is proposed to facilitate rolling behavior (Figure 6).

Fimbrial uncoiling may also occur, but only during times of axial fimbrial forces > 30 pN encountered at shear stresses higher than 1 Pa ((Andersson, Uhlin et al. 2007; Whitfield, Ghose et al. 2010). This happens to be near the range of forces experiences by *E.coli* while traversing the intestines. The viscous intestinal fluid (Jackson 2006) has been suggested to impart shear

stresses from 2-10 Pa causing a drag force of 64 pN (Yakovenko, Sharma et al. 2008). The interplay between fimbrial uncoiling/buffering along with FimH catch-bond formation is critical for *E.coli* to freely move about in the jostling environment of the intestines; emphasizing the complexity and importance of fimbrial mechanics to the natural behavior of *E.coli*.

*Basic FimH structure*

FimH consists of 2 immunoglobulin-like β sandwich domains known as the lectin and pilin domain which are interconnected via a three amino acid linker chain (Figure 7A) (Choudhury, Thompson et al. 1999). The N-terminal lectin domain (1-156 aa) possesses the binding pocket for mannose ligand at its tip, while the C-terminal pilin (160-273 aa) domain anchors the FimH lectin domain into the extending fimbriae (Aprikian, Tchesnokova et al. 2007). Proteins with immunoglobulin-like domains typically consist of two β sheets forming a "sandwich" construction with a Greek key topology and have a variety of functions. Some notable conformations are found in eukaryotic matrices, bacterial matrices, and adhesive proteins (Shan, Koch et al. 1999; Timpl, Tisi et al. 2000; Hashimoto 2006). Sense

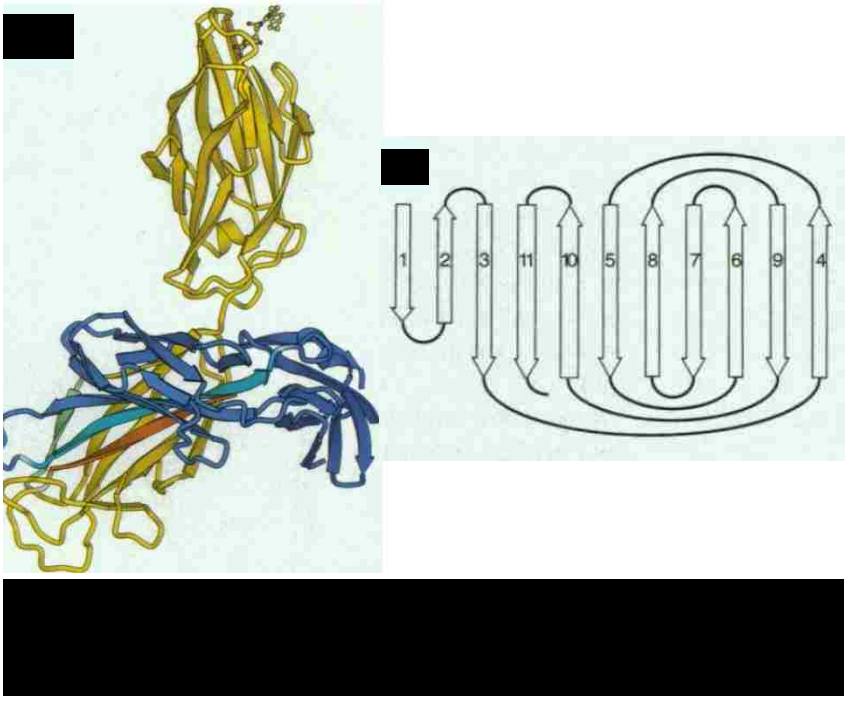

FimH is in a roughly all β-strand construction, residues making up the "ribbons" or strands of the sheet are in an antiparallel formation with typically (not always) alternating solvent exposed hydrophilic residues and inward core-facing hydrophobic residues. The lectin domain contains 11 strands in total that fold into a jellyroll-like construction to form its β sandwich with a hydrophobic core. A jellyroll topology looks like a Greek key, but with an extra "swirl" (Figure 7B). Although the pilin domain is in an immunoglobulin-like folding conformation, its conformation is a little different to that of the lectin domain and other immunoglobulin-like proteins. Six antiparallel β strands fold into a Greek key topology with a seventh β strand missing and leaving the hydrophobic core exposed. The core exposure is normally remedied with β strand donation by either the chaperone protein FimC or protein FimG depending on whether the system is independent of (Choudhury, Thompson et al. 1999) or incorporated into (Le Trong, Aprikian et al. 2010) the fibrillum, respectively.

*Mechanism of FimH catch-bond formation*

As mentioned previously, studies designed to examine *E. coli* binding to mannose-coated surfaces under physiological flow conditions have revealed a catch-bond mechanism of adhesion. The mechanism of catch-bond formation is more complex than selectins in that instead of one bound state, there are two bound states (Thomas, Forero et al. 2006; Yakovenko, Sharma et al. 2008). In flow chamber as well as single-molecule experiments, there is a switch from weak (fast dissociation rate) to strong binding (slow dissociation rate) under increasing force up to a peak force before all interactions resumed slip bond-like behavior

(Thomas, Forero et al. 2006; Yakovenko, Sharma et al. 2008). An allosteric mechanism for this particular switch from low- to high-affinity was proposed and experimentally confirmed under force (Aprikian, Tchesnokova et al. 2007) as well as in the presence of a monoclonal antibody (MAb 21), which only recognizes an epitope far from the binding pocket and exposed in the high-affinity conformation (Tchesnokova, Aprikian et al. 2008). In addition, the structure of the high-affinity (Choudhury, Thompson et al. 1999) and most recently the low-affinity state (Le Trong, Aprikian et al. 2010) combine to confirm the mechanical activation of FimH binding to be allosterically regulated.

The low-affinity structure was crystalized in the native fibrillum or tip-incorporated state without mannose while the high-affinity structure was crystalized with mannose either as a purified lectin domain (no pilin domain)(Bouckaert, Berglund et al. 2005; Wellens, Garofalo et al. 2008) or FimH complexed with chaperone FimC that wedged itself between the 2 domains (Choudhury, Thompson et al. 1999; Hung, Bouckaert et al. 2002). The reason why each conformational state was already identified and known was due to previously documented studies. The purified lectin domain has been demonstrated to constantly reside in the high-affinity state under static (Bouckaert, Berglund et al. 2005) and dynamic conditions (Aprikian, Tchesnokova et al. 2007). The FimH complexed with chaperone FimC has also been shown to have high affinity for mannose (Aprikian, Tchesnokova et al. 2007). The native fimbriae incorporated FimH has been observed extensively to form weak (low-affinity) bonds under static and low-shear or low force conditions and strong (high-affinity) bonds under high-shear

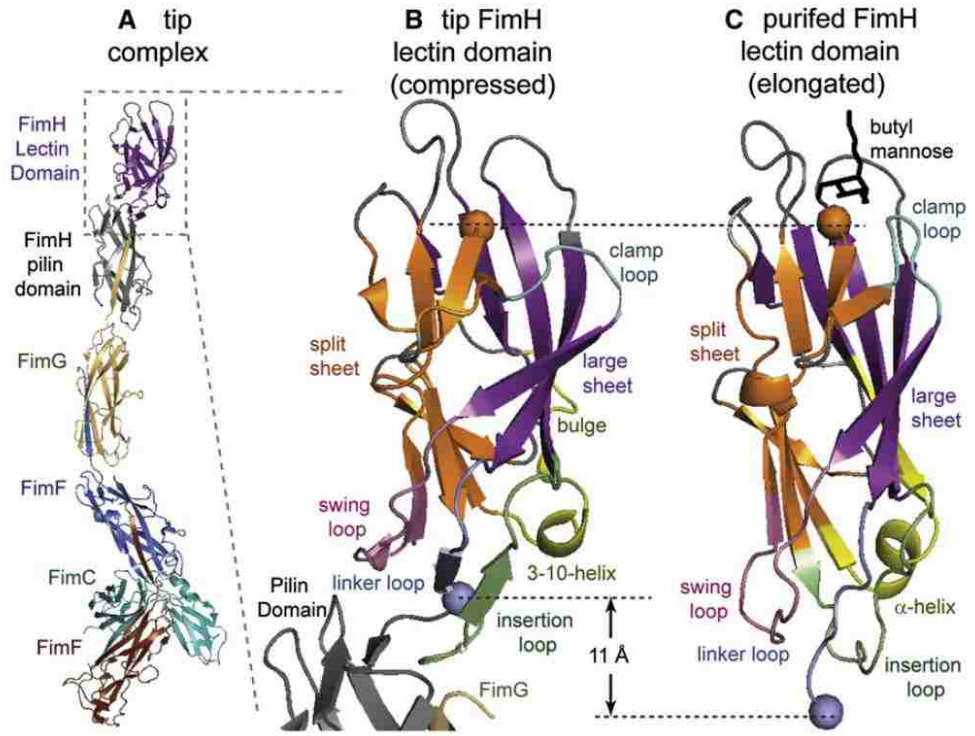


or high force conditions ((Thomas, Trintchina et al. 2002; Thomas, Nilsson et al. 2004; Aprikian, Tchesnokova et al. 2007; Yakovenko, Sharma et al. 2008).

The conversion of conformation in the FimH adhesin from low- to high-affinity or high- to low-affinity may be summarized by examining the low- and high-affinity crystal structures together side by side (Le Trong, Aprikian et al. 2010) (Figure 8). The β sandwich fold of any protein structure was originally considered to be too rigid to sustain movement. The profound conformational difference in the lectin domain between the crystalized low- and high-affinity structures disproves this general theory for FimH and reveals a new form of allostery: β-sheet twisting. The low-affinity structure varies from the high-affinity structure in that the lectin

domain has an overall compressed state and is in tight interaction with the pilin domain. In the tip incorporated structure vs. that of all previously published structures, the lectin-domain β sandwich was found to shorten by 11 Å at the back-end and open the mannose-binding pocket at the front end. The analogy of a finger trap toy has been used to describe the changes of FimH lectin domain in its native state when comparisons are made to the isolated lectin domain or high-affinity state. The FimH lectin domain compresses and opens its binding pocket while in the low-affinity, but stretches and clamps down on mannose while in the high-affinity. This is a result of pilin domain interacting and disconnecting with the lectin domain to cause finger trap-like compression (twisting) and elongation (untwisting, stretching), respectively, in the β sandwich folds of the lectin domain (Le Trong, Aprikian et al. 2010). *In this work, these key structural responses are paramount to FimH behavior and are exploited for the first time to introduce mutations in the lectin domain that will ultimately favor the low-affinity conformation under any condition.*

The page turning mechanism has been devised to describe the internal conformations adopted by the FimH lectin domain and will be briefly described here (Figure 9)(Le Trong, Aprikian et al. 2010). Residues 16 and 22 form a β strand at the edge of the long β sheet (in purple). The long β sheet sandwiches with the split β sheet (in orange). Following Figure 9 from right to left (high-affinity to low-affinity), if residue 22 were imagined to be at the bottom corner of a file folder with corresponding β sheet colors (purple for long, orange for split β sheet), than movement of residue 22 upward would cause residue 16 at the upper portion of the β sheet (and therefore the file folder) to move up as well. Much like a folder's top corner pulling away from its

adjacent sheet, the long β sheet pulls away from the split β sheet. This leaves the folder's top or lectin domain's top open, allowing anything inside to escape or at least loosens its grip in the form of fewer hydrogen bonds.

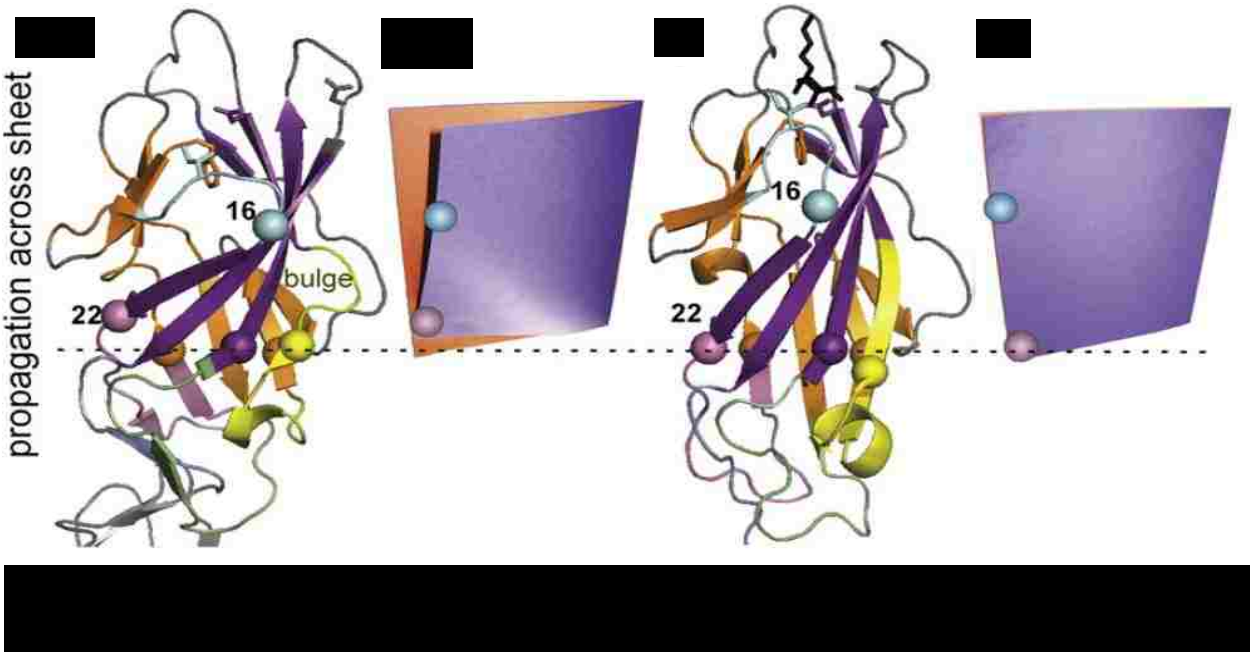


On an aside, all published high-affinity crystal structures were done using *E.coli* strain J96, a model uropathogenic isolate with a K12 background. The low-affinity state was crystalized using *E.coli* strain f18, a model fecal isolate with a KB91 background. The background strains differ in three amino acid residues at position 70, 78, and 27, but these were found by Le. Trong et al. *not* to cause the large differences in conformational changes observed in the low- vs. high-affinity structures (Le Trong, Aprikian et al. 2010) .

## Methodologies for bacterial synthesis and characterization

*Microbiology*

Microbiology-based techniques used in this work consist of the follow:

1. Point mutagenesis of a plasmid containing the gene for FimH
2. Synthesis of a plasmid construct containing the mutant lectin domain
3. Plasmid purification
4. DNA sequencing
5. Pili and lectin domain purification

All of these techniques are well established in the scientific community and will not be explained in detail here. If there is any interest in the methodology used to obtain these results, please see the specific Methods section within the following chapters. I have explained each of these methods in detail step by step to demonstrate my knowledge and understanding of each technique.

*Biophysical characterization*

Biophysical characterization of FimH mutations utilized in this work include whole cell *E.coli* binding to a substrate, enzyme-linked immunosorbent assay (ELISA), fluorescence-activated cell sorting, and atomic force microscopy. The latter two will be described in more detail within the following sections while the former two are well established and will be briefly discussed. Additionally, a more detailed description of these two techniques may be found in the Methods section of the following chapters.

*Binding to substrate*

Briefly, *E.coli* (possessing a FimH mutation) binding to a mannosylated substrate is a method in which the binding affinity of the contained FimH for mannose is assessed versus proper control

strain. After an incubation period and subsequent rinse step, *E.coli* bound to the substrate is assessed as a measure of affinity via crystal violet staining or radioactivity measurements (if a radioactive agent was included while seeding).

The ELISA based assays were included to characterize pili or lectin domain in one of two ways. First, the conformational state of FimH is determined via recognition with a specific primary antibody raised against one of its epitopes. A secondary antibody, conjugated to horse radish peroxidase, is then used to probe for the primary antibody. Horse radish peroxidase (HRP) is an enzyme that catalyzes the conversion of chromogenic substrates such as 3,3'-5,5'-tetramethylbenzidine (TMB) into a measurable colored product. Second, the phenotype of FimH is determined via binding to mannosylated substrate and later probed with the primary/secondary antibody method just described.

*Flow cytometry and fluorescence-activated cell sorting*

Flow cytometry is used in a variety of research and clinical settings to detect and count particles passing through a stream of fluid across an electronic detection apparatus. The main component of this instrument consists of a flow cell or liquid stream of sheath fluid that carries cells from a cell suspension and aligns them in preparation for a detection system. The detection system encompasses a light source which focuses a beam of light at the stream and a grouping of detectors which measure the light scatter and/or fluorescence at various angles. A detector in line with the laser beam usually detects the size or volume of the cells/particles, known as forward scatter (FSC). Several detectors positioned at perpendicular angle to the

laser beam detects side scatter (SSC), which is a measure of cell/particle complexity and/or content. A fluorescence detector is usually incorporated and may measure fluorescence emission given off by fluorescently labeled cells/particles. Signals from FSC, SSC, and fluorescence are then converted into an electronic signal, amplified, and stored for subsequent computational analysis. Analysis may be performed in 1-D histograms or 2-D plots to examine the number of cells of a certain size/fluorescence or compare FSC vs. SSC/fluorescence, respectively. Fluorescence-activated cell sorting (FACS) is a term used to describe a flow cytometer with the capability of sorting cells, but may be used in non-sorting applications. Most instruments available today are FACS machines, but for our purposes here, we have used it for non-sorting applications. The name is used only to distinguish the instrument.

*Atomic force microscopy*

Atomic force microscopy (AFM) is a high-resolution scanning probe microscopy with many useful applications including measuring, imaging, and manipulating on the nanoscale. For our purposes here, AFM is used as a form of force spectroscopy to measure the interaction of *E.coli* FimH with a mannosyl substrate (Figure 10). Briefly, a cantilever with a sharp tip and immobilized substrate is brought into contact with a surface coated with FimH expressing pili. The surface is then moved away from the cantilever and any interactions between the cantilever and surface deflects the cantilever. A laser spot sitting atop the cantilever measures

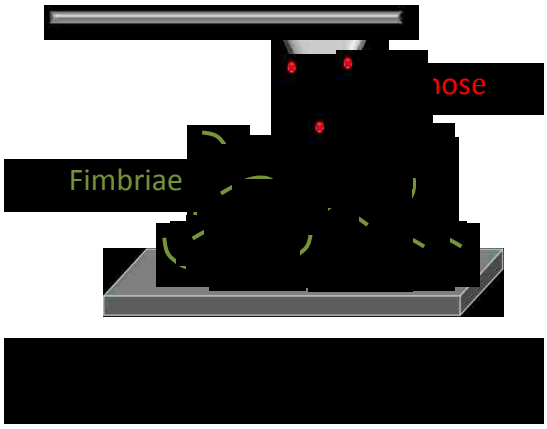

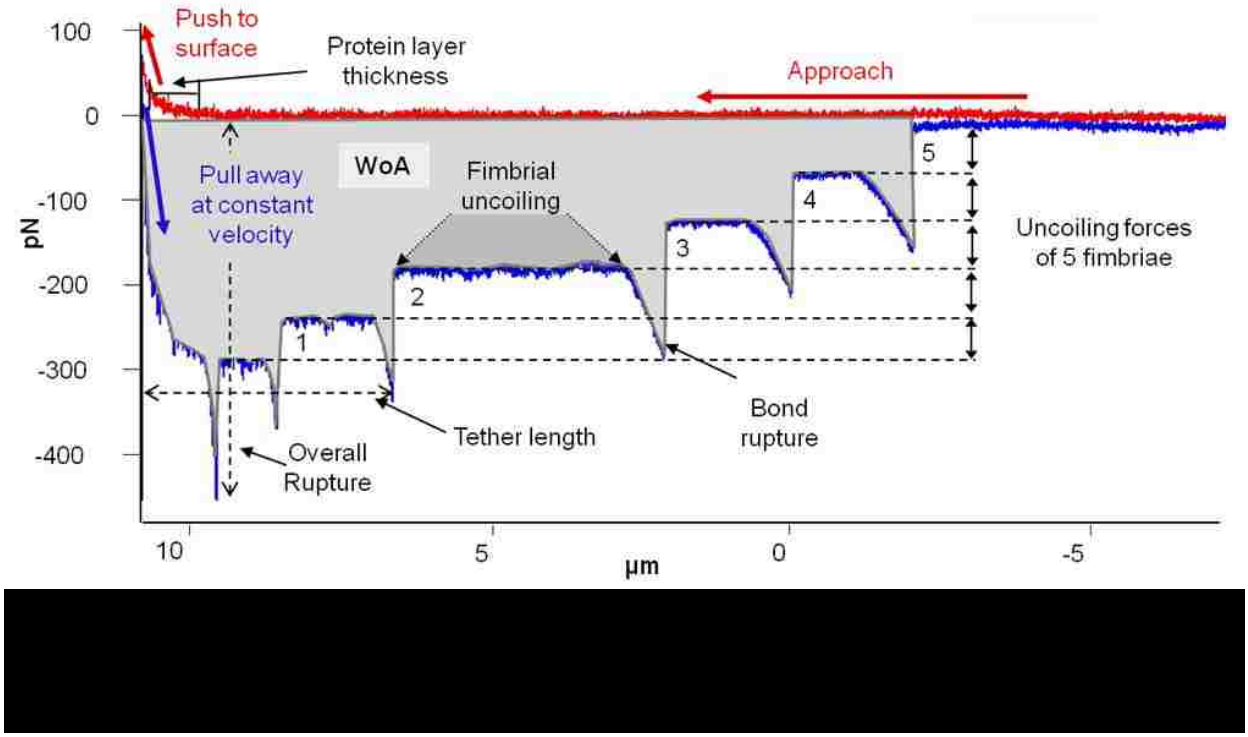


any deflection of the cantilever by reflection of its beam into an array of photodiodes. The photodiode then converts the reflected light into an electrical signal that may be interpreted by software into a force as a function of surface displacement (Figure 11). Knowing the cantilever's spring constant, $k_c$, any deflection by the cantilever can be converted into the force experienced by the fimbriae in contact:

$$F = -k_c \cdot d$$

and the trace that is created can be interpreted for other fimbrial mechanics such as uncoiling and overall rupture.

Atomic force microscopy was especially useful in this work in part due to the nature of the low-affinity FimH mutations synthesized. For particularly low-affinity mutants, the infrequency with

which the mutants bound a substrate-coated surface in a typical flow-chamber experiment caused difficulties in capturing strength/specificity of the bond in addition to identifying catch-bond formation. Because AFM is capable of measuring interactions on the single molecule scale, its sensitivity allowed for quantitative measurements of these characteristics. For this work, the *F* of the prevailing interactions was compared with that of the wild type in order to ensure that the binding pocket of each mutant remained intact. Additionally, the *F* value and frequency of each rupture peak allowed for the determination of catch-bond formation.

# Chapter III Multiple regions within the FimH lectin domain contribute to its allosteric pathway and may be mutated to sustain a low-affinity variant

**Victoria B. Rodriguez [†1], Brian A. Kidd [†1], Veronika Tchesnokova[2], Evgeni V. Sokurenko[2], Wendy E. Thomas[1]**

[1]Department of Bioengineering, Box 355061; [2]Department of Microbiology, Box 357242; University of Washington, Seattle, WA 98195, USA; [†]These authors contributed equally to this work.

**Acknowledgements**

Dr. Brian Kidd contributed to the rational design of FimH variants as well as offered general advisement for this chapter's structure. Dr. Veronika Tchesnokova contributed to the synthesis and assessment of the double-cysteine variants. Using human insight, Dr. Brian Kidd and Dr. Wendy Thomas evaluated variants suggested by rational design.

Support for this work comes from the NIH grant 1RO1 AI50940, NSF grant CBET-1132860, NIH-funded Molecular Biophysics Training Grant 1RO1 AI50940 at the UW (BAK and VBR), IGERT Fellowship Award NSF #DGE-0504573 (BAK) and the UW Initiatives Fund (BAK). The funders had no role in study design, data collection and analysis, decision to publish, or preparation of the manuscript.

**Publication**

This is a working manuscript and will be submitted for publication. The double cysteine variants, V27C-L34C and L34C-L109C, were also included in a recent publication:

Le Trong I, Aprikian P, Kidd BA, Forero-Shelton M, Tchesnokova V, Rajagopal P, Rodriguez V, Interlandi G, Klevit R, Vogel V, Stenkamp RE, Sokurekno EV, Thomas WE. "Structural basis for mechanical force regulation of the adhesin FimH via finger trap-like beta sheet twisting. " *Cell* 141 (4): 645-655. 2010.

## Abstract

The protein FimH is expressed by the majority of commensal and uropathogenic strains of *Escherichia coli (E.coli)* on the tips of type 1 fimbriae and mediates adhesion via catch-bonds to its ligand mannose. Crystal structures of FimH show an allosteric conformational change, but it remains unclear which differences between structures are due to the allosteric change versus ligand binding, point mutations, or even crystal contacts. Here we use the protein structural analysis tool RosettaDesign combined with human insight to identify and synthesize 10 mutations in four regions that we predicted would stabilize one of the conformational differences. The phenotype of each variant was characterized by measuring static binding to surfaces containing ligand and the preferred conformational state was elucidated with an enzyme-linked immunosorbent assay using a conformation-specific monoclonal antibody. These studies demonstrated that each region investigated was part of the FimH allosteric pathway. In addition, we identified many FimH variants that appear locked in the low-affinity state. Together, this information is critical to the future development of novel antiadhesive therapies designed to inhibit FimH by favoring the low-affinity state, which could provide an alternative treatment for antimicrobial drug resistant *E.coli*.

## Introduction

The most common bacteria associated with urinary tract infections (UTIs) are uropathogenic strains of *Escherichia coli* (*E.coli*) (Foxman 2010). Antimicrobial drugs used to treat UTIs are becoming increasingly less effective due to an increase in drug resistant *E.coli* (Karlowsky, Kelly et al. 2002; Zhanel, Hisanaga et al. 2005; Schito, Naber et al. 2009). Recently, research efforts have been focused on preventing bacterial adhesion and therefore colonization in the urinary tract through the use of antiadhesive therapies. The protein FimH, expressed by the majority of commensal and uropathogenic strains of *E.coli* on the tips of type 1 fimbriae, mediates adhesion and forms receptor-ligand bonds with terminal mannosyl residues on the surface of uroepithelial cells, intestinal epithelial cells, red blood cells, neutrophils, and yeast (Sokurenko, Chesnokova et al. 1997). Current antiadhesive therapies targeted at FimH include ligand-like inhibitors or vaccines. For the former, the complexity of both the carbohydrate environment *in vivo* and mechanics of bacterial adhesion has posed concerns for developing a successful competitive inhibitor (Thomas 2008; Hartmann and Lindhorst 2011). Moreover, several studies using FimH to immunize various animal models have shown protection against an *E.coli* infection, yet there exists no FDA approved vaccine on the market for humans (Langermann, Palaszynski et al. 1997; Langermann, Mollby et al. 2000). These observations suggest a need to understand the mechanism of FimH adhesion and how it is regulated to guide development of an effective therapy.

FimH has two domains: a lectin or mannose binding domain, and a pilin domain that anchors FimH to the fimbriae. Whereas most receptor-ligand interactions dissociate under force or high

flow conditions, FimH increases association under increasing tensile mechanical force. This phenomenon is known as a "catch bond". Mechanical activation of FimH has been demonstrated to result when tensile mechanical force allosterically switches FimH from a state with low affinity for mannose to one with high (Le Trong, Aprikian et al. 2010) (Figure 12). Tchesnokova et al., points out that although antibody therapy development is an alternative to antibiotic treatment of bacterial infections, the antibodies raised against FimH stabilized the

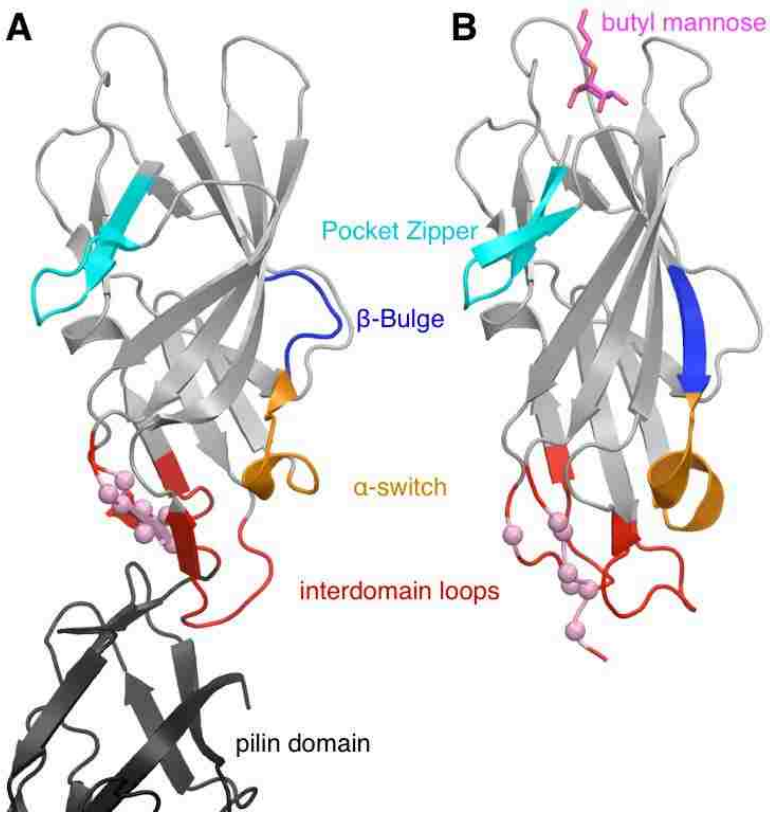


[redacted]

high-affinity conformation of the adhesin and actually enhanced bacterial adhesion to uroepithelial cells. An alternative strategy for preventing bacterial adhesion is thus to develop allosteric inhibitors or antibodies that stabilize the low-affinity state. To our knowledge, an

allosteric antiadhesive that targets the low-affinity state of FimH has never been reported. Characterization of the low-affinity conformation may provide the means to develop a successful allosteric inhibitor or antibody.

In order to design an antiadhesive therapy that targets the low-affinity state of FimH, it is necessary to understand the structural basis of the allosteric switch between the low- and high-affinity states. The crystal structure of the low-affinity state showed wide-spread conformational differences relative to previous structures (Le Trong, Aprikian et al. 2010). The three loops of the interdomain region, which directly contact the pilin domain, all dramatically changed structure (Figure 12) and these changes were shown to be due to the interaction with the pilin domain. In addition, the mannose-binding pocket had a looser conformation than in the high-affinity state, which was also shown to be caused by the presence of the pilin domain rather than by the absence of mannose in the structure. Furthermore, there were two additional large conformational changes. First, a short segment that is part of the β5-strand in the high-affinity crystal structure bulges out into a loop region in the low-affinity structure, which is referred to as the β-bulge. Second, a single-turn α-helix in the high-affinity structure becomes a $3_{10}$-helix in the low-affinity structure, which is referred to as the α-switch. It remains unclear whether these structural differences are associated with the allosteric conformational change, as they could also be caused by one or more of the differences in primary structure, since residues 27, 70, and 78, differ between the two crystalized proteins and are in or nearby the β-bulge and α-switch. Moreover, some changes in the mannose-binding pocket are ligand-induced (Nilsson, Yakovenko et al. 2007), whereas others are associated with the allosteric

switch (Le Trong, Aprikian et al. 2010), so it cannot be assumed that all conformational changes in or near the pocket are coupled to the allosteric pathway. Therefore, there remains a need to elucidate the contribution of each region of FimH to the allosteric pathway.

In this study, we used the protein structural analysis tool RosettaDesign combined with human insight to identify at least one mutation in each of four regions of the lectin domain that we predicted would stabilize the low- or high-affinity state if this region were part of the allosteric pathway. The mutations were introduced using site-directed mutagenesis to create 10 new variants that would together test whether each region was involved in allosteric control. The binding phenotype of each variant was characterized by measuring binding to mannosyl and oligomannosyl surfaces under static binding conditions. An enzyme-linked immunosorbent assay (ELISA) was used to elucidate each variant's conformation. These studies demonstrated that all four regions investigated were part of the FimH allosteric pathway. The resulting low-affinity variants provide tools for future fundamental FimH biophysics studies and establish a structural map of regulatory hotspots that can serve as targets for allosteric inhibitors or antibodies.

## Methods

*Software*

Images of protein structures were generated using PyMOL (DeLano 2002). The RosettaDesign source code is available without charge for academic users from: http://www.rosettacommons.org/software/. The MODIP server may be reached free of charge at http://caps.ncbs.res.in/dsdbase/modip.html.

*RosettaDesign Protocol*

Starting coordinates for the lectin domain structure were taken from the Protein Data Bank (PDB) (Berman, Westbrook et al. 2000) (pdb IDs: 1uwf chain A and 3jwn chain H for the high- and low-affinity states, respectively). The crystal structures of the lectin domain have been solved with proteins from slightly different genetic backgrounds: the high- and low-affinity state from the K12 and KB91 background, respectively (3 amino acid changes at 27, 70, & 78). Models were created for both parent strain backgrounds. Computational mutations were made by eliminating side chain atoms beyond the $C_\beta$ atom and allowing Rosetta to rebuild the side chains according to ideal bond lengths and angles. Finally, the side chain positions of the substitutions were optimized through repacking and rotamer trials (Kuhlman and Baker 2000), and the entire structure (all atoms) was minimized by optimizing the energy of the backbone and side chain dihedral angles.

Following repacking and minimization of the crystal structure, all amino acids were considered at each sequence position in the regions of the pocket zipper [N1-A10], β-bulge [Q59-S62], α-

switch [Y64-F71], and interdomain loops [A25-L34, P111-A119, N152-T158]. Side chain conformations were selected from the backbone dependent rotamer library (Dunbrack and Cohen 1997) generated from statistics of side chain conformers observed in structures found in the PDB. The backbone coordinates remained fixed while the side chain identity (and position) was varied. Only one position was varied at a time and each substitution was optimized for the local environment (all residues within 8 Å of the $C_\beta$ atom [$C_\alpha$ atom for glycine] of the original change were repacked). Each computational substitution was scored using the Rosetta all-atom energy function, which consists of a linear combination of the following terms; (i) Lennard-Jones attractive and repulsive, (ii) hydrogen bonding (Morozov, Kortemme et al. 2004), (iii) solvation (Lazaridis and Karplus 1999), (iv) statistical term ("pair") that approximates electrostatics and disulfide bonds, (v) statistical term ("rot") that estimates the backbone-dependent internal free energies of the rotamers, (vi) reference values for each amino acid that estimates the free energy of the denatured state. The energy difference from a substitution ($\Delta G = G_{mutant} - G_{wildtype}$) was computed for each state and the difference between states was determined ($\Delta\Delta G = \Delta G_{low\text{-}affinity} - \Delta G_{high\text{-}affinity}$). Since the goal was to find mutations that stabilize the low-affinity conformation relative to the high-affinity state, $\Delta\Delta G$ was arranged so negative values reflect a bias toward the low-affinity state.

*MODIP Design Protocol*

Two mutants containing double cysteines required a different technique in the design process. Briefly, MODIP evaluates a protein's geometry to identify residue pairs that could form disulfide

bonds without significantly altering the crystal structure, if mutated to cysteines (Sowdhamini, Srinivasan et al. 1989; Dani, Ramakrishnan et al. 2003). Based on stereochemical parameters, each attempted residue pairing is assigned a grade from A through D with A being the best.

*Mutagenesis*

The recombinant parent strain KB18 was constructed and described previously (Blomfield, McClain et al. 1991; Sokurenko, Chesnokova et al. 1997; Sokurenko, Schembri et al. 2001; Tchesnokova, Aprikian et al. 2008). Briefly, the *fim null E.coli* K12 derivative AAEC191A (donated by Dr. Ian Blomfield, University of Kent, UK), was transformed with the recombinant plasmid pPKL114 (donated by Dr. Per Klemm, Danish Technology University, Copenhagen, Denmark) to create KB18. Derived from the pBR322 plasmid, the pPKL114 plasmid contains the entire K12 *fim* gene cluster and a translational stop-linker inserted into the KpnI site of the *fimH* gene.

Site-directed mutagenesis followed Tchesnokova et al., (Tchesnokova, Aprikian et al. 2008). Briefly, primers were designed manually and ordered from Eurofins MWG Operon (Huntsville, AL). The K12 FimH-allele-containing plasmid, pGB2-24, was provided with one or two point mutations within the sequence encoding the FimH lectin domain (residues 1-160) via a Quick-Change Stratagene kit. Subsequent DNA sequencing confirmed each point mutation (University of Washington DNA sequencing facility). The resulting mutant plasmid (with chloramphenicol resistance) was then transformed into KB18 (with ampicillin resistance), thereby allowing the expression of fimbriae customized with the intended point mutation.

*Confirmation of fimbrial expression using fluorescence-activated cell sorting*

We examined the expression levels of mutant fimbriae versus wildtype (WT) K12 using fluorescence-activated cell sorting (FACS) and a previously published protocol with minor publications (Humphries, Raffatellu et al. 2003; Kisiela, Laskowska et al. 2006). First, *E.coli* were seeded in superbroth (SB) media with proper antibiotics (ampicillin at 100 μg/mL, chloramphenicol at 30 μg/mL) and incubated overnight at 37 °C under static conditions. The next morning, the bacteria were spun down, rinsed twice with 1X phosphate buffered saline (PBS), and resuspended at $A_{540}$ 10. Afterwards, 0.5 mL of bacteria were fixed with an equal amount of 3.7% formaldehyde for 30 min at room temperature. Fixed cells were rinsed with 1XPBS and blocked for nonspecific binding in 0.5 mL 0.2% BSA-PBS for 30 min with light rotation at room temperature. For the identification of FimH, the bacteria were spun down and resuspended in 0.5 mL 0.2% BSA-PBS containing 1:300 rabbit-anti-pilin-domain antibody (α-Pd PAb, Antibodies Inc., Davis, CA; immunogen: *E.coli* K12 FimH pilin domain). The bacteria were then incubated with light rotation for 1 hour at room temperature and rinsed twice with 1X PBS. Afterward, goat-anti-rabbit Immunoglobulin G (IgG) conjugated to Alexa-488 (Invitrogen) was mixed at 1:3000 in 0.2% BSA-PBS, covered, and incubated with light rotation for 1 hour at room temperature. After the final incubation, the bacteria were spun down, rinsed thrice with 1XPBS, resuspended in 0.5 mL 1XPBS, and immediately analyzed. A FACScan cell sorter (3 color Analyzer, Becton Dickinson, Department of Immunology's Cell Analysis Facility) quantified the expression levels based on Alexa-488 fluorescence up to 10,000 events per reading.

*Assessing variants' phenotype using radioactive-based binding assay*

In order to determine the phenotype of each variant, we performed static binding assays using radiolabeled bacteria on monomannosyl (1M) or trimannosyl (3M) coated surfaces as described previously (Sokurenko, Chesnokova et al. 1997; Sokurenko, Chesnokova et al. 1998; Sokurenko, Schembri et al. 2001). Briefly, *E.coli* expressing mutant FimH were seeded in superbroth (SB) media containing radiolabel Thymidine ($^3$H, PerkinElmer Life Sciences Inc.) and the proper antibiotics. Bacteria were incubated overnight at 37 °C under static conditions. Next, the bacteria were spun down, rinsed twice with 1XPBS, and resuspended at $A_{540}$ 2 with or without 1 % methyl α-D-mannopyranoside (αMMP or mannose). Meanwhile, detachable 96-well plates were incubated with 100µL of 20 µg/mL 1M (yeast mannin, Sigma) and 3M (bovine Rnase B, Sigma) in 0.02M $NaHCO_3$ buffer at 37 °C for 1 hour, blocked with 0.2 % BSA-PBS at 37 °C for 30 min, and aspirated. Wells with 0.2% BSA-PBS were included as a control substrate. The bacteria were then added to the coated plates and incubated for 45 min at 37 °C. Next, the plates were rinsed of unbound bacteria using 1XPBS, aspirated, dried at 65 °C for 15 min, broken into separate wells, and then placed in scintillation fluid. Radioactivity was measured for each sample (using Beckman LS 3801), done in triplicate, and the number of cells bound determined using calibration curves of known solution concentrations calculated with BIAevaluation software (GE Healthcare).

*Assessing the conformational change of variants in the presence of MAb21*

Prior to executing the ELISA, pili were purified from each variant according to a previously published protocol (Sokurenko, Chesnokova et al. 1997; Aprikian, Tchesnokova et al. 2007; Tchesnokova, Aprikian et al. 2008). In summary, *E.coli* were grown overnight at 37 °C in Terrific Broth (EMD Chemicals) media with proper antibiotics and under gentle shaking (125 rpm). The next morning, the bacteria were spun down at 8,000 rpm, resuspended in cold pili buffer (50 mM Tris-HCl at pH 7.0, 150 mM NaCl), and homogenized on ice three times for 1 min with a 1 min rest period in between (Pro 200 homogenizer, PRO Scientific Inc., Oxford, CT). Cell debris was spun down leaving the supernatant containing soluble pili. Pili were precipitated out of solution with 0.2 M $MgCl_2$ overnight at 4 °C, spun down at 15,000 rpm, and then resuspended in cold pili buffer. Any cell debris was then spun down at 15,000. Precipitation and resuspension was repeated several times before a final resuspension in cold 1XPBS. Protein concentration was determined using a BCA™ protein assay kit (Pierce) after heating in 0.1 M HCl for 5 min at 100 °C.

A basic ELISA using mouse-monoclonal antibody 21 (MAb21) was performed on the purified pili. MAb21 (from PickCell Inc., Netherlands) is an antibody raised against *E.coli* K12 FimH-lectin domain (residues 1-160) and previously determined to recognize or induce the high-affinity state of K12 FimH, especially in the presence of ligand (Tchesnokova, Aprikian et al. 2008; Tchesnokova, Aprikian et al. 2011). Pili were immobilized at 0.1 mg/mL in 0.02 M $NaHCO_3$ buffer in wells of 96-well-flat-bottom plates at 37 °C for 1 hour. Comparative controls consisted

of FocH (high-affinity with and without mannose) and WT K12 (high-affinity in presence of mannose). Free protein was rinsed off with 1XPBS twice and then quenched for 30 minutes in 0.2% BSA-PBS. MAb21 was added at 1:1500 dilution with and without 1% αMMP in 0.2% BSA-PBS for 137 min. Free reagent was rinsed off 4 times with 1XPBS. Horseradish-peroxidase conjugated to goat-anti-mouse (HRP-GAM) antibodies at 1:3000 in 0.2% BSA-PBS were incubated on the plate for 1 hour at 37 °C and then rinsed off 6 times with 1XPBS. Bound HRP-GAM was visualized with the addition of 3,3' 5,5' – tetramethylbenzidine (TMB) peroxidase enzyme from an immunoassay substrate kit (Bio-Rad). Absorbance was read at 650 nm using Molecular Devices Emaxx microtiter plate reader.

## Results

*Summary of Studies*

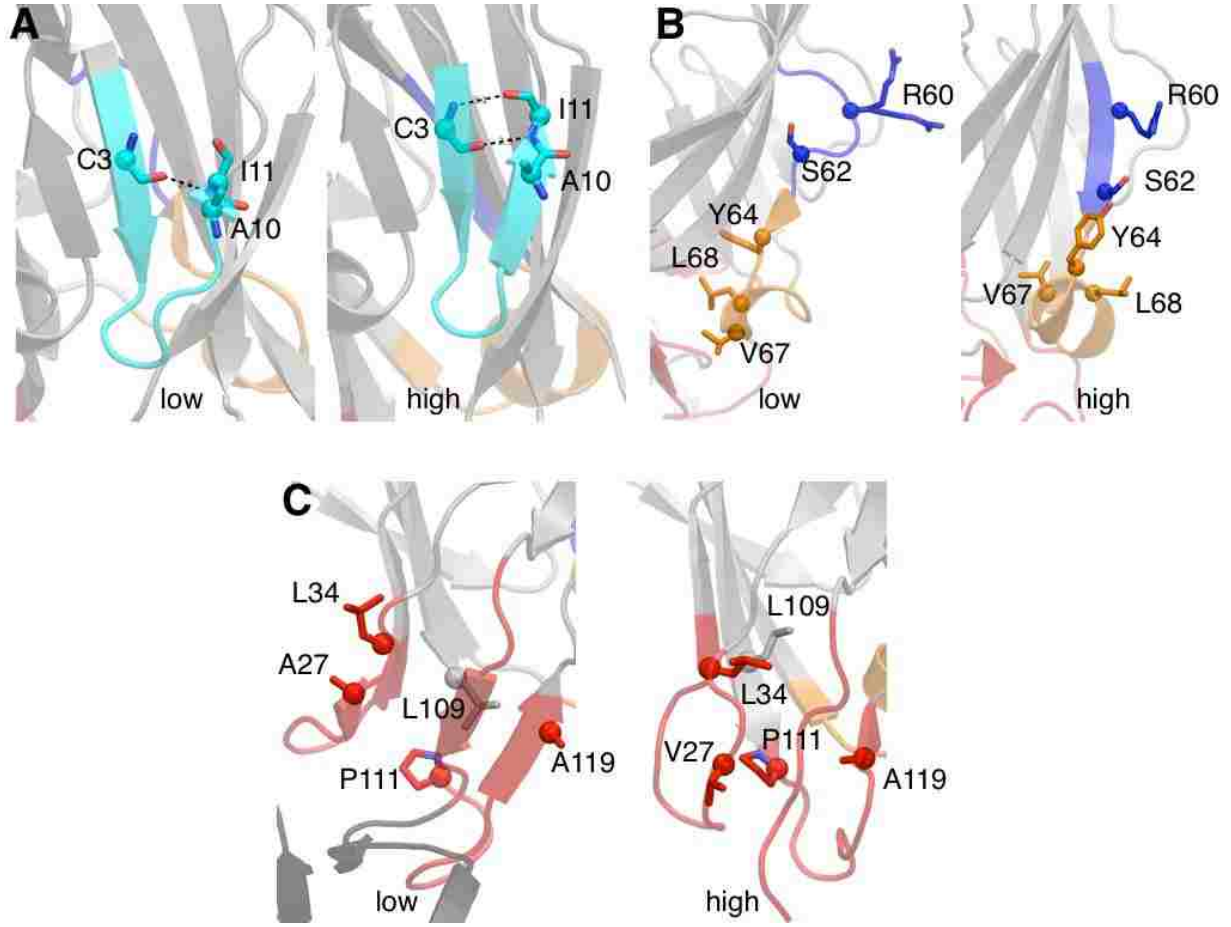


[redacted]

In this study, we used the crystal structures of FimH in two different states to predict point mutations that should stabilize one conformational state or the other. The amino acid substitutions were selected within four regions that we call the pocket zipper, β-Bulge, α-switch, and interdomain loops, to determine which of these regions are part of the allosteric pathway (Figure 13). Previously, only the interdomain loops were tested in this manner (Le Trong, Aprikian et al. 2010). We made a special effort to predict mutations that would stabilize the low-affinity state since almost all prior mutations have increased affinity, and both types of variants provide useful tools for future studies. In most cases, we used human intuition by analyzing the structures visually to identify amino acids that were solvent exposed in one conformation, but buried in the other. We then used RosettaDesign computational analysis to predict specific substitutions at these locations that would cause the largest $\Delta\Delta G$, or difference in energy between the two conformations.

We quantified the expression of FimH for each variant by detecting the amount of pilin domain in fluorescence-activated cell sorting of whole-cell *E. coli*. All variants demonstrated expression averaging 74-82% of wild type (WT) K12 (data not shown) and thus were concluded to not alter pilus biogenesis. In order to determine the phenotype of each variant, we performed static binding assays using radiolabeled bacteria on monomannosyl (1M) or trimannosyl (3M) coated surfaces (Figure 14A). The 1M/3M ratio was calculated to normalize the data since both high- and low-affinity variants bind similarly to RNAseB (Sokurenko, Chesnokova et al. 1997; Sokurenko, Chesnokova et al. 1998).

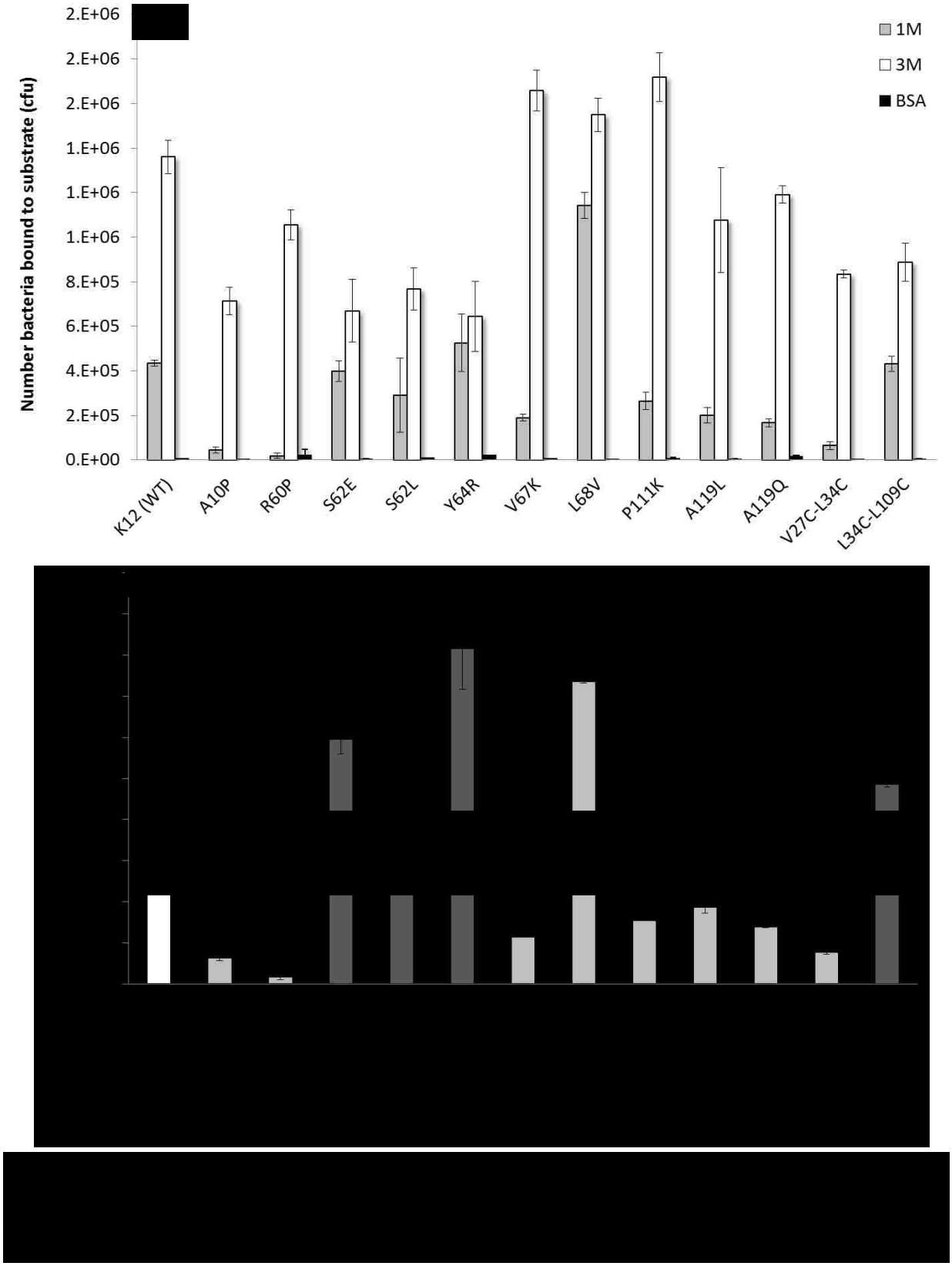
Number bacteria bound to substrate (cfu)
2.E+06
2.E+06
2.E+06
1.E+06
1.E+06
1.E+06
8.E+05
6.E+05
4.E+05
2.E+05
0.E+00
1M
3M
BSA
K12 (WT)
A10P
R60P
S62E
S62L
Y64R
V67K
L68V
P111K
A119L
A119Q
V27C-L34C
L34C-L109C

A low ratio relative to WT reflects low-affinity whereas a high ratio reflects high-affinity (Sokurenko, Chesnokova et al. 1997; Sokurenko, Chesnokova et al. 1998) (Figure 14B). To determine the conformation of each variant, we performed an ELISA using conformation-specific MAb21, in the presence and absence of the ligand mannose (Figure 15). The high-affinity variant FocH is strongly recognized by MAb21 even without ligand, whereas WT FimH requires ligand for strong recognition by MAb21, demonstrating that it switches to the high-affinity state when it binds ligand (Tchesnokova, Aprikian et al. 2008). These studies allowed us to determine which regions are exerting allosteric control over FimH.

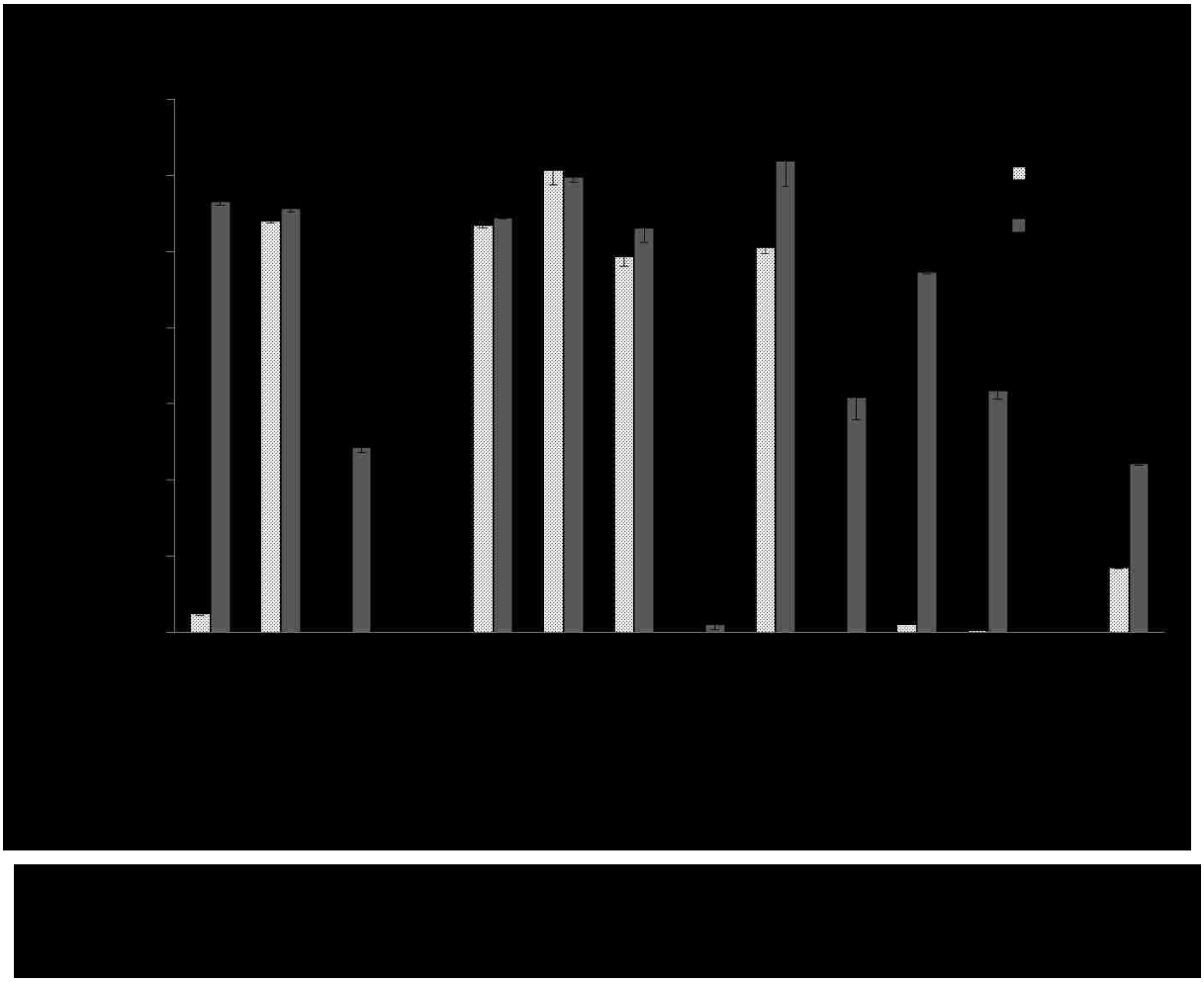

*Pocket Zipper (N1-A10)*

The pocket zipper is a two-strand β-hairpin that is “zipped” (tight) in the high-affinity conformation and is “unzipped” (loose) in the low-affinity conformation (Figure 13A). Analyses of the crystal structure suggests that the backbone hydrogen bond between residues C3 and I11 is critical for closing the angle (∠C3:N, N7:N, I11:N) in the tight conformation. We hypothesized that substituting proline for alanine at position 10 (A10P) would bias the structure toward the low-affinity conformation because the phi/psi angles for this residue are outside of the allowed region of the Ramachandran map for proline in the high-affinity conformation. We calculated using RosettaDesign that the predicted ΔΔG for this mutation is −29 kcal/mole, where a negative value indicates that the mutation should stabilize the low-affinity conformation. The 1M/3M ratio experiment showed that the A10P variant is a significantly weaker binder than WT and therefore demonstrates a low-affinity phenotype. In the absence of ligand, MAb21 binds more poorly to the A10P variant than to WT, suggesting that the A10P mutation stabilizes the low-affinity conformation rather than simply damaging the pocket. Ligand enhanced recognition by MAb21 for the A10P variant, but not to the levels observed for WT. The phenotype and conformation assays together suggest that A10P stabilizes the low-affinity conformation in a way that propagates from the mutation in the hairpin to the MAb21 epitope situated in the interdomain region.

*β-Bulge (Q59-S62)*

The β-bulge is a short segment that is part of a β-strand in the high-affinity conformation but bulges out into a small loop in the low-affinity conformation (Figure 13B). This bulge is hypothesized to act as a release valve for the strain caused by the more twisted conformation of the main β-sheet in the low-affinity state. Mutations were selected to stabilize the bulged configuration in order to test the importance of the bulge to the allosteric pathway by determining whether the overall structure should shift toward the low-affinity state. We hypothesized that a proline in position 60 would destabilize the high-affinity conformation since prolines destabilize β-sheets. The RosettaDesign calculation was a ΔΔG of −74 kcal/mole, favoring low-affinity as hypothesized. In experiments, the R60P variant demonstrated much weaker binding than WT or even A10P and therefore reveals a low-affinity phenotype. MAb21 failed to recognize R60P even with ligand, demonstrating that the R60P variant remained locked in the low-affinity state under these conditions.

The bulged conformation also requires an extra amino acid, which is provided by amino acids 62 through 63 shifting upward and rotating 180 °. For example, the sidechain of residue 62 is buried in the low-affinity conformation and solvent-exposed in the high-affinity conformation. To test whether this shift was coupled to the allosteric pathway, we hypothesized that the solvent-facing configuration would tolerate a change in amino acid more readily. RosettaDesign predicted that S62L & S62E would result in ΔΔG values of +112 & +28 kcal/mole respectively, favoring the high-affinity conformation. Both variants bound to mannose strongly relative to

WT and were recognized strongly by MAb21, suggesting that these mutations indeed favored the high-affinity conformation. In summary, mutants R60P, S62L, and S62E alter the overall phenotype and conformation of FimH, thereby demonstrating the importance of the β-Bulge to the FimH allosteric pathway.

*α-switch (Y64-F71)*

The α-switch is a single-turn $3_{10}$-helix in the low-affinity conformation that switches to an α-helix in the high-affinity conformation (Figure 13B). Structurally, this helical rearrangement is directly connected to the bulge segment because the $3_{10}$-helix conformation uses one less amino acid, allowing residue A63 to shift towards the β-bulge. To test whether this region is connected to the allosteric pathway, we selected mutations that were favorable for the $3_{10}$-helix while being unfavorable for the α-helix. Position 67 switches from solvent exposed in the low-affinity conformation to buried in the high-affinity conformation. RosettaDesign predicted that the V67K mutation would have the largest energy difference between conformations and favored the low-affinity conformation (ΔΔG = −5.3 kcal/mole). In experiments, the V67K variant binds significantly less than WT K12 and was not recognized by MAb21 in the absence or presence of ligand. The side chain at position 68 is buried in the low-affinity conformation and solvent exposed in the high-affinity. If packing is already optimized, any change should favor the high-affinity conformation. However, RosettaDesign predicted that a L68V mutation would result in a ΔΔG of –18 kcal/mole, favoring the low-affinity conformation. L68V demonstrated a high-affinity phenotype as indicated by 1M/3M ratio as well as by MAb21 recognition in the

absence and presence of ligand, supporting human insight over the Rosetta calculations. We also selected a mutation predicted to be favorable to the α-helix. The side chain of Y64 is buried in the $3_{10}$-helix conformation and exposed to solvent in the α-helix. RosettaDesign predicted that Y64R favored the high-affinity conformation with a ΔΔG of +25 kcal/mole. The Y64R variant did indeed show a high-affinity phenotype and was recognized by MAb21 in the absence and presence of ligand. Even with the one contradiction to Rosetta calculations, the fact that all three mutations in the α-switch significantly alter mannose binding in correlation with conformational state indicates that this region is also part of the allosteric pathway.

*Interdomain loops (A25-L34, P111-A119, 152-158)*

The interdomain region consists of three separate sequences in the mannose-binding lectin domain that contact the anchoring pilin domain (Figure 13C). The interdomain region changes configuration in the low-affinity state to enable interactions with the pilin domain, as previously described (Le Trong, Aprikian et al. 2010). The pilin domain is known to control affinity (Aprikian, Tchesnokova et al. 2007) and allosteric conformation (Tchesnokova, Aprikian et al. 2008), strongly suggesting that the interdomain loops are part of the allosteric pathway. In addition, two variants in this region affected both mannose binding and MAb21 recognition (Le Trong, Aprikian et al. 2010). Residue 34 shifts dramatically between the two configurations, so pilin-binding (docked) configuration was locked by a disulfide bond introduced with the double V27C-L34C mutation, while the undocked configuration was locked by a disulfide bond introduced with the double L34C-L109C mutation. As controls, we included the two variants

from Le Trong et al. for comparison in our experiments (Le Trong, Aprikian et al. 2010). Consistent with prediction, the V27C-L34C variant displayed a low-affinity in both phenotype and conformation, and the L34C-L109C variant displayed a high-affinity phenotype. Moreover, MAb21 recognized L34C-L109C better than K12 in absence of ligand, but more weakly in its presence. Together, this suggests that the two variants are in the predicted allosteric conformations, but that L109C may slightly interfere with the MAb21 binding site (Figure 12).

In addition, we predicted several new mutations in this region. We noted that A119 is buried in the high-affinity conformation and exposed in the low-affinity conformation. Accordingly, RosettaDesign predicted that long side chains at this position with point mutants A119L and A119Q would favor the low-affinity conformation ($\Delta\Delta G = -60$ and $-30$ kcal/mole, respectively). Indeed, both the A119L and A119Q variants demonstrated a low-affinity phenotype as well as a low-affinity conformation in the absence of ligand. However, in the presence of ligand, MAb21 recognized both mutants, demonstrating that this variant can switch to high-affinity in presence of ligand. Similar to residue 119, P111 is buried in the high-affinity conformation and exposed in the low-affinity conformation. A charged side-chain that is large (e.g. P111K) was predicted to strongly favor the low-affinity conformation ($\Delta\Delta G = -103$ kcal/mole). Similar to A119L and A11Q, P111K indicates a low-affinity phenotype and low-affinity conformation in the absence of ligand, but MAb21 recognizes P111K in the presence of ligand. In summary, A119L, A119Q, and P111K contribute to the allosteric pathway.

*Comparison of phenotype vs. conformation*

For the most part, the phenotype (1M/3M ratio) correlates with the conformation (MAb21 binding), as indicated by the trend lines in Figure 16. The wildtype K12 variant is at a key transition point in the correlation graph. MAb21 recognition is weak and dependent on mannose for variants with lower 1M/3M ratios. In contrast, recognition is strong regardless of mannose for variants with higher ratios. The trend lines illustrate this clearly, as they both remain high for all variants to the right of K12, but drop and separate to the left. The low-affinity variants (A10P, R60P, V27C-L34C, V67K, A119L/Q, P111K) are not recognized by MAb21 in the absence of ligand but only R60P and V27C-L34C show an insignificant shift in MAb21 recognition in the presence of ligand ($p > 0.05$, V67K had $p < 0.05$) indicating that they are locked in the low-affinity state even in the activating conditions of this assay. The outliers are also informative. Of the low-affinity variants, some are recognized by MAb21 with mannose more than expected given the 1M/3M ratio, while others less so, as reflected by their positions off the solid trend line. Also, recognition of L34C-L109C in presence of mannose is lower than expected given its phenotype, which is addressed in the discussion. Overall, the strong correlation of phenotype and conformation indicates that the primary determinant of binding strength is the allosteric state of the variants.

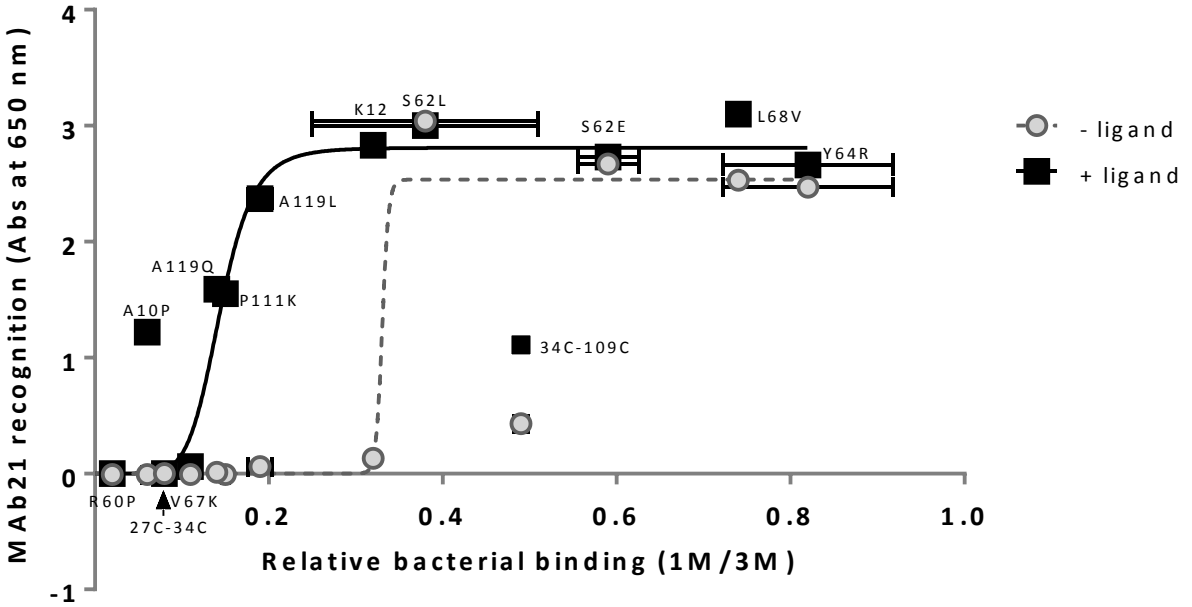


**Figure 16 Correlation of the 1M/3M ratio with MAb21 recognition of pili, in the absence (light circles) and presence (dark squares) of ligand mannose. Each data point contains a horizontal and vertical error bar. The dotted line and solid lines represent the empirical trend of MAb21 recognition in the absence and presence of ligand, respectively.**

*Identification of low-affinity FimH mutants*

In the course of this work, we identified six new low-affinity variants, which provide tools to complement the large number of previously identified high-affinity variants (Sokurenko, Courtney et al. 1995; Sokurenko, Chesnokova et al. 1997; Thomas, Trintchina et al. 2002; Thomas, Nilsson et al. 2004; Weissman, Chattopadhyay et al. 2006; Aprikian, Tchesnokova et al. 2007) for future studies about FimH allostery. Of these, A119L, A119Q, and P111K have only a slightly decreased 1M/3M ratio and switch at least partially to the high-affinity conformation in the presence of mannose in the MAb21 assays. A10P, R60P, V67K, and V27C-L34C variants have the lowest affinity for mannose and each represents a different region of the FimH lectin domain. However, the A10P variant can switch to the high-affinity conformation with mannose,

while the other three remain locked in the low-affinity conformation in all conditions tested here. Thus, R60P, V67K and V27C-L34C are the most promising candidates for future studies requiring low-affinity variants.

## Discussion

In this study, we applied human insight and RosettaDesign to crystal structures of FimH in two allosteric conformations in order to predict 10 mutations that would stabilize one or the other conformation. We genetically engineered variants with these mutations using site-directed mutagenesis. We evaluated them for phenotype by testing ability to bind to mannose-coated surfaces and for conformation by testing MAb21 binding, which specifically recognizes the high-affinity state. Every variant that was designed using both human and computational analysis demonstrated the predicted phenotype. In one case, human insight and RosettaDesign contradicted each other, and this variant demonstrated the phenotype predicted by human insight. In every case, binding of the conformation-sensitive antibody correlated with phenotype, demonstrating that the changes in ligand-binding strength were caused by a change in the allosteric conformation. This suggests that the combination of human and computational analysis is needed for successful prediction of mutations that affect the allosteric state of a protein. The fact that all predicted variants affected phenotype demonstrates that all four regions are part of the allosteric pathway. Previously, only the role of the interdomain region was tested with point mutations based on the crystal structures (Le Trong, Aprikian et al. 2010).

To draw the conclusions above, we assumed that binding to MAb21 directly reflected the conformational state of FimH, so it is worth evaluating this assumption in depth. Two other mechanisms could cause loss of MAb21 binding. First, a mutation may directly interfere with the MAb21 epitope. However, the MAb21 epitope is restricted to residues 26, 29, and 153-157 (Tchesnokova, Aprikian et al. 2011) which includes none of our mutations. Moreover, MAb21

recognized all variants given the right conditions. A10P, R60P and V67K were recognized normally by MAb21 when expressed with the FocH pilin domain and incubated with mannose, which lacks the ability of the wild type pilin domain to stabilize the low-affinity state (Tchesnokova, Aprikian et al. 2011). V27C-L34C was recognized normally by MAb21 in the presence of mannose and DTT, which breaks the disulfide bond that maintains the low-affinity conformation for this variant (Le Trong, Aprikian et al. 2010). It might be noted that the L34C-L109C only reaches 50% to 80% of MAb21 binding compared to WT even with mannose (Figure 15) and (Le Trong, Aprikian et al. 2010)), and the FocH pilin domain (Tchesnokova, Aprikian et al. 2011), suggesting that the disulfide bond in the hydrophobic core subtly distorts the nearby MAb21 epitope. However, the slightly reduced MAb21 binding does not interfere with our ability to observe the increased recognition of MAb21 in the absence of mannose, which demonstrates the allosteric activation by this double mutation. A second alternative explanation could be that some variants are misfolded or fail to express, so that both mannose binding and MAb21 binding would be lost, but not because FimH is in the low-affinity state. However, the FACS data demonstrated that expression levels are comparable, and the ability to bind RNAseB (Figure 14) demonstrates that the proteins are folded properly. Thus, the level of MAb21 binding reflects the population of FimH in the high- vs. the low-affinity state.

While the interdomain region was already shown to exert allosteric control over FimH (Thomas, Trintchina et al. 2002; Thomas, Nilsson et al. 2004; Le Trong, Aprikian et al. 2010), here we showed that three other novel regions – the pocket zipper, the β-bulge and the α-helix – are also part of the allosteric pathway. This knowledge expands the targets for allosteric

antiadhesives. Indeed, it may be most advantageous to target an allosteric antiadhesive to a region other than the interdomain region so that it does not compete with the pilin domain's natural allosteric inhibition (Aprikian, Tchesnokova et al. 2007; Le Trong, Aprikian et al. 2010), allowing the two to work in synchrony to stabilize FimH in the low-affinity state. Our data can also be used to determine how tightly each of these regions is coupled to the conformation of the mannose-binding versus pilin-binding regions. For instance, the A10P mutation was tightly coupled to mannose binding but only weakly coupled to MAb21 binding, which is near the pilin-binding site. In contrast, V67K and V27C-L34C were more tightly coupled to MAb21 binding than to mannose binding, while R60P appears tightly coupled to both. Interestingly, this coupling reflects the proximity of each region to the two binding sites. In summary, each region of FimH investigated herein is part of the allosteric pathway, and their degree of coupling to the mannose- or pilin-binding regions can be predicted by the proximity to these sites. This information should be useful in choosing binding sites for computational design of allosteric inhibitors or antibodies to prevent an *E.coli* infection.

Here we also characterized six new low-affinity variants. A previous study showed that antibodies raised against high-affinity FimH structures increased rather than decreased bacterial adhesion to uroepithelial cells because they stabilized the high-affinity state of FimH (Tchesnokova, Aprikian et al. 2011). This suggests that particular antibodies raised against the low-affinity variants may inhibit bacterial adhesion because they stabilize the low-affinity state of FimH. If so, these low-affinity variants may be used either directly in patients as a vaccine or used as an immunogen to develop a passive-immunity formulation. The variants A10P, R60P,

V67K, and V27C-L34C represent all 4 regions investigated herein and provided the strongest stabilization of a low-affinity phenotype and conformation. Variant A10P's low 1M/3M ratio and recognition by MAb21 in the presence of ligand suggests that the mutation to proline may directly affect the binding pocket nearby and contribute to the low-affinity phenotype. Therefore, A10P is not as stable in the low-affinity conformation as R60P, V67K, and V27C-L34C and may not be the preferred candidate for an antiadhesive therapy. The remaining variants were capable of maintaining a low-affinity conformation in the absence and presence of ligand. These low-affinity variants may also be useful to screen for allosteric inhibitors or antibodies. It may be important to use more than one low-affinity variant for both immunogen and screening, to address the issue that some antibodies may recognize an epitope that includes one of the mutations and thus be ineffective against WT FimH.

The low-affinity variants identified here should also be useful for understanding FimH-mediated bacterial adhesion. Many pathogenic clinical isolates express variants that have a high-affinity for mannose (Sokurenko, Courtney et al. 1995; Sokurenko, Chesnokova et al. 1998; Weissman, Chattopadhyay et al. 2006), and more high-affinity variants have been engineered (Sokurenko, Schembri et al. 2001; Thomas, Trintchina et al. 2002; Aprikian, Tchesnokova et al. 2007). These were critical for showing that FimH forms strong slip bonds if it is already allosterically activated. These variants also mediated strong stationary adhesion that is not shear-enhanced, demonstrating the role of catch bonds in shear-enhanced adhesion. These studies were essential for understanding the biological importance of the allosteric inhibition of FimH. However, the corresponding questions have not been asked to understand the importance of

the allosteric activation of FimH. It is possible that the low-affinity variants are locked in the low-affinity state so that they can't be activated by force, or that they will simply require more force for activation, like a loss-of-function variant of the catch-bond forming protein von Willebrand Factor (Auton, Sedlak et al. 2009). It has been suggested that FimH that is locked in the low-affinity state could still mediate shear-enhanced adhesion due to mechanical properties of the type 1 pili that anchor FimH (Bjornham and Axner 2010; Whitfield, Ghose et al. 2010). The low-affinity variants developed here can be used to address these and other fundamental questions about bacterial adhesion.

Most bacterial adhesins have never been tested in controlled flow conditions, so the prevalence of shear-enhanced adhesion is still being determined. Nevertheless, this phenomenon has already been reported for the collagen receptor of *Staphylococcus aureus* (Li, Mohamed et al. 2000), P-pili (Nilsson, Thomas et al. 2006) and CfaI (Tchesnokova, McVeigh et al. 2010) of *E. coli,* Hsa and GspB of *Steptococcus gordonii* (Ding, Palmer et al. 2010), and type 1 fimbriae of *Salmonella enterica* (Kisiela, Kramer et al. 2011). These adhesins contribute to virulence, so are also targets of antiadhesive therapies. While none of these other adhesins have been shown to have allosteric properties, *E. coli* FimH was studied for over 100 years and crystallized in 6 unique crystals with nearly identical conformations, both with and without ligand (Choudhury, Thompson et al. 1999; Hung, Bouckaert et al. 2002; Bouckaert, Berglund et al. 2005; Wellens, Garofalo et al. 2008) before the alternative allosteric conformation was finally crystallized (Le Trong, Aprikian et al. 2010). This suggests that allostery may also be overlooked in other

bacterial adhesins, and our success in using the crystal structure for allosteric design demonstrates the value of obtaining alternative structures.

# Chapter IV A low-affinity FimH lectin domain independent of its pilin domain promises new frontiers in catch-bond biophysics and antiadhesive therapies targeted at *E.coli*

**Victoria B. Rodriguez[1], Nichole S. Tyler[1], Veronika Tchesnokova[2], Matt Whitfield[1], Evgeni V. Sokurenko[2], Wendy E. Thomas[1]**

[1]Department of Bioengineering, Box 355061; [2]Department of Microbiology, Box 357242; University of Washington, Seattle, WA 98195, USA.

**Acknowledgements**

Dr. Whitfield provided the advisement, design, and execution of the preliminary AFM experiments as well as created a costume-made "do-it" program for Igor Pro 5.05A used in the AFM curve analyses. Nichole Tyler performed the AFM experiments that were included in this chapter. Dr. Veronika Tchesnokova kindly provided results for assays performed on all FocH variants.

Support for this work comes from the NIH grant 1RO1 AI50940, NSF grant CBET-1132860, NIH-funded Molecular Biophysics Training Grant 1RO1 AI50940 at the UW (VBR). The funders had no role in study design, data collection and analysis, decision to publish, or preparation of the manuscript.

**Publication**

This is a working manuscript and will be submitted for publication.

## Abstract

Expressed by most commensal and uropathogenic Escherichia coli (E.coli), the adhesive protein FimH facilitates urinary tract colonization and has become a significant antigen for antiadhesive therapies that may prevent urinary tract infections. FimH, which contains a mannose-binding lectin domain (LD) and pilin domain, possesses 2 different affinities and conformations for ligand mannose with previous work strongly suggesting that the pilin domain interacts with and stabilizes the LD's low-affinity conformation. This may explain evidence of antibodies raised against the isolated LD biasing the high-affinity state and allosterically enhancing FimH adhesion. To investigate this, a previously described low-affinity mutant V27C-L34C was characterized in new forms that physically altered the pilin domain's interaction with the LD in order to assess the LD's independence. Mutant "locked-low" may be unlocked to increase binding via reducing agent dithiothreitol (DTT). Under native conditions (without ligand and DTT in solution), our investigation discovered that locked-low pili containing an altered pilin domain, FocH, were unrecognized by high-affinity-binding MAbs and weakly bound to monomannosyl (1M) substrate. Under the same conditions, a locked-low isolated LD was also unrecognized by high-affinity binding MAb21 and bound 1M and trimannosyl substrate with low-affinity. Our study strongly suggests that under native conditions, LD interaction with the pilin domain is not required to stabilize a low-affinity state. This is also the first native low-affinity isolated LD that switches states via DTT to be useful in future biophysical characterization and as an alternative antigen in antiadhesive therapy development.

## Introduction

Uropathogenic strains of *Escherichia coli* (*E.coli*) are the most common bacteria associated with urinary tract infections (UTIs) (Foxman 2010) and are becoming increasingly resistant to current antimicrobial drugs (Karlowsky, Kelly et al. 2002; Zhanel, Hisanaga et al. 2005; Schito, Naber et al. 2009). Antiadhesive therapies, such as vaccines, have been a recent focus in order to provide an alternative measure in preventing initial bacterial adhesion to the urinary tract. A significant antigen to target on *E.coli* is the protein FimH, expressed by the majority of commensal and uropathogenic strains of *E.coli* on the tips of type 1 fimbriae covering each bacterium's surface. FimH mediates adhesion and forms receptor-ligand bonds with terminal mannosyl residues exposed on the surface of a variety of cell types (Sokurenko, Chesnokova et al. 1997). Several studies using FimH to immunize various animal models were successful in protection against an *E.coli* infection (Langermann, Palaszynski et al. 1997; Langermann, Mollby et al. 2000), but there is no evidence of an FDA approved vaccine on the market. One possible explanation is that the development of a vaccine is effected by the conformation of the original antigen used during immunization and FimH happens to have two different conformations that bind mannose with different affinities: a low and a high-affinity state (Aprikian, Tchesnokova et al. 2007; Tchesnokova, Aprikian et al. 2008; Le Trong, Aprikian et al. 2010) (Figure 17A and Figure 17B, respectively). Tchesnokova et al., demonstrated that antibodies raised against the isolated binding-domain of FimH, known as the lectin domain (LD), are biased solely to epitopes of the high-affinity state, are able to allosterically *enhance* FimH adhesion, and may easily be shed if the low-affinity conformation is favored (Tchesnokova, Aprikian et al. 2011). The outcome

suggests that the potential antigen for immunization resides in the high-affinity state when isolated and in fact, all isolated FimH LDs crystallized previously exist in this conformation (Choudhury, Thompson et al. 1999; Hung, Bouckaert et al. 2002; Bouckaert, Berglund et al. 2005; Wellens, Garofalo et al. 2008).

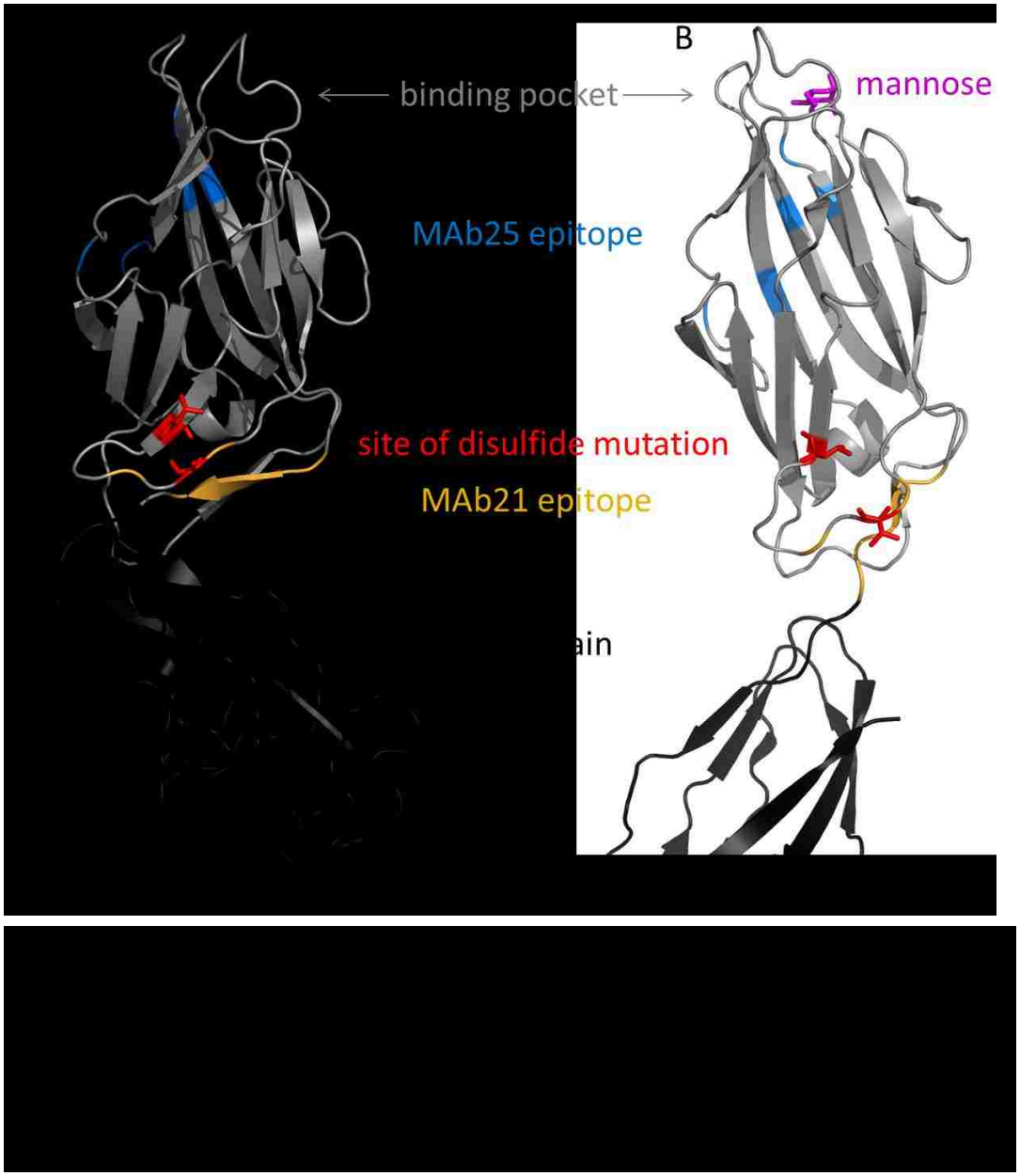

Tchesnokova's discovery motivates the use of a low-affinity-state FimH as the antigen for antiadhesive therapy development, but the antigen's preferred high-affinity conformation when isolated creates a potential road block and suggests why there is not a licensed vaccine for UTI infections. Perhaps a way around the road block is to investigate the mechanism of how FimH switches conformations and how the low-affinity state may be stabilized. FimH's LD contains the binding pocket for ligand at its tip, while the pilin domain anchors the FimH LD into the extending fimbriae. FimH has been documented to be force activated at higher fluid flow, thus increasing its affinity for mannosyl residues, a phenomenon known as a "catch bond." An allosteric mechanism for FimH's switch from low to high-affinity was experimentally confirmed under force (Aprikian, Tchesnokova et al. 2007) as well as in the presence of a monoclonal antibody, which recognizes an epitope far from the binding pocket near the interdomain region (Tchesnokova, Aprikian et al. 2008) (MAb 21 in Figure 17). The pilin domain's physical contact with the LD, as seen in the low-affinity crystal structure (Le Trong, Aprikian et al. 2010) and disruption of that contact to cause a high-affinity phenotype (Aprikian, Tchesnokova et al. 2007; Le Trong, Aprikian et al. 2010), confirms that the pilin domain's interaction with the LD allosterically regulates FimH binding. Therefore, all previous work strongly suggests that the pilin domain's interaction with the LD is required to stabilize the LD's conformation in the low-affinity state. This hypothesis would explain why all crystal structures of the isolated LD are in a high-affinity conformation and why using it as an antigen would cause antibodies that recognize and perhaps stabilize the high-affinity conformation.

Although the pilin domain is an effective allosteric regulator of FimH, other regions within the LD have been recently found to contribute to the allosteric pathway (Thomas, Trintchina et al. 2002; Thomas, Nilsson et al. 2004; Le Trong, Aprikian et al. 2010; Rodriguez, Kidd et al. 2012). Each region is also amenable to point mutations that cause whole fimbriae to exhibit a low-affinity phenotype and conformation (Rodriguez, Kidd et al. 2012). If the pilin domain of these variants was prevented from interacting with the LD, it is unknown what phenotype or conformation each would exhibit. If these low-affinity variants are capable of demonstrating a stable low-affinity state without the autoinhibitory pilin domain, they also may stabilize the isolated LD for use as a novel immunogen for antiadhesive therapy development. In this work, we chose to characterize double-cysteine mutant V27C-L34C located in the interdomain loops of FimH LD (Figure 17) because of these previous studies (Le Trong, Aprikian et al. 2010; Rodriguez, Kidd et al. 2012), the location and strength of the variant's disulfide bond, and its demonstrated ability to switch into a high-affinity state via reduction of the disulfide bond with dithiothreitol (DTT) (Le Trong, Aprikian et al. 2010).

Mutant V27C-L34C, or "locked-low", was investigated in various forms that physically altered the pilin domain's interaction with the LD in order to determine the LD's capacity to stabilize the low-affinity state of FimH. A special engineered variant that alters the lectin and pilin domain contacts, known as FocH (Sokurenko, Schembri et al. 2001; Aprikian, Tchesnokova et al. 2007), was used as the background strain for conformation-based MAb recognition and monomannosyl binding assay under native and non-native (meaning ligand and DTT in solution) conditions. We also investigated locked-low pili, without the altered pilin domain, interacting

with a mannose-coated cantilever tip while under the mechanical force of atomic force microscopy (AFM). Additionally, an isolated LD with the locked-low mutation was characterized for conformation-based MAb recognition and mannosyl binding under native and non-native conditions. All studies together revealed that each pilin-domain-independent form of V27C-L34C demonstrated a native low-affinity state activatable under non-native conditions such as the presence of ligand, DTT, and mechanical force. The results suggest the idea that interaction with the pilin domain is not required to stabilize the LD. Through the use of DTT to reduce its disulfide bond, we have also demonstrated the first isolated lectin domain to transform from a low-affinity to high-affinity state that will be useful in future catch-bond biophysics research. Most intriguing of all, the native low-affinity isolated LD may be exploited in future antiadhesive therapy development targeted at uropathogenic *E.coli*.

## Methods

*FocH background strain used for conformation ELISA and phenotypic binding assay*

Point mutations at residues 27 and 34 were introduced as previously described (Tchesnokova, Aprikian et al. 2008) into a FimH-FocH background previously described (Knudsen and Klemm 1998) and modified (Aprikian, Tchesnokova et al. 2007). Briefly, FocH consists of *E.coli* WT K12 background with aa 186-201 (YCAKSQNLGYYLSGTH) replaced by the amino acids of adhesin FocH (RCDQTQSVSYTLSGSV), which has 36% sequence identity and 80% homology with $FimH_{K12}$ (Knudsen and Klemm 1998; Sokurenko, Schembri et al. 2001; Aprikian, Tchesnokova et al. 2007). The replacement of amino acids in this portion of the pilin domain alters the interaction between the lectin and pilin domains, causing the LD of FocH pili to convert into the high-affinity conformation.

*Assessing the conformation of locked-low pili in the presence of MAb21 and MAb25*

Prior to executing the conformation-based ELISA, pili were purified according to a previously published protocol (Sokurenko, Chesnokova et al. 1997; Aprikian, Tchesnokova et al. 2007; Tchesnokova, Aprikian et al. 2008) with the resultant suspension in 1X PBS. A basic ELISA using mouse-monoclonal antibody 21 and 25 (MAb21 and MAb25, respectively) was performed on the purified pili. MAb21 and MAb25 (from PickCell Inc., Netherlands) are antibodies raised against *E.coli* K12 FimH-lectin domain (residues 1-160) and previously determined to recognize or induce the high-affinity state of K12 FimH, especially in the presence of ligand (Tchesnokova, Aprikian et al. 2008; Tchesnokova, Aprikian et al. 2011). Pili were immobilized at 0.4 mg/mL in

0.02 M $NaHCO_3$ buffer in wells of 96-well-flat-bottom plates at 37 °C for 1 hour. Comparative controls consisted of FocH (high-affinity with and without mannose). Free protein was rinsed off with 1X PBS twice and then quenched for 30 minutes in 0.2% BSA-PBS. MAb21 and MAb25 were added at 1:400 and 1:250 dilution, respectively, with and without 1% αMMP or 2 mM DTT in 0.2% BSA-PBS for 137 min. Free reagent was rinsed off 4 times with 1XPBS. Horseradish-peroxidase conjugated to goat-anti-mouse (HRP-GAM) antibodies at 1:3000 in 0.2% BSA-PBS were incubated on the plate for 1 hour at 37 °C and then rinsed off 6 times with 1XPBS. Bound HRP-GAM was visualized with the addition of 3,3' 5,5' – tetramethylbenzidine (TMB) peroxidase enzyme from an immunoassay substrate kit (Bio-Rad). Absorbance was read at 650 nm using Molecular Devices Emaxx microtiter plate reader.

*Assessing locked-low's phenotype using radioactive-based binding assay*

We performed static binding assays using radiolabeled *E.coli* on monomannosyl (1M) or trimannosyl (3M) coated surfaces as described previously (Sokurenko, Chesnokova et al. 1997; Sokurenko, Chesnokova et al. 1998; Sokurenko, Schembri et al. 2001). Briefly, *E.coli* expressing locked-low $FimH_{K12}$ with a FocH pilin domain were seeded in superbroth (SB) media containing radiolabel Thymidine ($^3H$, PerkinElmer Life Sciences Inc.) and the proper antibiotics. Bacteria were incubated overnight at 37 °C under static conditions. Next, the bacteria were spun down, rinsed twice with 1XPBS, and resuspended at $A_{540}$ 2 with or without 1 % methyl α-D-mannopyranoside (αMMP or mannose). Meanwhile, detachable 96-well plates were incubated with 100µL of 20 µg/mL 1M (yeast mannin, Sigma) and 3M (bovine Rnase B, Sigma) in 0.02M

$NaHCO_3$ buffer at 37 °C for 1 hour, blocked with 0.2 % BSA-PBS at 37 °C for 30 min, and aspirated. Wells with 0.2% BSA-PBS were included as a control substrate. The bacteria were then added to the coated plates and incubated for 45 min at 37 °C. Next, the plates were rinsed of unbound bacteria using 1XPBS, aspirated, dried at 65 °C for 15 min, broken into separate wells, and then placed in scintillation fluid. Radioactivity was measured for each sample (using Beckman LS 3801), done in triplicate, and the number of cells bound determined using calibration curves of known solution concentrations calculated with BIAevaluation software (GE Healthcare).

*Probing catch-bond formation of locked-low pili using atomic force microscopy (AFM)*

A previously published protocol was used with minor modifications (Yakovenko, Sharma et al. 2008). Briefly, 10-20 µg/mL purified pili in 0.02 M $NaHCO_3$ buffer were immobilized on 35 mm tissue culture dishes (Corning) for 75 min at 37 °C. After, the plates were gently rinsed with 0.2 % BSA-PBS three times and blocked in 1 mL 0.2% BSA-PBS at 4 °C until applied to the AFM set-up. Each sample plate was tested before and after the addition of 1 mM DTT. Positive control WT K12 and a negative control BSA-coated plate were also included. Olympus Biolever cantilevers were prepared by incubation in 200 µg/mL 1M-BSA for 75 min at 37 °C. After, the cantilevers were stored/blocked in 0.2% BSA-PBS in the refrigerator overnight prior to the experiment.

An Asylum MFP-3D AFM was used to examine the binding behavior of the immobilized pili. Prior to the experiment, the cantilever was initially calibrated to check on its spring constant

(varies between 4.38 and 7.17 pN/nm for various cantilevers). After, the tip would contact the surface and depending on the number of bonds formed, the dwell time would be adjusted (at 1 s, K12 is considered to saturate the tip with bonds). For the following experiment, a dwell of 0 s was used. Each sample plate underwent constant velocity pulls of 2 µm/s with the cantilever. Three spots were probed for all control plates with a BSA-coated plate as a negative control. For the locked-low sample, up to 9 spots were probed in order to collect enough data. This bias was accounted for using the appropriate statistics. Bond rupture forces were calculated using an automated program and defined as the difference between the peak tensile and average baseline force post rupture. Analysis of each pull used a costume-made "do-it" program in Igor Pro 5.05A. Further analysis of the population of rupture force was organized and analyzed using a custom-written Matlab script.

*Ld construct synthesis and purification*

Lectin domain (LD) construct synthesis and purification followed previously published methods (Schembri, Hasman et al. 2000; Bouckaert, Berglund et al. 2005) with minor modifications from (Aprikian, Tchesnokova et al. 2007). The original V27C-L34C plasmid synthesized in Le Trong et al. (Le Trong, Aprikian et al. 2010) with the same FimH allele encoded in *E.coli* J96 (all codons coding for 1-156 residues and signal peptide) was used here as the template plasmid for the PCR reaction and subsequent ligation into the Ndel-HindIII digested pET-22b. The expression of LD incorporated a $His_6$ at the c-terminal end.

*Assessing Locked-low LD's conformation in the presence of MAb21*

An ELISA protocol for antibody binding to immobilized locked-low LD was followed with slight modifications (Tchesnokova, Aprikian et al. 2008). A control LD was included and consisted of a purified LD isolate with a KB91 background and a $His_6$ at the c-terminal end. The background strain differs from locked-low's background strain in three amino acid residues at position 70, 78, and 27, but these were found *not* to cause the large differences in conformational changes observed in the low- vs. high-affinity structures (Le Trong, Aprikian et al. 2010) and possess functionally equivalent affinities towards mannosyl substrates (Bouckaert, Mackenzie et al. 2006; Aprikian, Tchesnokova et al. 2007). Briefly, 0.02 mg/mL of locked-low or control LD in 0.02 M $NaHCO_3$ buffer was immobilized in wells of a 96-well flat bottom plate for 1 hour at 37 °C. After rinsing the plate 2x in 1X PBS, the plate was blocked for 30 min with 0.2% BSA-PBS. MAb21 was added at a 1:800 final dilution in the absence and presence of α-MMP and/or DTT each at 1% and 1 mM in 0.2% BSA-PBS. A protein-concentration control of Tetra-His antibody at a 1:1,000 final dilution was also added to designated wells. The plates were incubated for 1 hour at 37 °C and washed 6x with 1XPBS. Next, the bound antibodies were probed with goat-anti-mouse antibody conjugated with HRP at 1:3,000 dilution in 0.2% BSA-PBS for 45 min at 37 °C. After washing 6x with 1X PBS, the reaction was visualized with the addition TMB peroxidase enzyme immunoassay substrate (Bio-Rad). Absorbance was read within several minutes at 650 nm using Molecular Devices Emaxx microtiter plate reader. All samples/conditions were run in duplicate.

*Assessing Locked-low LD's phenotype by binding to mannosylated substrates*

An ELISA assay using purified locked-low LD was performed on monomannosyl (1M) and trimannosyl (3M) coated surfaces in order to observe the isolated LD's predicted binding behavior versus control LD. The control LD was also the same used during the LD ELISA assay previously described. Briefly, 96-well plates were allowed to incubate with 100µL of 20 µg/mL 1M (yeast mannin, Sigma) or 3M (bovine Rnase B, Sigma) in 0.02M $NaHCO_3$ buffer at 37 °C for 1 hour, rinsed twice with 1X PBS, then blocked with 0.2 % BSA-PBS at 37 °C for 30 min, and tapped to remove any spare solution. LD samples were applied to the 1M or 3M substrate at 0.02 mg/mL in the presence and absence of α-methyl-D-mannopyranoside (α-MMP) and/or dithiothreitol (DTT) in 0.2% BSA-PBS. The solutions were incubated 1 hour at 37 °C. After, the plates were rinsed of unbound LD 3x with 1X PBS and bound LD was probed using 1:1,000 dilution of anti-His·Tag® mouse-monoclonal antibody (Tetra-His antibody by Qiagen) in 0.2% BSA-PBS for 1 hour at 37 °C. Unbound antibody was rinsed off 4x with 1X PBS and the Tetra-His antibody was probed with goat-anti-mouse antibody conjugated with horseradish peroxidase (HRP) at 1:3,000 dilution in 0.2% BSA-PBS for 45 min at 37 °C. Unbound antibody was rinsed off 6x with 1X PBS and the reaction was visualized with the addition of 3,3' 5,5' – tetramethylbenzidine (TMB) peroxidase enzyme immunoassay substrate (Bio-Rad). Absorbance was read within several minutes at 650 nm using Molecular Devices Emaxx microtiter plate reader. All samples were performed in duplicate.

## Results

*The native locked-low's pilin domain is not required to maintain the low-affinity state*

In this work, FimH mutant V27C-L34C was characterized in various forms that physically altered the pilin domain's interaction with the lectin domain (LD) in order to determine its capacity to stabilize the low-affinity state of FimH LD without the autoinhibitory pilin domain. This "locked-low" mutant is low-affinity and may be unlocked to increase its binding for ligand mannose in the presence of reducing agent dithiothreitol (DTT) (Le Trong, Aprikian et al. 2010). Throughout this work, DTT was used to sever the disulfide bond and assess changes in conformation or phenotype attributed to the bond's presence. In order to determine conformation, we performed an ELISA using conformation-specific MAb21 and MAb25 on immobilized pili in native and non-native (ligand and DTT in solution) conditions (Figure 18). MAb21 and MAb25 are well documented ligand-inducing binding site (LIBS) antibodies that each recognizes different non-linear epitopes of the high-affinity LD of FimH (Tchesnokova, Aprikian et al. 2008; Tchesnokova, Aprikian et al. 2011) (Figure 17). Like LIBS epitopes in integrins (Hynes 1987; Frelinger, Du et al. 1991; Mould, Travis et al. 2005), the interaction is allosteric and reciprocal. Briefly, the binding of FimH to mannose activates a conformational shift or epitope exposure both MAbs are capable of recognizing and the ability of MAbs to recognize and bind the particular conformation enhances the binding of FimH to mannose. Throughout all studies herein, the background strain of pilin domain used is distinguished by the use of wildtype (WT) "WT" or "FocH". FocH consists of *E.coli* WT K12 background with aa 186-201 (YCAKSQNLGYYLSGTH) replaced by the amino acids of adhesin FocH (RCDQTQSVSYTLSGSV),

which has 36% sequence identity and 80% homology with $FimH_{K12}$ (Knudsen and Klemm 1998; Sokurenko, Schembri et al. 2001; Aprikian, Tchesnokova et al. 2007). The replacement of amino acids in this portion of the pilin domain alters the interaction between the lectin and pilin domains, causing the LD of FocH pili to convert into the high-affinity conformation and is therefore strongly recognized by MAb21 (Figure 18A) and MAb25 (Figure 18B) even in the absence of ligand (Tchesnokova, Aprikian et al. 2008).

Conversely, locked-low pili with a FocH pilin domain are not recognized by MAb21 or MAb25 in the absence of ligand and indicate a native low-affinity conformation near the interdomain region and near the binding pocket, respectively. MAb21 exclusively recognizes locked-low pili in the presence of DTT, in which the locked-low pili demonstrate a high-affinity conformation similar to FocH pili. MAb 25 recognizes locked-low pili in the presence of ligand or DTT. This result indicates that under non-native conditions, such as the presence of ligand, the conformation of FimH near the binding pocket converts to the high-affinity. Therefore, the disulfide bond located near the interdomain region of FimH is tightly coupled to the conformation of its home region and is moderately coupled to the conformation of a distant region near the binding pocket.

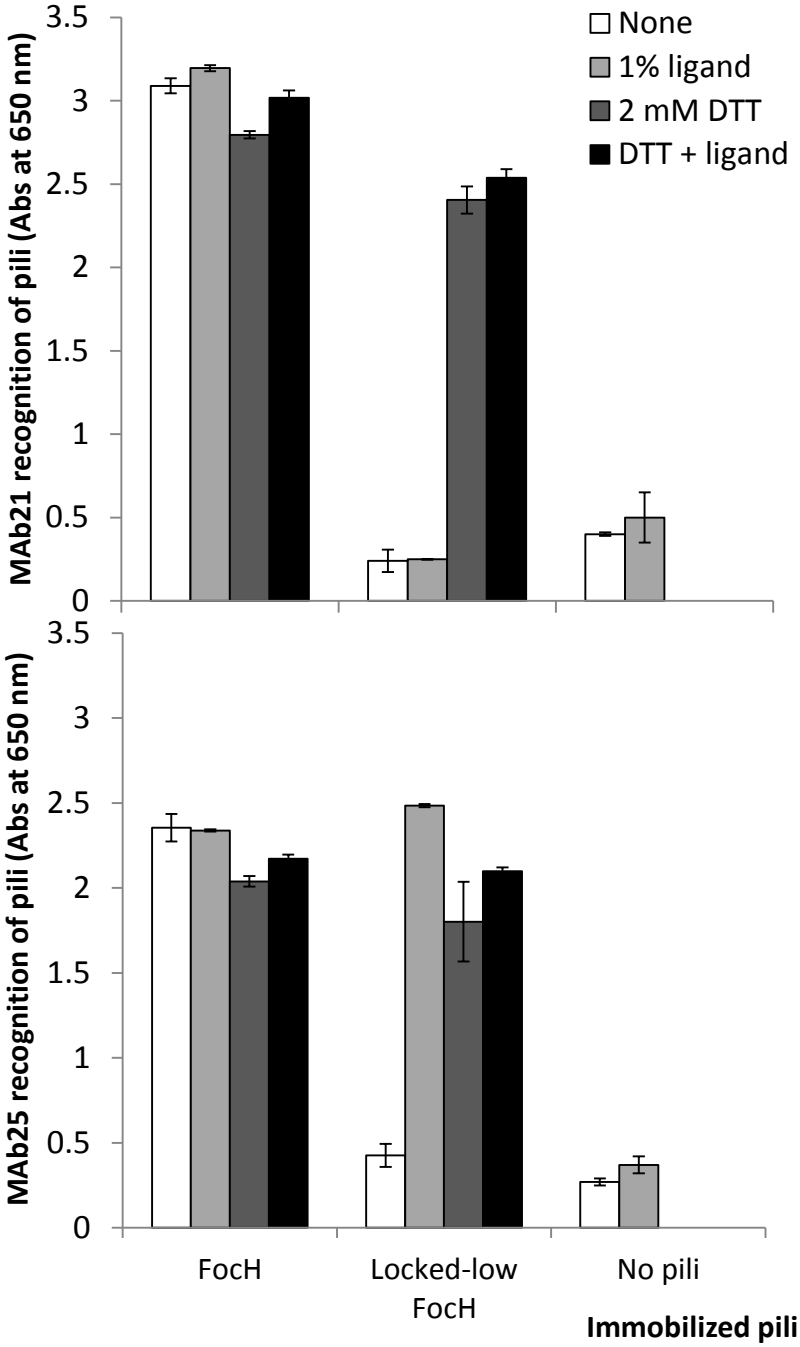
None
1% ligand
2 mM DTT
DTT + ligand
MAb21 recognition of pili (Abs at 650 nm)
MAb25 recognition of pili (Abs at 650 nm)
3.5
3
2.5
2
1.5
1
0.5
0
FocH
Locked-low FocH
No pili
Immobilized pili

[redacted]

Phenotype was determined by measuring the binding of radiolabeled whole-cell *E.coli* to a monomannosyl (1M) surface with our without DTT (Figure 19). *E.coli* containing the locked-low mutation with a FocH pilin domain bound 1M with low-affinity in the absence of DTT and high-affinity in the presence of DTT. For comparison, WT *E.coli* was also included as an example of a low-affinity interaction with 1M and reveals that in the absence of DTT, locked-low *E.coli* are lower binders than WT ($p < 0.05$). Together, the phenotype and conformation results suggest that when the pilin domain's interaction with the LD is altered, the locked-low mutation is capable of stabilizing the low-affinity conformation of FimH enough to maintain a low-affinity phenotype.

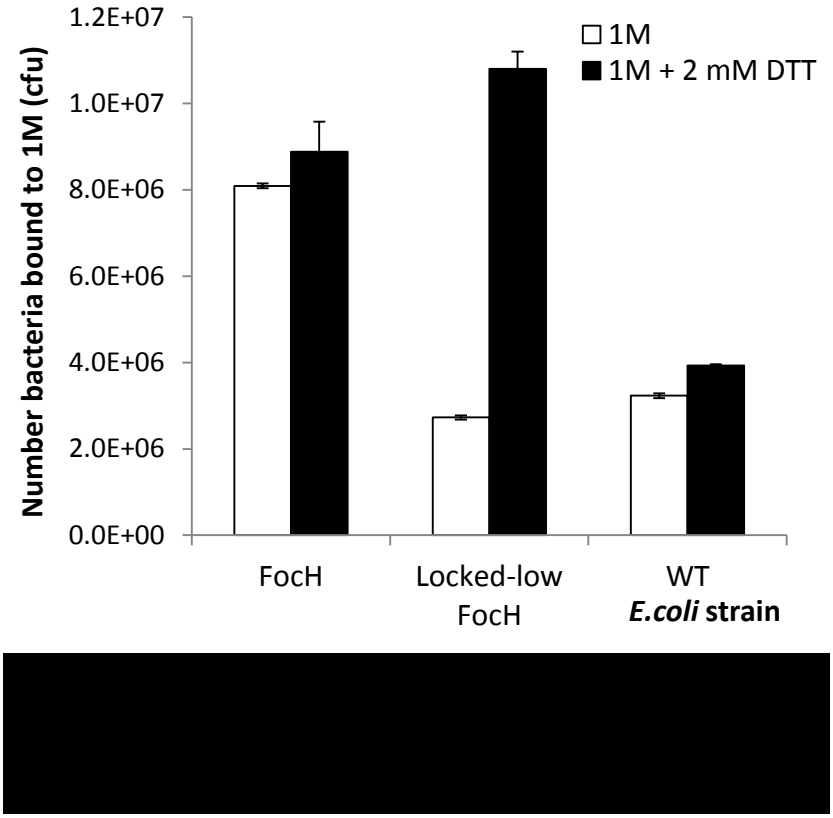


*Under mechanical force, locked-low shifts to a destabilized high-affinity state*

AFM was used to probe for catch-bond formation of locked-low pili, containing a WT pilin domain, while contacting mannose-BSA (1M-BSA) under high-force conditions (Figure 20). AFM

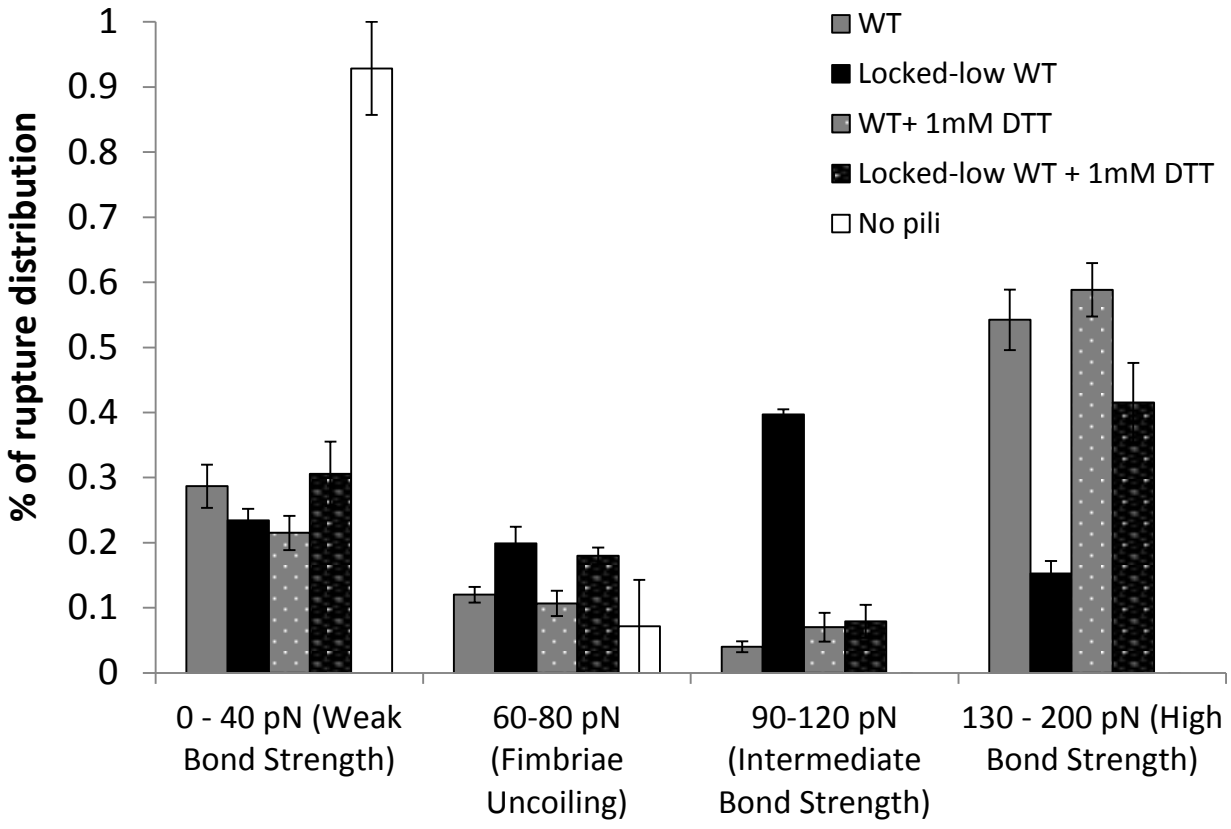


[redacted]

uses an extreme condition of force to explore the biomechanics not necessarily revealed under native conditions. By interacting with ligand on the AFM cantilever tip's surface, it is hypothesized that the pilin domain physically pulls away from the LD and allows for any high-affinity interactions to be recorded on the pN scale. Once all rounds of testing were completed on control WT and locked-low pili, DTT was added to investigate any changes in the force of each rupture.

DTT diminished the frequency of rupture (# ruptures/ # pulls) for all pili tested (data not shown) and is most likely due to the severing of the C3-C44 bond in the binding pocket as previously suggested (Nilsson, Yakovenko et al. 2007).Nevertheless, DTT did not affect the strength of ruptures for control pili, which maintained the majority of ruptures at high bond strength (130-200 pN) indicative of catch-bond formation (Yakovenko, Sharma et al. 2008). Without DTT, locked-low pili demonstrate significantly fewer high bond strength ruptures (15 %) to WT pili (54 %). Interestingly, 40 % of locked-low's ruptures were at a far lower strength (90-120 pN) that we consider to be destabilized catch-bonds termed "intermediate bond strength". For comparison, WT pili only showed 4 % within this regime. When the unlocking agent DTT is added to the locked-low pili, it allowed ruptures in this regime to disappear (8 %) and reappear (42 %) at high bond strength.

Through the use of mechanical force, AFM clearly distinguished two different high-affinity conformations when locked-low's disulfide bond is present: a novel intermediate bond strength and the well characterized high bond strength (Yakovenko, Sharma et al. 2008). Like the MAb data, the AFM data suggests that although the high-affinity state is perhaps short lived, it dictates that the FimH structure likely cannot withstand certain non-native conditions such as outside mechanical force. *

** For additional mechanical studies, please see Appendix B for preliminary flow-chamber experiments performed on several low-affinity variants, including the locked-low variant.*

*Isolated LD with locked-low mutation is in low-affinity state and only switches to high-affinity when DTT is present*

A plasmid (with $His_6$) for the isolated LD construct was successfully mutated with cysteines at residue 27 and 34, transformed, and purified (data not shown). The conformation of nonspecifically immobilized locked-low LD was assessed in an ELISA via recognition by MAb21 in the presence and absence of ligand and/or DTT (Figure 21). Control LD was recognized by MAb21 no matter the condition. Similar to the conformation ELISA performed on locked-low pili, recognition of locked-low LD by MAb21 occurred exclusively in the presence of DTT. The result confirms the native conformational state of locked-low LD as low-affinity in addition to demonstrating that it is not misfolded and may be induced to switch to a high-affinity conformation via the addition of DTT.

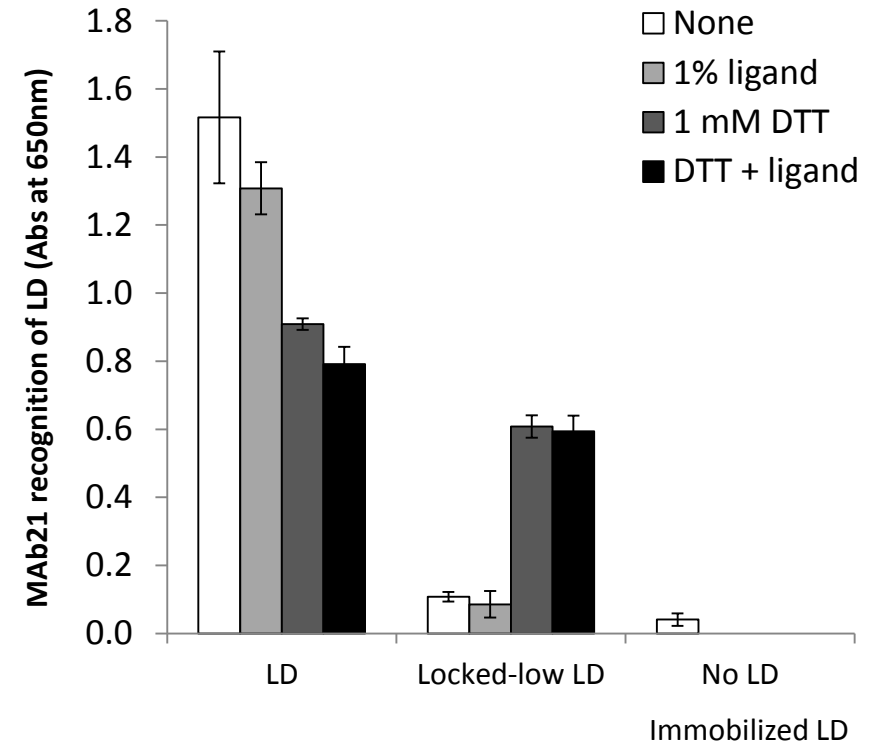

Locked-low LD's phenotype was examined by measuring its binding to 1M and a trimannosyl substrate (3M) with and without DTT (Figure 22). The presence of LD on the surface was measured using its $His_6$ tag. Control LD bound 1M and 3M irrespective of condition. Conversely, locked-low LD did not bind to the 1M surface in the absence of DTT. However, it did show affinity for the 3M surface as was observed previously in whole cell *E.coli* (Rodriguez, Kidd et al. 2012). DTT caused a dramatic and significant increase of binding for locked-low LD to 1M and 3M. It may be proposed that by adding DTT, the cysteine bond between residues 27 and 34 is severed and allows locked-low LD to bind 1M and enhance its affinity for 3M.

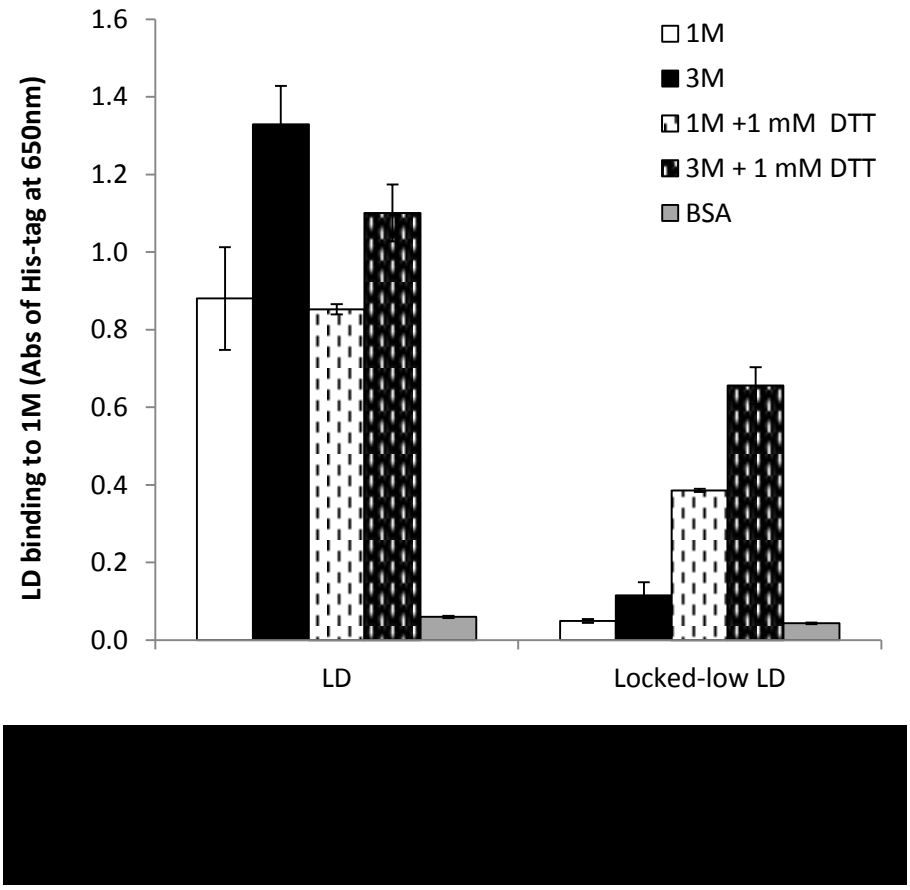


To our knowledge, this is the first time an isolated lectin domain has ever been recorded to demonstrate a low-affinity conformation and phenotype. Through the use of DTT to reduce its disulfide bond, we have also demonstrated the first isolated lectin domain to transform from a low-affinity to high-affinity state. These results also indicate that a native low-

affinity LD is possible both in structure and function without the autoinhibitory pilin domain, a result that may be exploited in future antiadhesive therapy development.

## Discussion

In this work, a previously described mutation V27C-L34C (Le Trong, Aprikian et al. 2010; Rodriguez, Kidd et al. 2012) of the adhesin FimH was characterized in new forms that physically altered the pilin domain's interaction with the LD in order to assess the LD's ability to independently sustain a low-affinity state. This "locked-low" mutant is low-affinity and may be unlocked to increase its binding for ligand mannose in the presence of reducing agent DTT (Le Trong, Aprikian et al. 2010). Previous work investigating the isolated LD crystal structure (Choudhury, Thompson et al. 1999; Hung, Bouckaert et al. 2002; Bouckaert, Berglund et al. 2005; Wellens, Garofalo et al. 2008) and phenotype (Aprikian, Tchesnokova et al. 2007) of various strains have all exhibited a high-affinity state. Under native conditions (without ligand and DTT in solution), our investigation discovered that locked-low pili containing an altered pilin domain, FocH, were unrecognized by high-affinity-binding MAbs and weakly bound to 1M substrate. Under the same conditions, an isolated LD with the locked-low mutation was also unrecognized by high-affinity binding MAb21 and bound 1M and 3M with low-affinity. Our study strongly suggests that the interaction with the pilin domain is not required to stabilize a low-affinity state.

Although the native conformation exhibits a low-affinity state, locked-low pili exhibited partial activation under non-native conditions as demonstrated by MAb25 recognition in the presence of ligand or intermediate bond strength in the presence of mechanical force. In addition to being a LIBS antibody that binds the high-affinity conformation (Tchesnokova, Aprikian et al. 2011), MAb25 is located near the binding pocket and far away from the mutation near the

FimH interdomain region, which happens to be proximal to the MAb21 epitope (Figure 17). While MAb21 did not recognize the conformation in the presence of ligand, MAb25 was able to bind and thereby indicate a high-affinity conformation. Based on previous work (Le Trong, Aprikian et al. 2010; Rodriguez, Kidd et al. 2012) and our data that DTT facilitates MAb21 to recognize the high-affinity conformation of both locked-low pili and locked-low isolated LD, it may be ruled out that MAb21's epitope is disrupted by the mutation. Irrespective of partial activation near the binding pocket, our data indicate that locked-low pili clearly demonstrated an overall low-affinity phenotype. It may be concluded that although the conformation near the binding pocket is high-affinity, the conformation of the interdomain region is perhaps what dictates the phenotype of FimH.

Partial activation was also demonstrated using AFM to probe locked-low pili (containing a WT pilin domain) interacting with 1M-BSA. Although the % of high-bond-strength ruptures (15 %) is significantly less than control WT pili (54 %), it is still evidence of previously defined high-affinity interactions (Yakovenko, Sharma et al. 2008). The locked-low pili also showed 40 % of ruptures within 90-120 pN and distinguished a separate regime we consider to be intermediate bond strength. This data suggests that although the high-affinity state is perhaps short lived, the evidence of intermediate and high bond strength ruptures dictates the FimH structure likely cannot withstand certain amounts of outside mechanical force. Combining the partial activation evidence from the MAb and AFM studies, the MAb studies indicate that removal of the pilin domain does not facilitate a shift into the high-affinity state, rather mechanical activation does.

The strength of binding under mechanical force supports the use of the locked-low FimH for further biophysical characterization in various forms, in particular the study of the locked-low isolated LD. Indeed, this is the first documented isolated LD that switches from the low-affinity to high-affinity state via reduction of its disulfide bond. Utilizing this clever attribute not only allowed us to confirm the novel isolated LD is functional rather than a misfolded protein, but opens up new research to characterize FimH biophysical properties. Specifically, the isolated lectin domain is the portion of FimH that is responsible for adhesion and now may be studied without interference from other parts of the fimbriae that provide their own biomechanical properties to *E.coli* adhesion (Forero, Yakovenko et al. 2006; Whitfield, Ghose et al. 2010; Aprikian, Interlandi et al. 2011; Whitfield and Thomas 2011). As an additional bonus, it has already been synthesized within a well-studied plasmid construct and may be efficiently purified in high quantities. In conclusion, the novel protein therefore offers itself as an accessible and relevant tool to further our knowledge of FimH catch-bond biophysics and allostery.

This is the first documentation of an isolated FimH LD exhibiting a low-affinity conformation and phenotype that will be useful in future development of antiadhesive therapies targeted at uropathogenic *E.coli*. Prior to this work, antibodies raised against the isolated LD (Langermann, Palaszynski et al. 1997; Tchesnokova, Aprikian et al. 2011) exhibited bias towards high-affinity epitopes and allosterically enhanced FimH adhesion (Tchesnokova, Aprikian et al. 2011), which may be explained by the innate high-affinity conformation of the isolated LD. The same hypothesis may be why successful studies of animal models immunized with FimH protein have

not produced an FDA approved vaccine over a decade post publication (Langermann, Palaszynski et al. 1997; Langermann, Mollby et al. 2000). The FimH protein used during immunization was complexed with chaperone protein FimC (Langermann, Palaszynski et al. 1997; Langermann, Mollby et al. 2000) or was a derived natural truncate (Jones, Pinkner et al. 1995), FimHt, purified away from a complex of proteins in the fimbrial tip (includes FimH, FimC, FimF, and FimG) (Langermann, Palaszynski et al. 1997). The crystal structure of FimH-FimC has been documented in the high-affinity state (Choudhury, Thompson et al. 1999), while FimHt's structure is still unknown. Regardless of the exact cause for the lack of a vaccine on the market, the novel isolated LD reported here has the potential of expanding the library of antibodies produced during immunization due to exposure of inherently different epitopes. And based off our knowledge of the past attempts with a vaccine, the implementation of the novel isolated LD may be expanded to include seeking effective epitopes for allosteric inhibitors or applications in passive immunity with this protein acting as immunogen. Fortunately, partial activation during immunization research is not of concern due to the low concentration of mannose in human serum (~41-55 μM)(Etchison and Freeze 1997; Alton, Hasilik et al. 1998; Sone, Shimano et al. 2003) and animal serum (~75 μM)(Alton, Hasilik et al. 1998) versus the high concentration (111,000 μM) used in our studies. Furthermore, the immunogen is not anchored to allow for the mechanical activation observed in AFM. Overall, the novel isolated LD provides an alternative approach in antiadhesive research that increases the likelihood of overcoming current issues faced in preventing adhesion of uropathogenic *E.coli*.

# Chapter V Monoclonal antibodies raised against low-affinity FimH lectin domain prevent *E.coli* adhesion to urothelial cells *in vitro*

**Victoria B. Rodriguez[1], Dagmara Kisiela[2], Veronika Tchesnokova[2], Evgeni V. Sokurenko[2], Wendy E. Thomas[1]**

[1]Department of Bioengineering, Box 355061; [2]Department of Microbiology, Box 357242; University of Washington, Seattle, WA 98195, USA.

**Acknowledgements**

We greatly appreciate our collaboration with contract research organization, Covance Inc. (Denver, PA), for custom polyclonal and monoclonal antibody production. Dr. Dagmara Kisiela and Dr. Veronika Tchesnokova provided tremendous advice during experimental procedures. Dr. Dagmara Kisiela also executed several experiments using the antibodies Covance Inc., produced and is acknowledged within the text.

Support for this work comes from the NIH grant 1RO1 AI50940, NSF grant CBET-1132860, NIH-funded Molecular Biophysics Training Grant 1RO1 AI50940 at the UW (VBR). The funders had no role in study design, data collection and analysis, decision to publish, or preparation of the manuscript.

**Publications**

This is a working manuscript and will be submitted for publication.

## Abstract

Expressed by most commensal and uropathogenic *Escherichia coli* (*E.coli*), the protein FimH mediates adhesion to ligand mannose exposed on a variety of cell types and has become a significant antigen for antiadhesive therapies targeted at urinary tract infections (UTIs). Previous work strongly suggests that the FimH ligand-binding lectin domain (LD) exists in the high-affinity conformation as opposed to its other, low-affinity conformation, which may explain why antibodies raised against the isolated LD bias the high-affinity state and enhance FimH adhesion. In this study, 5 mice were immunized against a recently-synthesized novel low-affinity LD and the majority of mice indicated average or greater titers against the immunogen. One mouse was selected for monoclonal antibody (MAb) development and created 55 MAbs that positively recognized the immunogen. Of these 55 MAbs, MAb10 and MAb926 significantly reduced the adhesion of both wildtype K12- and high-affinity A188D-expressing *E.coli* to a monomannosyl surface ($p < 0.05$). Additionally, both MAbs significantly reduced the adhesion of wildtype K12-expressing *E.coli* to urothelial cells *in vitro* ( $p < 0.05$) and partially inhibited the adhesion of *E.coli* expressing high-affinity A188D ($0.1 < p < 0.5$). The results of this work support our hypothesis of alternative antiadhesive therapies targeted at the prevention of UTI causing *E.coli*.

## Introduction

Expressed by most commensal and uropathogenic *Escherichia coli* (*E.coli*), the protein FimH mediates adhesion and forms receptor-ligand bonds with terminal mannosyl residues on a variety of cell types (Sokurenko, Chesnokova et al. 1997). Due to increasing numbers of antimicrobial-drug-resistant *E.coli* (Karlowsky, Kelly et al. 2002; Zhanel, Hisanaga et al. 2005; Schito, Naber et al. 2009), FimH has become a significant antigen for antiadhesive therapies such as vaccines. Despite successful FimH vaccine studies in animal models (Langermann, Palaszynski et al. 1997; Langermann, Mollby et al. 2000), there still remains a lack of an FDA approved vaccine on the market. One possible explanation is that the development of a vaccine is effected by the conformation of the original antigen used during immunization. FimH is composed of a mannose-binding or lectin domain (LD) and a fimbrial-anchoring pilin domain that combine to form two significantly different conformations with different affinities: a low and a high-affinity state (Aprikian, Tchesnokova et al. 2007; Tchesnokova, Aprikian et al. 2008; Le Trong, Aprikian et al. 2010) (Figure 12). The likely immunogen is the adhesive unit or isolated LD, which demonstrates a high-affinity conformation for all published crystal structures (Choudhury, Thompson et al. 1999; Hung, Bouckaert et al. 2002; Bouckaert, Berglund et al. 2005; Wellens, Garofalo et al. 2008). Due to this preferred structure of the isolated LD, antibodies raised against it are biased solely to epitopes of the high-affinity state, are able to *enhance* FimH adhesion, and may easily be shed if the low-affinity conformation is favored (Tchesnokova, Aprikian et al. 2011). Perhaps antibodies raised against a novel low-affinity FimH LD may inhibit bacterial adhesion by binding and stabilizing the low-affinity state. We

hypothesize that the investigation of a “locked” low-affinity FimH LD is an alternative strategy for antiadhesive therapies and will foster more informed research in the prevention of uropathogenic *E.coli* infections.

FimH responds to tensile mechanical force by allosterically switching from a low- to high-affinity state for its ligand (Le Trong, Aprikian et al. 2010) and it is this allosteric pathway that has been harnessed previously to produce 4 candidate low-affinity variants, each representing 1 of 4 regions that contribute to the allosteric pathway (Rodriguez, Kidd et al. 2012). The isolated LD of one of these variants, V27C-L34C or “locked-low”, demonstrated both a low-affinity conformation (Figure 21) and phenotype (Figure 22) (Rodriguez 2012). It has yet to be determined whether this novel protein is capable of producing antibodies in an animal model. As long as it maintains its conformation *in vivo*, we hypothesize that antibodies raised against the isolated “locked-low” LD will bind and stabilize the low-affinity state of FimH thereby preventing *E.coli* adhesion.

In this study, a previously described novel LD isolate (Rodriguez 2012) with low-affinity conformation and phenotype was used as an immunogen in order to develop polyclonal and monoclonal antibodies targeted at the adhesin FimH of *E.coli*. Five mice were immunized against the locked-low LD and 3 of the 5 indicated average or greater titers against the immunogen. With its sufficient titer, recognition of native pili, and no cross-reactivity to the immunogen’s His·Tag®, mouse WA 616 was selected for MAb development and created a panel of 55 MAbs that positively recognized the immunogen. Of these 55 MAbs, MAb10 and MAb926

significantly reduced the adhesion of both WT K12 and high-affinity A188D expressing *E.coli* to a monomannosyl surface ($p < 0.05$). Additionally, both MAbs significantly reduced the adhesion of *E.coli* expressing WT FimH to urothelial cells *in vitro* ( $p < 0.05$) and partially inhibited the adhesion of *E.coli* expressing high-affinity A188D ($0.1 < p < 0.5$). The results of this work support our hypothesis of alternative antiadhesive therapies targeted at the prevention of uropathogenic *E.coli*.

## Methods

*Mutant Ld purification for immunization*

Lectin domain (LD) construct synthesis and purification followed previously published methods (Schembri, Hasman et al. 2000; Bouckaert, Berglund et al. 2005) with minor modifications from (Aprikian, Tchesnokova et al. 2007). The original V27C-L34C or "locked-low" plasmid synthesized in Le Trong et al. (Le Trong, Aprikian et al. 2010) with the same FimH allele encoded in *E.coli* J96 (all codons coding for 1-156 residues and signal peptide) was used here as the template plasmid for the PCR reaction and subsequent ligation into the NdeI-HindIII digested pET-22b. The expression of LD incorporated a $His_6$ at the c-terminal end. An SDS-PAGE was run vs. standard protein ladder (PageRulerTM Prestained Protein Ladder SM0671) to check the size/purity and the protein concentration was checked with a Coomassie Plus™ Protein Assay kit.

*Mouse immunization with immunogen LD for polyclonal and monoclonal antibody development*

Immunization was contracted out to Covance Inc. at their animal facility in Denver, Pennsylvania. After a total of 2.15 mgs of pure V27C-L34C LD, or immunogen, was shipped to the facility, a 3-month-long procedure followed that consisted of immunization, booster immunization, polyclonal sera collection, and care of 5 mice (see Appendix C for Covance Inc., "Master Schedule List" detailing their procedures). Polyclonal antiserum was collected from each of the 5 mice and 1 mouse was selected to undergo monoclonal development based off the results of an enzyme-linked immunosorbent assay (ELISA) indicating the mouse with the

strongest recognition for the immunogen (performed by Covance Inc.) and fimbrial incorporated immunogen (performed by our laboratory) without cross-reactivity from the His·Tag® (performed by our laboratory). The selected mouse underwent one last booster immunization several days prior to euthanization. The spleen was then collected from the mouse and *in vitro* hybridoma development followed Covance Inc. protocol. For a detailed methodology of this entire process please see Appendix D.

*Fimbriae purification*

For all assays described that included the use of fimbriae or "pili", purification of fimbriae followed a previous protocol (Tchesnokova, Aprikian et al. 2008) with the resultant suspension in 1x PBS.

*Recognition of immunogen fimbriae by 55 MAbs*

A basic ELISA with all 55 MAb supernatants provided by Covance Inc. was performed. Fimbriae containing the immunogen (locked-low LD) used for antibody development were immobilized in wells of the 96-well plates in the interest of carrying on MAbs that had a positive reactivity to the immunogen's native form.

Briefly, fimbriae were immobilized at 0.02 mg/mL in 0.02 M $NaHCO_3$ buffer in wells of 96-well flat bottom plates overnight at 4 °C. The plates were then rinsed of free fimbriae 2x with 1X PBS and blocked with 0.2% BSA-PBS at 37 °C for 30 min. Following these steps, 55 MAb supernatants were mixed at 1:150 dilution with or without 1% αMMP. The mixtures were incubated 1.5 hrs at 37 °C. After the incubation, the wells were rinsed 4x with 1X PBS and HRP-

conjugated goat-anti-mouse antibodies were added at 1:3000 in 0.2% BSA-PBS followed by an incubation of 45 min at 37 °C. Free antibodies were then rinsed off 6x in 1X PBS and the reaction was visualized with the addition of TMB peroxidase enzyme immunoassay substrate (Bio-Rad). A negative control consisted of 0.2% BSA coated wells and a positive control consisted of the use of rabbit-anti-pilin-domain antibodies (α-PD PAbs) in place of the MAb supernatants (goat-anti-rabbit-HRP was required to probe for these wells instead of the goat-anti-mouse-HRP). All samples were performed in duplicate in the interest of conserving time and reagents. Absorbance was read a few minutes later at 650 nm using Molecular Devices Emaxx microtiter plate reader.

*Recognition of WT and immunogen fimbriae by the selected 10 of 55 MAbs*

From the assay just described, 10 of the 55 clones were selected to be carried on to an in-depth ELISA on WT K12 fimbriae and immunogen fimbriae. The ELISA followed the previous protocol with the exception of increasing the MAb final dilution to 1:100.

*Inhibition of fimbrial binding to HRP in the presence of MAbs*

*Dr. Dagmara Kisiela performed this experiment with advisement from Dr. Veronika Tchesnokova and me.* A previous protocol for testing of HRP-inhibited binding to fimbriae in the presence of the selected 10 monoclonal antibodies was followed with several modifications (Tchesnokova, Aprikian et al. 2008). Briefly, WT K12 and high-affinity FocH fimbriae were immobilized at 0.3 mg/mL on 96-well plates in 0.02 M $NaHCO_3$ buffer at 37 °C for 1 hour, rinsed 2x in 1 XPBS, then blocked with 0.2 % BSA at 37 °C for 15 min. Monoclonal antibodies were then incubated at 50

µL at varying concentrations (1:10, 1:20, 1:40, etc.) for 1 hour at 37 °C prior to the addition of 50 µL of HRP at 100 µg/mL (final concentration) and a final 1 hour incubation at 37 °C. Controls consisted of immobilized fimbriae with no antibodies and immobilized fimbriae in contact with MAb21 at varying concentrations. Mouse WA PAb 616 sera was included in a separate experiment. Once the HRP incubation had taken place, free HRP was rinsed off 6x with 1X PBS. The reaction was visualized using TMB peroxidase enzyme immunoassay substrate (Bio-Rad). Absorbance was read a few minutes later at 650 nm using Molecular Devices Emaxx microtiter plate reader. All samples were done in singles to conserve the MAb sera.

*Inhibition of* E.coli *adhesion to monomannosyl surface in presence of MAb10 & MAb926*

An assay testing the binding of K12 background strains (WT and A188D) to a monomannosylated (1M) surface was performed using 2 particular MAbs (10 and 926) selected from the previous assay. Briefly, *E.coli* containing the respective FimH background was seeded in superbroth (SB) media and incubated overnight at 37 °C under static conditions. All bacteria were seeded with the proper antibiotic(s). The following morning, wells of 96-well flat bottom plates were incubated with 100µL of 20 µg/mL 1M (yeast mannin, Sigma) in 0.02 M $NaHCO_3$ buffer at 37 °C for 1 hour, rinsed 2x with 1X PBS, then blocked with 0.2 % BSA at 37 °C for 15 min. The bacteria were spun down, rinsed once with 1X PBS, and resuspended at $A_{540}$ OD 4 along with MAbs at 1:20 or PAb WA 616 at 1:800. The bacteria and antibody mixture was then pre-incubated at 37 °C for 1 hour prior to adding 50 µL of the mixture to wells with either 50 µL 0.2 % BSA or 50 µL 2% αMMP. All the bacteria at the various conditions were allowed to incubate for 45 min at 37 °C. Finally, the plates were rinsed of unbound bacteria 6x in 1X PBS

and dried at 60 °C for 15 min. Crystal violet was then added at 0.1% for 10 min at room temperature and then rinsed with water 3 times. To visualize bound bacteria, 100 µL of 50% EtOH was added and the absorbance measured at 600 nm on a Molecular Devices Emaxx microtiter plate reader. Controls consisted of no antibodies (Abs) + *E.coli,* no Abs, and no *E.coli* (BSA). All experimental samples were performed in triplicate.

*Inhibition of* E.coli *adhesion to urothelial cells* in vitro *& in presence of MAb10 & MAb926*

*Dr. Dagmara Kisiela and I performed this assay together. In vitro* cell culture assay used a previously established protocol by Kisiela et al., with minor modifications (Kisiela, Kramer et al.). In summary, T24 cells were seeded in wells of 96-well flat bottom plates (Cellstar) with culture media (McCoy, 10 FBS, Pen/Strep) and allowed to reach 100% confluence over a 2 day period at 37 °C, 5 % $CO_2$. On the day prior to the assay, *E.coli* (WT K12 and A188D with K12 background) were seeded in SB media and incubated overnight at 37 °C under static conditions. All bacteria were seeded with the proper antibiotic(s). The following morning, the bacteria were spun down, rinsed once with culture media, OD measured at $A_{540}$, and resuspended at $10^8$ cells/mL. The bacteria were then pre-incubated for 1 hour at 37 °C with MAbs at a final concentration of 1:20 in culture media. The bacteria were then added to the confluent T24 monolayers at a final concentration of 2.5 X $10^6$ cells/well in the presence and absence of 1% αMMP. The bacteria then incubated with the T24 cells for 1 hour at 37 °C, 5% $CO_2$. The T24 monolayers were next rinsed 5-6 x with culture media and the T24 cells were lysed with 0.5% Triton X-100 for 10 min at room temperature. The lysed media underwent serial dilutions followed by seeding on LB plates and then an overnight incubation at 37 °C. Adherent bacteria

were quantified by counting the number of colonies formed during the incubation period. All samples were performed in triplicate.

## Results

*Immunogen purification successful*

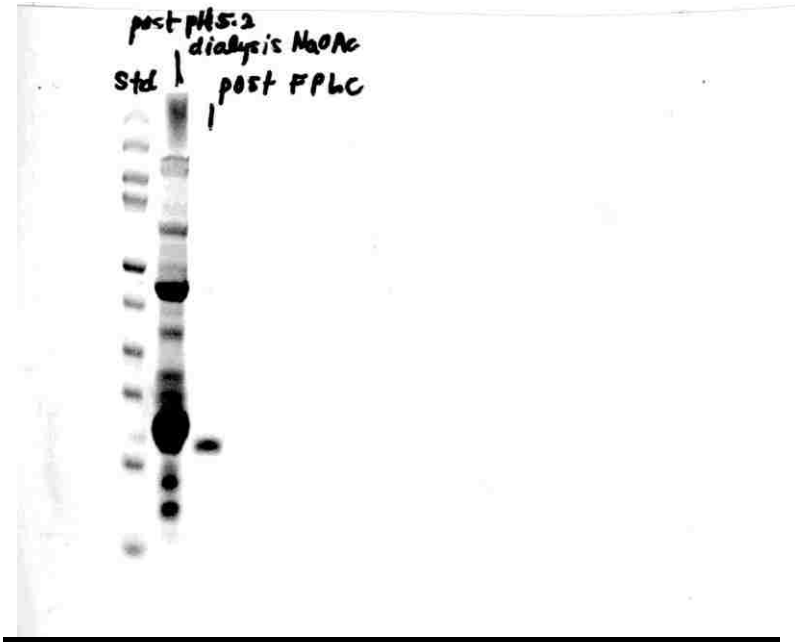


Protein purification was carried out in 4 separate rounds to ensure a high concentration for immunization. The final step of fast protein liquid chromatography (FPLC) to enhance the purity of the locked-low isolated LD, or immunogen, was successful as indicated by the SDS-PAGE (Figure 23). The collective concentration was at 1.72 mg/mL (data not shown). A volume of 1.25 mL (2.15 mg total) was packed on ice and shipped overnight to Covance Inc.

*The majority of mice were successfully immunized to produce polyclonal antibodies, 1 mouse chosen for monoclonal antibody (MAb) production*

Covance Inc. completed the scheduled immunization of five mice (WA 616-620) over the course of several months (December 2011 – February 2012). Covance Inc. indicated a low response of PAb titers for WA 618 and WA 619, an average response for WA 616 and 620, and a high response for WA 617 (data not shown). Based off of these results, WA 618 and WA 619 were

thrown out of consideration for MAb development. In several ELISAs performed at the University of Washington, WA 616 demonstrated the highest recognition of immunogen pili overall without any indication of cross-reactivity to His·Tag® (data not shown). Mouse WA 616 was therefore selected for monoclonal antibody development.

Covance Inc. completed fusion of mouse WA 616 spleen cells with myeloma cells to produce a hybridoma (immortal) cell-line capable of producing monoclonal antibodies each specific to one epitope of the immunogen. Covance Inc. reported 55 separate clones demonstrating recognition for the immunogen and the frozen stocks of supernatants (containing antibodies) were later shipped to our laboratory for the following studies.

*A population of MAbs recognized both immunogen and WT pili*

Two separate ELISAs were performed using immunogen-recognizing MAbs on immobilized pili in order to first, select MAbs that would recognize immunogen pili and second, use those selected MAbs to investigate the recognition of WT pili that had a K12 background (same as the immunogen). For the first study, 15 of the 55 hybridoma supernatants recognized immunogen pili (data not shown). Even though all 55 supernatants indicated a positive recognition of the immunogen, not all may recognize FimH while incorporated into pili. This is due to the pilin domain physically blocking epitopes that are exposed by the isolated LD. The 10 supernatants with the strongest recognition were then carried onto recognize both immunogen and WT pili in the presence and absence of ligand. For the second study, all 10 MAbs recognized immunogen and WT pili (Figure 24). The response to the conditions fell into several groups: a

MAb that universally recognized pili (ligand independent): 172, 241, 320; a MAb that cannot recognize pili while in the presence of ligand (ligand dependent): 475, 844; and a MAb that

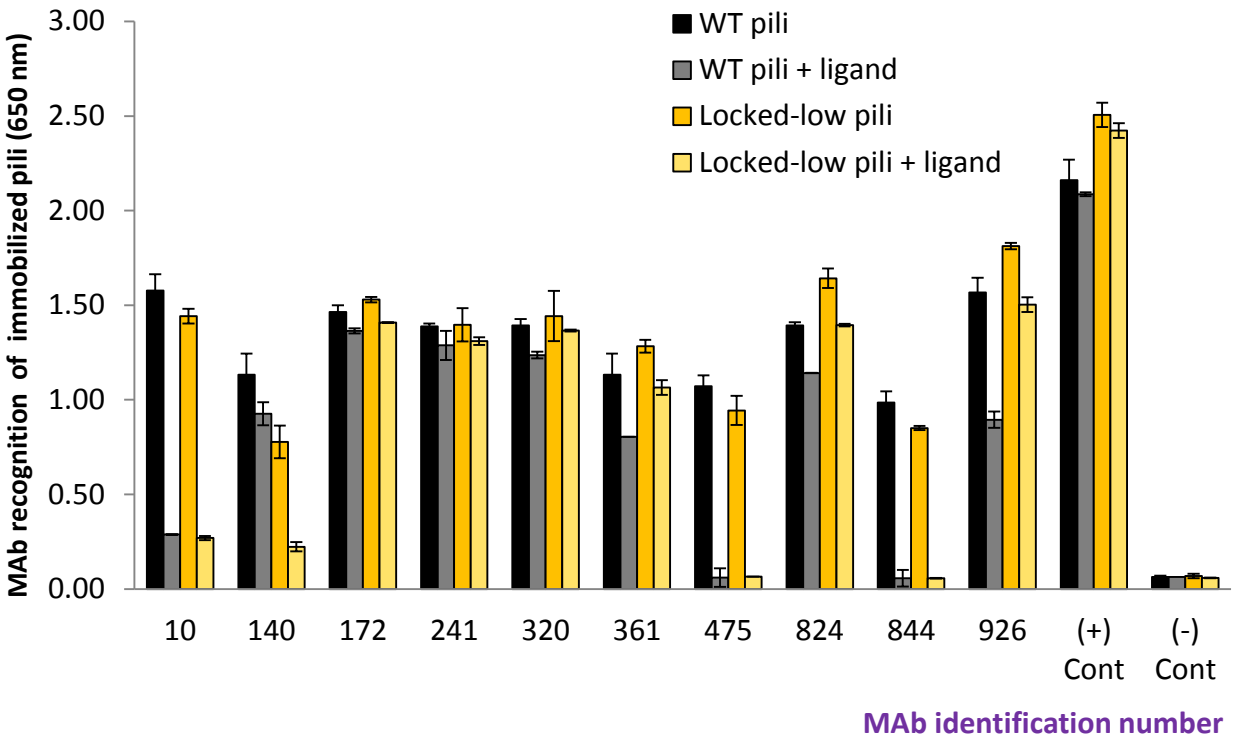


[redacted]

shows decreased recognition of pili while in the presence of mannose: 10, 140, 361, 824, 926.

This data strongly suggests that the presence of ligand provides a clue as to each MAb's binding epitope. It was demonstrated previously herein (Figure 15)(Rodriguez, Kidd et al. 2012) and in a separate study (Le Trong, Aprikian et al. 2010) that WT and locked-low pili maintain a low-affinity conformation in the absence of ligand. But in the presence of ligand, WT pili indicated a high-affinity conformation while the locked-low pili still maintained a low-affinity conformation. In our study here, we hypothesize ligand independent MAbs universally bind epitopes shared

by both low and high-affinity state conformations. For ligand dependent MAb475 and MAb844, we hypothesize these epitopes to be conformation independent when considering the two different conformations of WT and locked-low pili in the presence of ligand. Therefore, we suggest these epitopes are near or in the FimH binding pocket, which become blocked by the binding to ligand. As for the MAbs that decreased recognition of pili in the presence of ligand, the location of these epitopes may be in places indicating nuanced changes in conformation that require additional investigation. In conclusion, these results encouraged additional studies to probe each MAb's ability to prevent pili binding to a mannose-like ligand, HRP.

*Majority of MAbs did not increase the binding of pili to HRP*

Immobilized WT K12 and FocH pili were co-incubated with antibodies and HRP to seek MAbs capable of preventing FimH from binding HRP (Figure 25), much like how an antiadhesive therapy would prevent *E.coli* binding to the urinary tract. Additionally, FocH was included to assess the ability of these MAbs to prevent a FimH persistently in the high-affinity conformation. The results from a separate study of sera from mouse WA PAb 616 (Figure 25A) was also included for comparison and indicate that although it appears to decrease WT binding to HRP, the serum increased FocH binding to HRP. The results also indicate that a variety of MAbs were derived from the immunogen and collectively change the binding behavior of FimH. Therefore, the results strongly encouraged continued investigation of MAbs as a potential antiadhesive therapy rather than using the locked-low LD as an immunogen for a conventional vaccine.

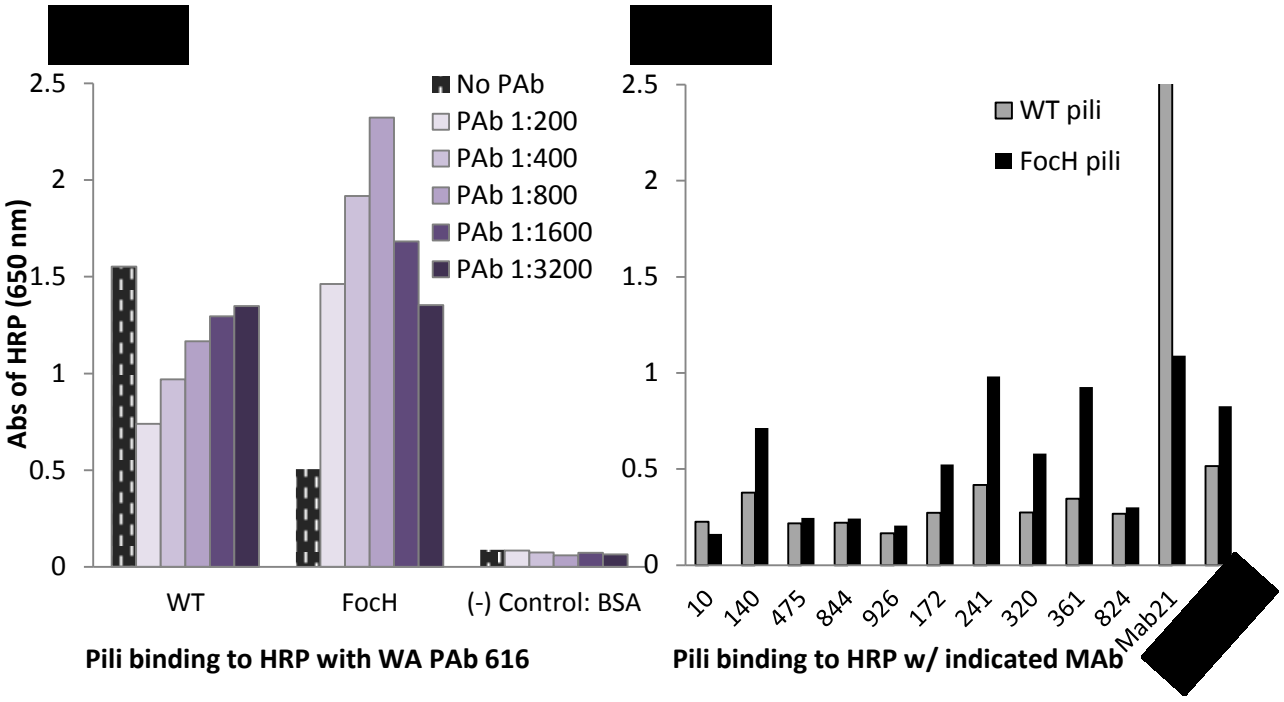


Other than MAb241 and MAb361 for FocH, it may be interpreted that the majority of newly synthesized MAbs do not increase the binding of HRP. WT pili were prevented from adhering the most to HRP in the presence of MAb926, followed by MAb10, MAb475, MAb844 at equivalent inhibition. FocH pili were prevented from adhering the most to HRP in the presence of MAb10 and MAb926. Therefore, MAb10 and MAb926 were carried on to investigate each one's capability of preventing bacterial adhesion to a mannosylated surface as well as urothelial cells.

*MAb10 and MAb926 significantly inhibited the adhesion of WT and high-affinity A188D to 1M*

To investigate the prevention of bacterial adhesion in the presence of selected MAbs, we measured the adhesion of *E.coli* that was pre-incubated with MAbs to a monomannosyl (1M) substrate (Figure 26). The bacterial strains expressed FimH with two K12 background strains: WT and high-affinity A188D. Variant A188D is a derivative of FocH and is 1 of 2 crucial point mutations that cause its high-affinity conformation (Aprikian, Tchesnokova et al. 2007). The bacteria demonstrated specificity in the presence of mannose (data not shown) and in a separate study (data not shown), heat inactivated MAb10/926 also demonstrated specificity.

The PAb sera from mouse WA 616 did prevent bacterial adhesion of A188D ($p < 0.05$), while the sera had no effect on the WT ($p > 0.05$). An opposite effect was observed in the HRP binding study in the previous section. This may be justified when considering the mixture of antibodies within a sample of serum. Each antibody likely recognizes various epitopes all over the targeted immunogen as well as

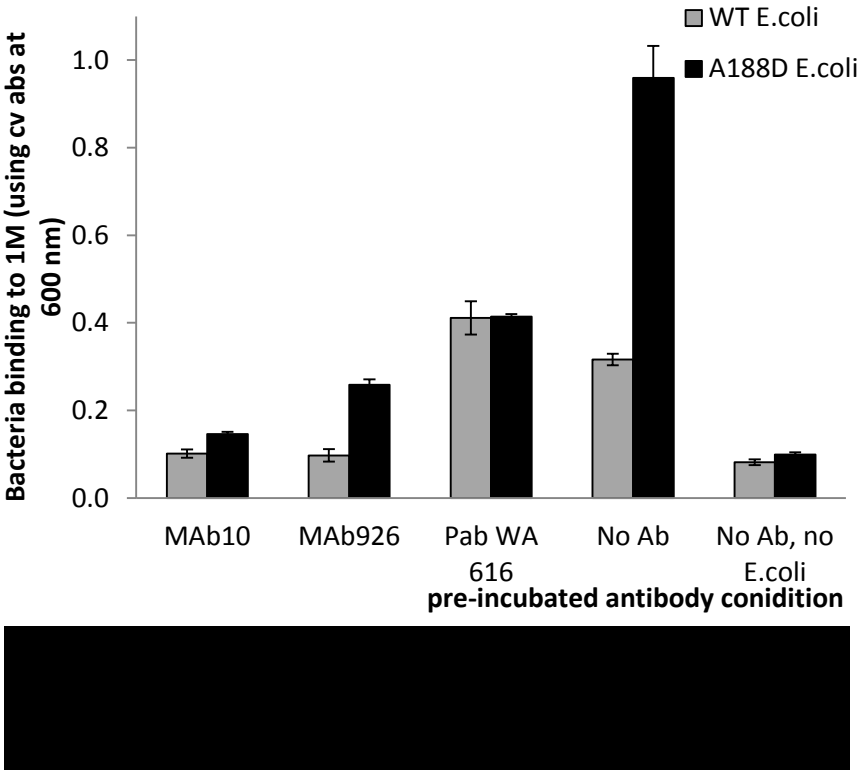

antibodies that are completed unrelated and belong to the host's immunological history. The particular PAb serum is therefore inconsistent and confirms the HRP binding study's conclusion that the locked-low LD is not the most effective immunogen for a conventional vaccine.

In future antiadhesive research targeting uropathogenic *E.coli* (UPEC), it is imperative that the antibodies are capable of preventing various strains of FimH-expressing *E.coli*. MAb10 and MAb926 significantly inhibit the binding of WT and high-affinity A188D FimH ($p < 0.05$). Although both *E.coli* used in this assay belong to K12 background strain, they represent each of FimH's two conformations and thereby demonstrate potential as an antiadhesive therapy targeted at other UPEC strains.

*MAb10 and MAb926 significantly inhibited the adhesion of WT* E.coli *to urothelial cells* in vitro

In order to determine the antiadhesive properties of MAb10 and MAb926 *in vitro*, *E.coli* were pre-incubated with these MAbs prior to a 1 hour exposure to confluent T24 cells. Both MAb10 and MAb926 significantly inhibited the adhesion of *E.coli* expressing WT FimH ($p < 0.05$) (Figure 27). Although both MAbs decreased the adhesion of *E.coli* expressing A188D FimH, the variability between plates prevented the decrease from being significant ($0.1 < p < 0.5$). Additionally, it must be noted that this *in vitro* study showed nonspecific adhesion of bacteria to T24 cells based off the high colony counts for those containing soluble ligand. When this is taken into consideration, MAb10 may be considered more effective at inhibiting bacterial adhesion. Overall, the significant inhibition of WT FimH by these MAbs encourages the pursuit

of antiadhesive research in light of the fact that this strain is derived from *E.coli* strain J96, a model uropathogenic isolate.

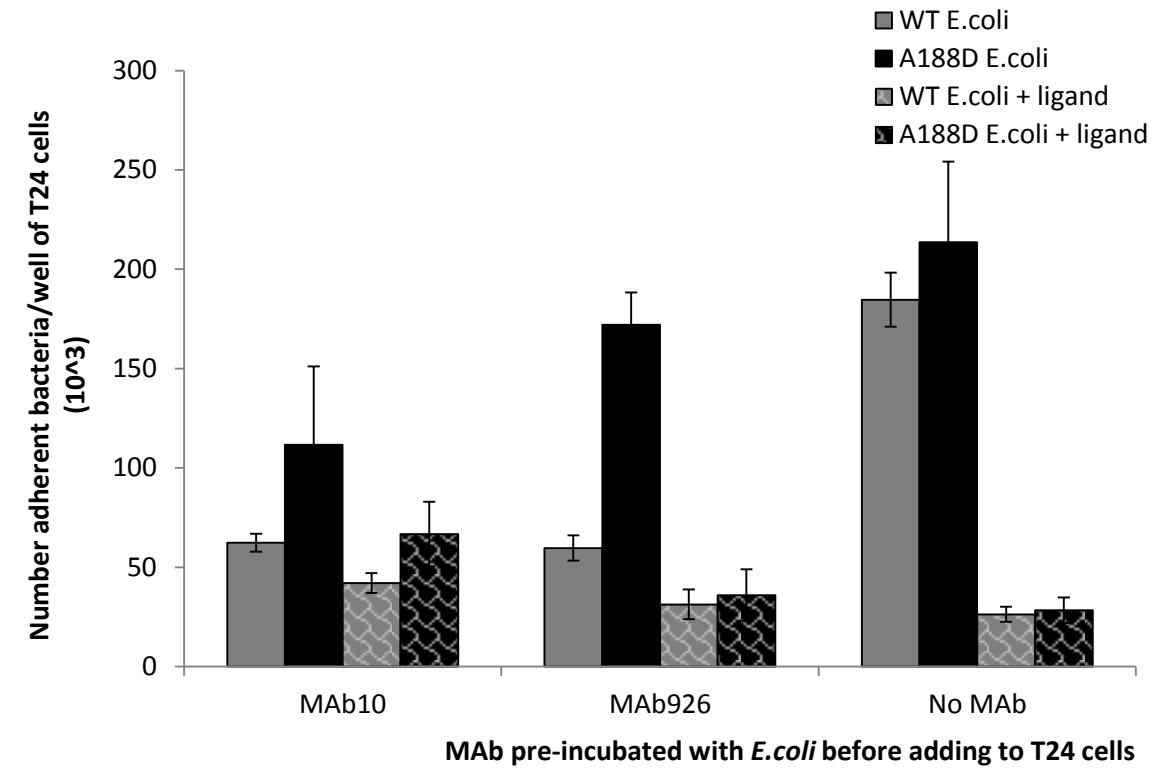


[redacted]

## Discussion

In this study, a previously described novel LD isolate (Rodriguez 2012) with low-affinity conformation and phenotype (see Figure 21 and Figure 22, respectively) was used as an immunogen in order to develop polyclonal and monoclonal antibodies targeted at the adhesin FimH of *E.coli*. This represents a novel immunogen in that the isolated LD crystal structure (Choudhury, Thompson et al. 1999; Hung, Bouckaert et al. 2002; Bouckaert, Berglund et al. 2005; Wellens, Garofalo et al. 2008) and phenotype (Aprikian, Tchesnokova et al. 2007) of various strains have all exhibited a high-affinity state. Because of its low-affinity conformation, the immunogen also represents an alternative path in antiadhesive therapies that have not produced a commercial vaccine despite successful FimH vaccines studies in animal models (Langermann, Palaszynski et al. 1997; Langermann, Mollby et al. 2000). Here, 5 mice were immunized against the locked-low LD and 3 of the 5 indicated average or greater titers against the immunogen. This also confirmed the immunogen's stability during the immunization phase. With its average titer, recognition of the native pili containing the immunogen, and no cross-reactivity to the immunogen's His·Tag®, mouse WA 616 was selected for MAb development and created a panel of 55 MAbs that positively recognized the immunogen. Of these 55 MAbs, MAb10 and MAb926 significantly reduced the adhesion of both WT K12 and high-affinity A188D expressing *E.coli* to a 1M surface ($p < 0.05$). Additionally, both MAbs significantly reduced the adhesion of *E.coli* expressing WT K12 to urothelial cells *in vitro* ( $p < 0.05$) and partially inhibited the adhesion of *E.coli* expressing high-affinity A188D ($0.1 < p < 0.5$). The results of this work

support our hypothesis of alternative antiadhesive therapies targeted at the prevention of UTI causing *E.coli*.

Although mouse WA 616's sera indicated mixed results in preventing fimbrial adhesion or *E.coli* adhesion to ligand HRP or a 1M substrate (respectively), these results do not discount the immunogen as we have significant proof of MAbs from this mouse that are capable of preventing WT bacterial adhesion to a 1M substrate as well as *in vitro*. What can be said with certainty is that this particular immunogen is not likely sustainable as a candidate for a conventional vaccine. Rather, it's a precursor vaccine in that the MAbs generated from it indicate the potential for previously documented low-affinity FimH variants (Rodriguez, Kidd et al. 2012) as candidates for similar immunization studies.

A way to select the next low-affinity FimH variant as a candidate for future immunization studies would be to understanding the mechanism of MAb10 and MAb926. Using a previously developed methodology (Tchesnokova, Aprikian et al. 2011) along with a library of FimH variants, basic ELISA assays may identify the epitopes the monoclonal antibodies recognize. Pinpointing epitopes gives a map of regions important in preventing FimH adhesion and may be used to select current immunogen candidates or allow for the custom synthesis of new ones. In addition, knowing these target regions allows for the custom synthesis of small-molecule inhibitors and expands our knowledge of vital regions involved in the FimH catch-bond mechanism. With additional characterization, these MAbs may be immediately used as an alternative preventative measure in medicine such as passive immunity of patients prior to

high-risk surgical procedures and for those undergoing short- or long-term catheterization. In conclusion, our investigation demonstrated a promising antiadhesive therapy that will assist current issues faced in preventing adhesion of uropathogenic *E.coli*.

# Chapter VI Conclusions

This work will aide future development of novel antiadhesive therapies designed to inhibit the adhesion of uropathogenic *E.coli*. Although past vaccine studies using animal models have reported successful immunization against UPEC, this work emphasizes that FimH as an immunogen is likely more complex than what is used during conventional vaccine development. Over the course of moving this project from conception to monoclonal antibody (MAb) development, we have discovered that in-depth knowledge of the FimH mechanism combined with alternative therapies that go beyond a conventional vaccine is the bridge to eradicating uropathogenic *E.coli* (UPEC) infections. As an additional bonus, we have created several biological "tools" that we hope will contribute to the current knowledge base of catch-bonds for FimH as well as other systems such as leukocyte selectins, muscle myosin, and blood platelets.

This work has exceeded the expectations made while developing the original plans of a "locked-low" FimH adhesin, but ultimately did not lead to a panacea for the prevention of urinary tract infections. That panacea is currently considered to be a conventional vaccine for UPEC in which an immunogen injected into a patient stimulates the production of antibodies against UPEC. The mouse selected for MAb production (Chapter 5) demonstrated sera that showed mixed results at preventing fimbrial and bacteria adhesion to ligand. This result is analogous to a patient receiving an injection of the immunogen, but failing to gain full immunity against a disease or infection. This should not discount the locked-low immunogen as we have significant

proof of MAbs from this mouse that are capable of preventing wildtype bacterial adhesion to a monomannosyl substrate as well as *in vitro*. Additionally, we did not do in-depth screening of the other mice involved in the immunization study. What can be said with certainty is that this particular immunogen is not likely sustainable as a candidate for a conventional vaccine. Rather, it's a precursor vaccine in that the MAbs generated from it indicate the potential for previously documented low-affinity FimH variants (Chapter 3) as candidates for similar immunization studies. Therefore, we believe this is a promising feasibility study.

In light of this result and the lack of a commercial vaccine for UPEC on the market, we also believe that perhaps alternative strategies should be considered in order to expand our arsenal against UPEC. The implementation of the novel isolated locked-low LD (Chapter 4) may be expanded to include seeking effective epitopes for allosteric inhibitors. Or, the MAbs produced in this work may be immediately used as an alternative preventative measure in medicine such as passive immunity of patients prior to high-risk surgical procedures and for those undergoing short- or long-term catheterization.

In conclusion, no research project is an island and we hope to discover more about the adhesin FimH from adjacent FimH researchers as well as those investigating other catch-bond systems. Even if it is to be discovered that this is not the proper path in the prevention of urinary tract infections, we have made one step closer to making such a conclusion. That is the basis of scientific discovery: small steps together may advance any field.

# References

(2005). Urinary Tract Infections in Adults. U. S. D. o. H. H. a. Services. Bethesda, MD, National Kidney and Urologoic Diseases Information Clearinghouse.

Alberts B, J. A., Lewis J, Raff M, Roberts K, Walter P (2002). Molecular Biology of the Cell. New York, Garland Science.

Alton, G., M. Hasilik, et al. (1998). "Direct utilization of mannose for mammalian glycoprotein biosynthesis." Glycobiology **8**(3): 285-295.

Andersson, M., B. E. Uhlin, et al. (2007). "The biomechanical properties of E-coli Pili for urinary tract attachment reflect the host environment." Biophysical Journal **93**(9): 3008-3014.

Aprikian, P., G. Interlandi, et al. (2011). "The Bacterial Fimbrial Tip Acts as a Mechanical Force Sensor." Plos Biology **9**(5): 16.

Aprikian, P., V. Tchesnokova, et al. (2007). "Interdomain interaction in the FimH adhesin of Escherichia coli regulates the affinity to mannose." Journal of Biological Chemistry **282**(32): 23437-23446.

Auton, M., E. Sedlak, et al. (2009). "Changes in thermodynamic stability of von Willebrand factor differentially affect the force-dependent binding to platelet GPIbalpha." Biophys J **97**(2): 618-27.

Bell, G. I. (1978). "MODELS FOR SPECIFIC ADHESION OF CELLS TO CELLS." Science **200**(4342): 618-627.

Berman, H. M., J. Westbrook, et al. (2000). "The Protein Data Bank." Nucleic Acids Res. **28**(1): 235--242.

Bjornham, O. and O. Axner (2010). "Catch-bond behavior of bacteria binding by slip bonds." Biophys J **99**(5): 1331-41.

Blomfield, I. C., M. S. McClain, et al. (1991). "TYPE-1 FIMBRIAE MUTANTS OF ESCHERICHIA-COLI K12 - CHARACTERIZATION OF RECOGNIZED AFIMBRIATE STRAINS AND CONSTRUCTION OF NEW FIM DELETION MUTANTS." Molecular Microbiology **5**(6): 1439-1445.

Bouckaert, J., J. Berglund, et al. (2005). "Receptor binding studies disclose a novel class of high-affinity inhibitors of the Escherichia coli FimH adhesin." Molecular Microbiology **55**(2): 441-455.

Bouckaert, J., J. Berglund, et al. (2005). "Receptor binding studies disclose a novel class of high-affinity inhibitors of the Escherichia coli FimH adhesin." Mol Microbiol **55**(2): 441-55.

Bouckaert, J., J. Mackenzie, et al. (2006). "The affinity of the FimH fimbrial adhesin is receptor-driven and quasi-independent of Escherichia coli pathotypes." Molecular Microbiology **61**(6): 1556-1568.

Choudhury, D., A. Thompson, et al. (1999). "X-ray structure of the FimC-FimH chaperone-adhesin complex from uropathogenic Escherichia coli." Science **285**(5430): 1061-6.

Choudhury, D., A. Thompson, et al. (1999). "X-ray Structure of the FimC-FimH Chaperone-Adhesin Complex from Uropathogenic Escherichia coli." Science **285**(5430): 1061-1066.

Dani, V. S., C. Ramakrishnan, et al. (2003). "MODIP revisited: re-evaluation and refinement of an automated procedure for modeling of disulfide bonds in proteins." Protein Engineering **16**(3): 187-193.

DeLano, W. L. (2002). The PyMOL User's Manual, DeLano Scientific, Palo Alto, CA, USA.

Dembo, M., D. C. Torney, et al. (1988). "THE REACTION-LIMITED KINETICS OF MEMBRANE-TO-SURFACE ADHESION AND DETACHMENT." Proceedings of the Royal Society of London Series B-Biological Sciences **234**(1274): 55-83.

Ding, A. M., R. J. Palmer, Jr., et al. (2010). "Shear-enhanced oral microbial adhesion." Appl Environ Microbiol **76**(4): 1294-7.

Dunbrack, J. R. L. and F. E. Cohen (1997). "Bayesian statistical analysis of protein side-chain rotamer preferences." Protein Sci. 6(8): 1661-1681.

Etchison, J. R. and H. H. Freeze (1997). "Enzymatic assay of D-mannose in serum." Clinical Chemistry 43(3): 533-538.

Evans, E. (2001). "Probing the relation between force - Lifetime - and chemistry in single molecular bonds." Annual Review of Biophysics and Biomolecular Structure 30: 105-128.

Finger, E. B., K. D. Puri, et al. (1996). "Adhesion through L-selectin requires a threshold hydrodynamic shear." Nature 379(6562): 266-269.

Forero, M., O. Yakovenko, et al. (2006). "Uncoiling mechanics of Escherichia coli type I fimbriae are optimized for catch bonds." Plos Biology 4(9): 1509-1516.

Foxman, B. (2002). "Epidemiology of urinary tract infections: Incidence, morbidity, and economic costs." American Journal of Medicine 113: 5S-13S.

Foxman, B. (2010). "The epidemiology of urinary tract infection." Nature Reviews Urology 7(12): 653-660.

Frelinger, A. L., X. P. Du, et al. (1991). "Monoclonal antibodies to ligand-occupied conformers of integrin alpha IIb beta 3 (glycoprotein IIb-IIIa) alter receptor affinity, specificity, and function." Journal of Biological Chemistry 266(26): 17106-17111.

Goto, S., Y. Ikeda, et al. (1998). "Distinct mechanisms of platelet aggregation as a consequence of different shearing flow conditions." The Journal of Clinical Investigation 101(2): 479-486.

Guo, B. and W. H. Guilford (2006). "Mechanics of actomyosin bonds in different nucleotide states are tuned to muscle contraction." Proceedings of the National Academy of Sciences of the United States of America 103(26): 9844-9849.

Hahn, E., P. Wild, et al. (2002). "Exploring the 3D molecular architecture of Escherichia coli type 1 pili." Journal of Molecular Biology 323(5): 845-857.

Hartmann, M. and T. K. Lindhorst (2011). "The Bacterial Lectin FimH, a Target for Drug Discovery - Carbohydrate Inhibitors of Type 1 Fimbriae-Mediated Bacterial Adhesion." European Journal of Organic Chemistry(20-21): 3583-3609.

Hashimoto, H. (2006). "Recent structural studies of carbohydrate-binding modules." Cellular and Molecular Life Sciences **63**(24): 2954-2967.

Humphries, A. D., M. Raffatellu, et al. (2003). "The use of flow cytometry to detect expression of subunits encoded by 11 Salmonella enterica serotype Typhimurium fimbrial operons." Molecular Microbiology **48**(5): 1357-1376.

Hung, C. S., J. Bouckaert, et al. (2002). "Structural basis of tropism of Escherichia coli to the bladder during urinary tract infection." Mol Microbiol **44**(4): 903-15.

Hung, C. S., J. Bouckaert, et al. (2002). "Structural basis of tropism of Escherichia coli to the bladder during urinary tract infection." Molecular Microbiology **44**(4): 903-915.

Hynes, R. O. (1987). "Integrins: A family of cell surface receptors." Cell **48**(4): 549-554.

Jackson, M. (2006). Molecular and Cellular Biology. New York, Cambridge University Press.

Jones, C. H., J. S. Pinkner, et al. (1995). "FIMH ADHESIN OF TYPE-1 PILI IS ASSEMBLED INTO A FIBRILLAR TIP STRUCTURE IN THE ENTEROBACTERIACEAE." Proceedings of the National Academy of Sciences of the United States of America **92**(6): 2081-2085.

Karlowsky, J. A., L. J. Kelly, et al. (2002). "Trends in antimicrobial resistance among urinary tract infection isolates of Escherichia coli from female outpatients in the United States." Antimicrobial Agents and Chemotherapy **46**(8): 2540-2545.

Kisiela, D., A. Laskowska, et al. (2006). "Functional characterization of the FimH adhesin from Salmonella enterica serovar Enteritidis." Microbiology-Sgm **152**: 1337-1346.

Kisiela, D. I., J. J. Kramer, et al. "Allosteric Catch Bond Properties of the FimH Adhesin from Salmonella enterica Serovar Typhimurium." Journal of Biological Chemistry **286**(44): 38136-38147.

Kisiela, D. I., J. J. Kramer, et al. (2011). "Allosteric catch bond properties of the FimH adhesin from Salmonella enterica serovar Typhimurium." J Biol Chem **286**(44): 38136-47.

Knudsen, T. B. and P. Klemm (1998). "Probing the receptor recognition site of the FimH adhesin by fimbriae-displayed FimH-FocH hybrids." Microbiology-Uk **144**: 1919-1929.

Krogfelt, K. A., H. Bergmans, et al. (1990). "DIRECT EVIDENCE THAT THE FIMH PROTEIN IS THE MANNOSE-SPECIFIC ADHESIN OF ESCHERICHIA-COLI TYPE-1 FIMBRIAE." Infection and Immunity **58**(6): 1995-1998.

Kuhlman, B. and D. Baker (2000). "Native protein sequences are close to optimal for their structures." Proc. Natl. Acad. Sci. U.S.A. **97**(19): 10383-8.

Langermann, S., R. Mollby, et al. (2000). "Vaccination with FimH adhesin protects cynomolgus monkeys from colonization and infection by uropathogenic Escherichia coli." Journal of Infectious Diseases **181**(2): 774-778.

Langermann, S., S. Palaszynski, et al. (1997). "Prevention of mucosal Escherichia coli infection by FimH-adhesin-based systemic vaccination." Science **276**(5312): 607-611.

Lazaridis, T. and M. Karplus (1999). "Effective energy function for proteins in solution." Proteins **35**(2): 133-152.

Le Trong, I., P. Aprikian, et al. (2010). "Structural Basis for Mechanical Force Regulation of the Adhesin FimH via Finger Trap-like beta Sheet Twisting." Cell **141**(4): 645-655.

Li, Z. J., N. Mohamed, et al. (2000). "Shear stress affects the kinetics of Staphylococcus aureus adhesion to collagen." Biotechnol Prog **16**(6): 1086-90.

Lou, J. Z., T. Yago, et al. (2006). "Flow-enhanced adhesion regulated by a selectin interdomain hinge." Journal of Cell Biology **174**(7): 1107-1117.

Lou, J. Z. and C. Zhu (2007). "A structure-based sliding-rebinding mechanism for catch bonds." Biophysical Journal **92**(5): 1471-1485.

Marshall, B. T., M. Long, et al. (2003). "Direct observation of catch bonds involving cell-adhesion molecules." Nature 423(6936): 190-193.

Morozov, A. V., T. Kortemme, et al. (2004). "Close agreement between the orientation dependence of hydrogen bonds observed in protein structures and quantum mechanical calculations." Proc. Natl. Acad. Sci. U.S.A. 101(18): 6946--6951.

Mould, A. P., M. A. Travis, et al. (2005). "Evidence That Monoclonal Antibodies Directed against the Integrin Î² Subunit Plexin/Semaphorin/Integrin Domain Stimulate Function by Inducing Receptor Extension." Journal of Biological Chemistry 280(6): 4238-4246.

Mulvey, M. A., J. D. Schilling, et al. (2000). "Bad bugs and beleaguered bladders: Interplay between uropathogenic Escherichia coli and innate host defenses." Proceedings of the National Academy of Sciences of the United States of America 97(16): 8829-8835.

Munera, D., C. Palomino, et al. (2008). "Specific residues in the N-terminal domain of FimH stimulate type I fimbriae assembly in Escherichia coli following the initial binding of the adhesin to FimD usher." Molecular Microbiology 69(4): 911-925.

Nelson, D. L. and M. M. Cox (2005). Lehninger Priciples of Biochemistry. New York, NY, W.H. Freeman and Company.

Nilsson, L. M., W. E. Thomas, et al. (2006). "Catch bond-mediated adhesion without a shear threshold: trimannose versus monomannose interactions with the FimH adhesin of Escherichia coli." J Biol Chem 281(24): 16656-63.

Nilsson, L. M., O. Yakovenko, et al. (2007). "The cysteine bond in the Escherichia coli FimH adhesin is critical for adhesion under flow conditions." Molecular Microbiology 65(5): 1158-1169.

Pereverzev, Y. V., E. Prezhdo, et al. (2011). "The Two-Pathway Model of the Biological Catch-Bond as a Limit of the Allosteric Model." Biophysical Journal 101(8): 2026-2036.

Pereverzev, Y. V., O. V. Prezhdo, et al. (2005). "The two-pathway model for the catch-slip transition in biological adhesion." Biophysical Journal 89(3): 1446-1454.

Remaut, H., R. J. Rose, et al. (2006). "Donor-strand exchange in chaperone-assisted pilus assembly proceeds through a concerted beta strand displacement mechanism." Molecular Cell **22**(6): 831-842.

Rodriguez, V. (2012). "in preparation."

Rodriguez, V., B. Kidd, et al. (2012). "in preparation."

Saint, S. (2000). "Clinical and economic consequences of nosocomial catheter-related bacteriuria." American Journal of Infection Control **28**(1): 68-75.

Sauer, F. G., H. Remaut, et al. (2004). "Fiber assembly by the chaperone-usher pathway." Biochimica Et Biophysica Acta-Molecular Cell Research **1694**(1-3): 259-267.

Saulino, E. T., E. Bullitt, et al. (2000). "Snapshots of usher-mediated protein secretion and ordered pilus assembly." Proceedings of the National Academy of Sciences of the United States of America **97**(16): 9240-+.

Schembri, M. A., H. Hasman, et al. (2000). "Expression and purification of the mannose recognition domain of the FimH adhesin." FEMS Microbiology Letters **188**(2): 147-151.

Schito, G. C., K. G. Naber, et al. (2009). "The ARESC study: an international survey on the antimicrobial resistance of pathogens involved in uncomplicated urinary tract infections." International Journal of Antimicrobial Agents **34**(5): 407-413.

Shan, W. S., A. Koch, et al. (1999). "The adhesive binding site of cadherins revisited." Biophysical Chemistry **82**(2-3): 157-163.

Shapiro, B. E. and H. Qian (1997). "A quantitative analysis of single protein-ligand complex separation with the atomic force microscope." Biophysical Chemistry **67**(1-3): 211-219.

Sokurenko, E. V., V. Chesnokova, et al. (1997). "Diversity of the Escherichia coli type 1 fimbrial lectin - Differential binding to mannosides and uroepithelial cells." Journal of Biological Chemistry **272**(28): 17880-17886.

Sokurenko, E. V., V. Chesnokova, et al. (1998). "Pathogenic adaptation of Escherichia coli by natural variation of the FimH adhesin." Proceedings of the National Academy of Sciences of the United States of America **95**(15): 8922-8926.

Sokurenko, E. V., H. S. Courtney, et al. (1995). "Quantitative differences in adhesiveness of type 1 fimbriated Escherichia coli due to structural differences in fimH genes." J. Bacteriol. **177**(13): 3680-3686.

Sokurenko, E. V., M. A. Schembri, et al. (2001). "Valency conversion in the type 1 fimbrial adhesin of Escherichia coli." Molecular Microbiology **41**(3): 675-686.

Sone, H., H. Shimano, et al. (2003). "Physiological changes in circulating mannose levels in normal, glucose-intolerant, and diabetic subjects." Metabolism-Clinical and Experimental **52**(8): 1019-1027.

Sowdhamini, R., N. Srinivasan, et al. (1989). "STEREOCHEMICAL MODELING OF DISULFIDE BRIDGES - CRITERIA FOR INTRODUCTION INTO PROTEINS BY SITE-DIRECTED MUTAGENESIS." Protein Engineering **3**(2): 95-103.

Tchesnokova, V., P. Aprikian, et al. (2011). "Type 1 Fimbrial Adhesin FimH Elicits an Immune Response That Enhances Cell Adhesion of Escherichia coli." Infection and Immunity **79**(10): 3895-3904.

Tchesnokova, V., P. Aprikian, et al. (2011). "in preparation."

Tchesnokova, V., P. Aprikian, et al. (2008). "Integrin-like allosteric properties of the catch bond-forming FimH adhesin of Escherichia coli." Journal of Biological Chemistry **283**(12): 7823-7833.

Tchesnokova, V., A. L. McVeigh, et al. (2010). "Shear-enhanced binding of intestinal colonization factor antigen I of enterotoxigenic Escherichia coli." Mol Microbiol **76**(2): 489-502.

Thomas, W. (2008). "Catch bonds in adhesion." Annual Review of Biomedical Engineering **10**: 39-57.

Thomas, W., M. Forero, et al. (2006). "Catch-bond model derived from allostery explains force-activated bacterial adhesion." Biophysical Journal 90(3): 753-764.

Thomas, W. E., L. M. Nilsson, et al. (2004). "Shear-dependent 'stick-and-roll' adhesion of type 1 fimbriated Escherichia coli." Molecular Microbiology 53(5): 1545-1557.

Thomas, W. E., E. Trintchina, et al. (2002). "Bacterial adhesion to target cells enhanced by shear force." Cell 109(7): 913-923.

Thomas, W. E., V. Vogel, et al. (2008). Biophysics of catch bonds. Annual Review of Biophysics. Palo Alto, Annual Reviews. 37: 399-416.

Timpl, R., D. Tisi, et al. (2000). "Structure and function of laminin LG modules." Matrix Biology 19(4): 309-317.

Vetsch, M., D. Erilov, et al. (2006). "Mechanism of fibre assembly through the chaperone-usher pathway." Embo Reports 7(7): 734-738.

Vetsch, M., C. Puorger, et al. (2004). "Pilus chaperones represent a new type of protein-folding catalyst." Nature 431(7006): 329-332.

Waksman, G. and S. J. Hultgren (2009). "Structural biology of the chaperone-usher pathway of pilus biogenesis." Nature Reviews Microbiology 7(11): 765-774.

Weissman, S. J., S. Chattopadhyay, et al. (2006). "Clonal analysis reveals high rate of structural mutations in fimbrial adhesins of extraintestinal pathogenic Escherichia coli." Molecular Microbiology 59(3): 975-988.

Wellens, A., C. Garofalo, et al. (2008). "Intervening with urinary tract infections using anti-adhesives based on the crystal structure of the FimH-oligomannose-3 complex." PLoS ONE 3(4): e2040.

Wellens, A., C. Garofalo, et al. (2008). "Intervening with Urinary Tract Infections Using Anti-Adhesives Based on the Crystal Structure of the FimH-Oligomannose-3 Complex." Plos One 3(4): 13.

Whitfield, M., T. Ghose, et al. (2010). "Shear-Stabilized Rolling Behavior of E. coli Examined with Simulations." Biophysical Journal **99**(8): 2470-2478.

Whitfield, M., T. Ghose, et al. (2010). "Shear-stabilized rolling behavior of E. coli examined with simulations." Biophys J **99**(8): 2470-8.

Whitfield, M. and W. E. Thomas (2011). "A Nanoadhesive Composed of Receptor-Ligand Bonds." Journal of Adhesion **87**(5): 427-446.

Yakovenko, O., S. Sharma, et al. (2008). "FimH forms catch bonds that are enhanced by mechanical force due to allosteric regulation." Journal of Biological Chemistry **283**(17): 11596-11605.

Yakovenko, O., V. Tchesnokova, et al. (2011). "in preparation, potential title: Catch bonds enable rapid adhesion in high flow."

Zhanel, G. G., T. L. Hisanaga, et al. (2005). "Antibiotic resistance in outpatient urinary isolates: final results from the North American Urinary Tract Infection Collaborative Alliance (NAUTICA)." International Journal of Antimicrobial Agents **26**(5): 380-388.

# Appendix

**A** Epitopes of FimH lectin domain recognized by indicated groups of antibodies. Group A, B, C, and D are represented by A-B, C-D, E-F, and G-H, respectively. Tip incorporated lectin domain is on the left (A, C, E, G) while isolated lectin domain is on the right (B, D, F, H). Epitopes are in red, binding site is in yellow, and interdomain-bonding residues in dark green for lectin domain and dark-cyan for pilin domain. All epitopes mapped by Tchesnokova et al., (Tchesnokova, Aprikian et al. 2011)**.**

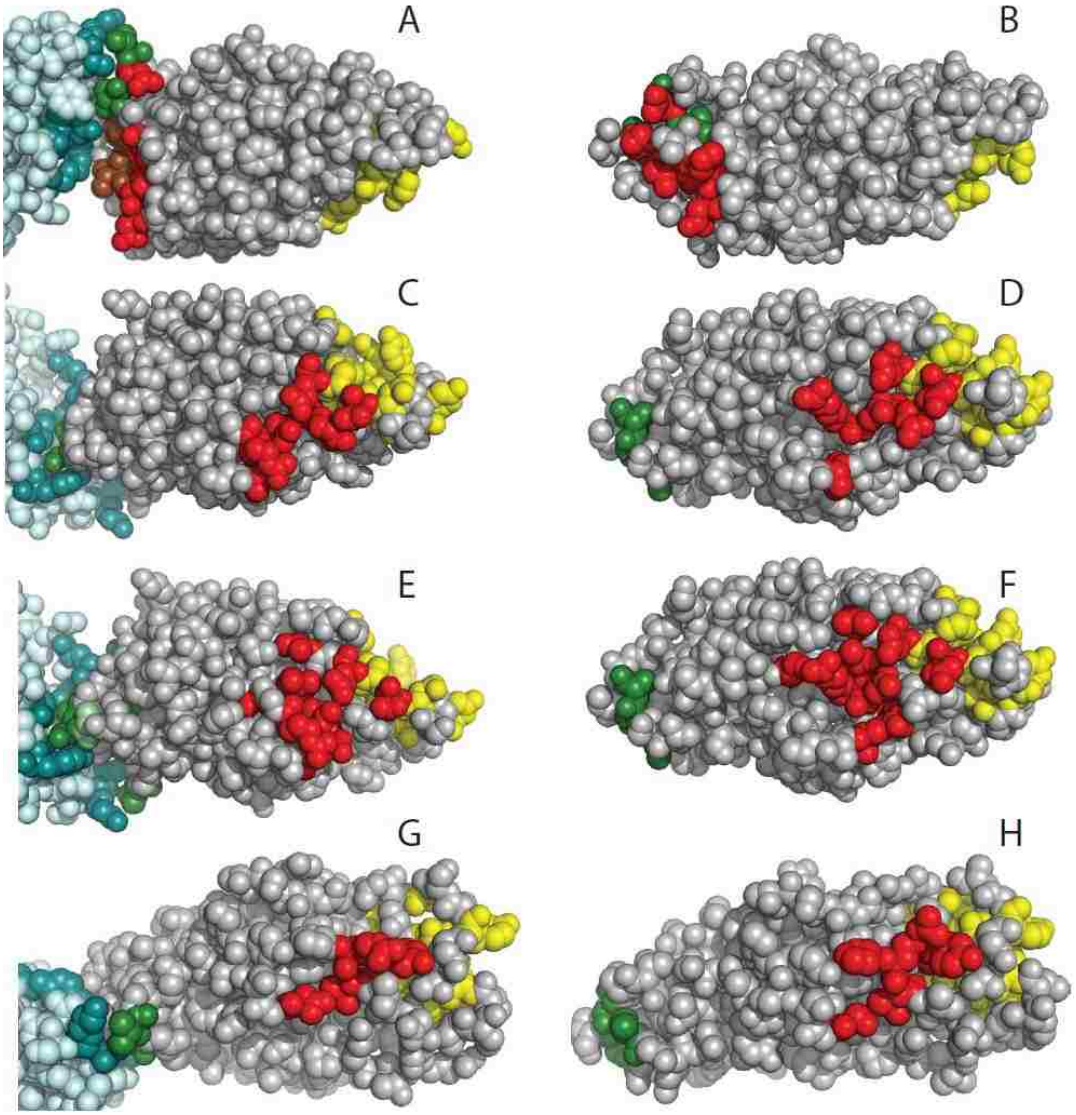

**B** Preliminary mechanical studies on FimH variants using parallel-plate flow chamber

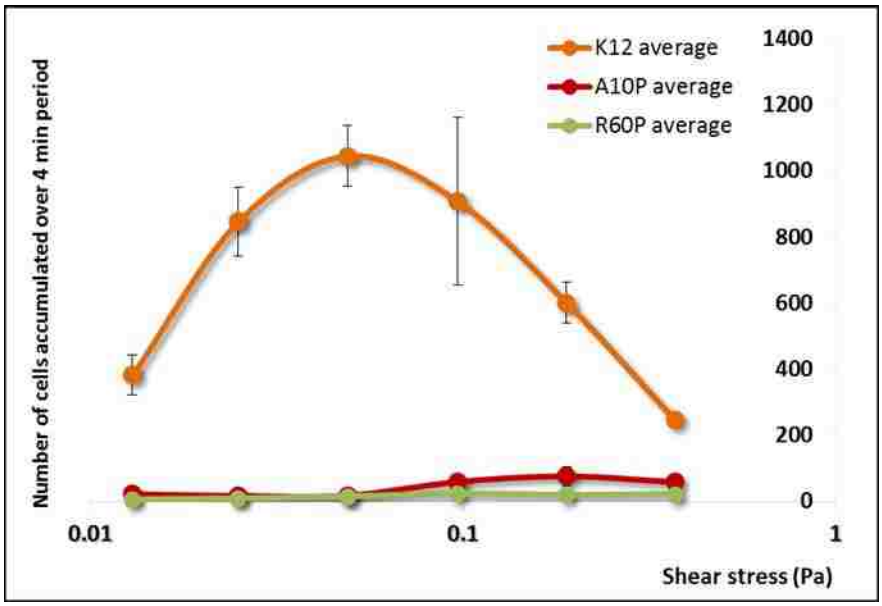


[redacted]

[redacted]

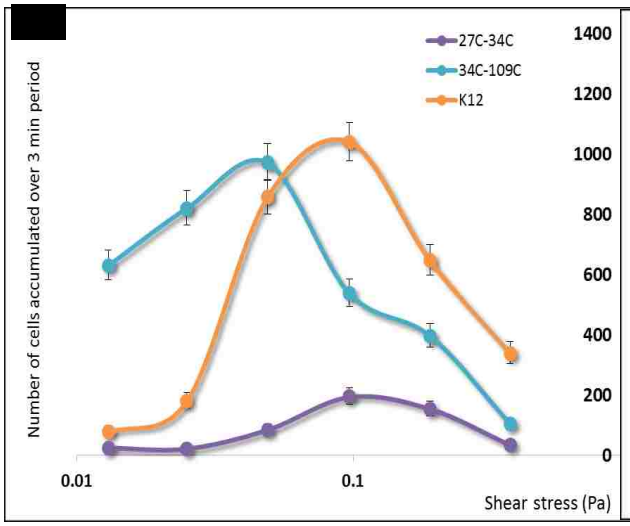


[redacted]

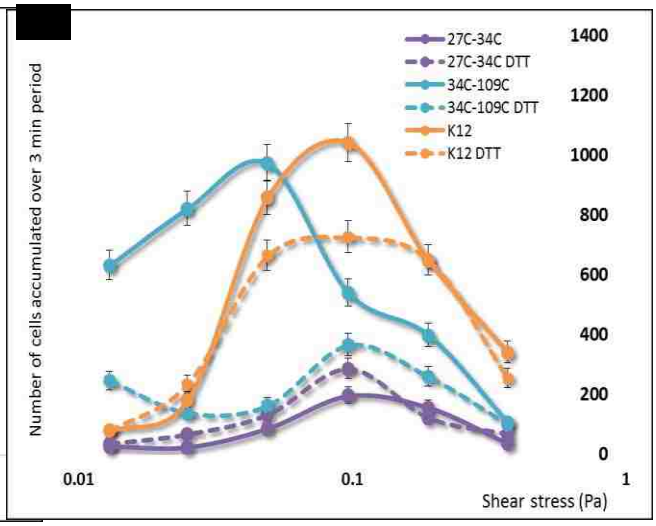


[redacted]

**C** "Master Schedule List" detailing the particular procedure performed on all mice throughout the process with specific dates of sera shipment to our lab for general testing.

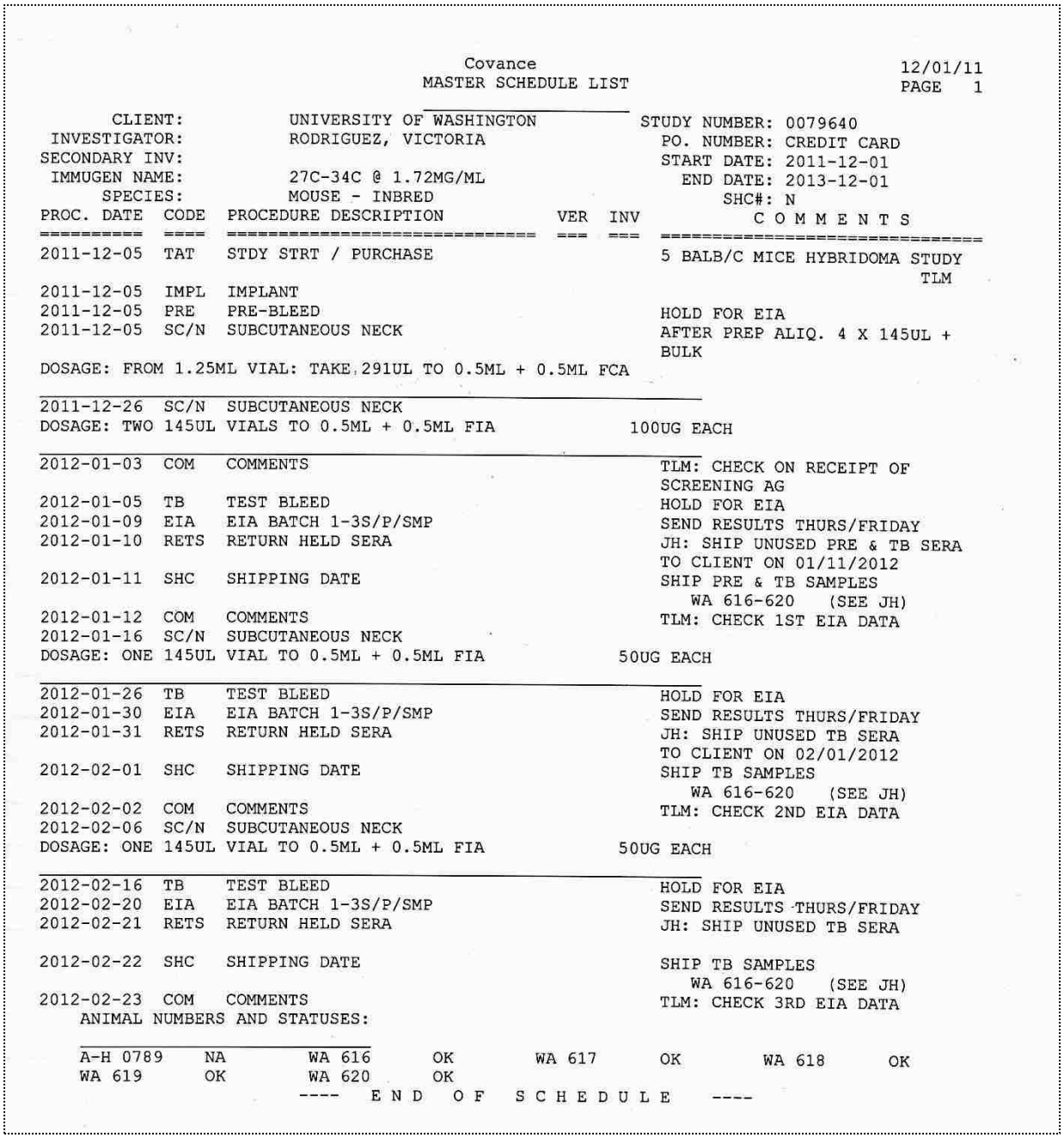

Covance
MASTER SCHEDULE LIST

12/01/11
PAGE 1

CLIENT: UNIVERSITY OF WASHINGTON
INVESTIGATOR: RODRIGUEZ, VICTORIA
SECONDARY INV:
IMMUGEN NAME: 27C-34C @ 1.72MG/ML
SPECIES: MOUSE - INBRED

STUDY NUMBER: 0079640
PO. NUMBER: CREDIT CARD
START DATE: 2011-12-01
END DATE: 2013-12-01
SHC#: N

| PROC. DATE | CODE | PROCEDURE DESCRIPTION | VER | INV | COMMENTS |
|---|---|---|---|---|---|
| 2011-12-05 | TAT | STDY STRT / PURCHASE | | | 5 BALB/C MICE HYBRIDOMA STUDY TLM |
| 2011-12-05 | IMPL | IMPLANT | | | |
| 2011-12-05 | PRE | PRE-BLEED | | | HOLD FOR EIA |
| 2011-12-05 | SC/N | SUBCUTANEOUS NECK | | | AFTER PREP ALIQ. 4 X 145UL + BULK |
| DOSAGE: FROM 1.25ML VIAL: TAKE 291UL TO 0.5ML + 0.5ML FCA | | | | | |
| 2011-12-26 | SC/N | SUBCUTANEOUS NECK | | | |
| DOSAGE: TWO 145UL VIALS TO 0.5ML + 0.5ML FIA | | | | | 100UG EACH |
| 2012-01-03 | COM | COMMENTS | | | TLM: CHECK ON RECEIPT OF SCREENING AG |
| 2012-01-05 | TB | TEST BLEED | | | HOLD FOR EIA |
| 2012-01-09 | EIA | EIA BATCH 1-3S/P/SMP | | | SEND RESULTS THURS/FRIDAY |
| 2012-01-10 | RETS | RETURN HELD SERA | | | JH: SHIP UNUSED PRE & TB SERA TO CLIENT ON 01/11/2012 |
| 2012-01-11 | SHC | SHIPPING DATE | | | SHIP PRE & TB SAMPLES WA 616-620 (SEE JH) |
| 2012-01-12 | COM | COMMENTS | | | TLM: CHECK 1ST EIA DATA |
| 2012-01-16 | SC/N | SUBCUTANEOUS NECK | | | |
| DOSAGE: ONE 145UL VIAL TO 0.5ML + 0.5ML FIA | | | | | 50UG EACH |
| 2012-01-26 | TB | TEST BLEED | | | HOLD FOR EIA |
| 2012-01-30 | EIA | EIA BATCH 1-3S/P/SMP | | | SEND RESULTS THURS/FRIDAY |
| 2012-01-31 | RETS | RETURN HELD SERA | | | JH: SHIP UNUSED TB SERA TO CLIENT ON 02/01/2012 |
| 2012-02-01 | SHC | SHIPPING DATE | | | SHIP TB SAMPLES WA 616-620 (SEE JH) |
| 2012-02-02 | COM | COMMENTS | | | TLM: CHECK 2ND EIA DATA |
| 2012-02-06 | SC/N | SUBCUTANEOUS NECK | | | |
| DOSAGE: ONE 145UL VIAL TO 0.5ML + 0.5ML FIA | | | | | 50UG EACH |
| 2012-02-16 | TB | TEST BLEED | | | HOLD FOR EIA |
| 2012-02-20 | EIA | EIA BATCH 1-3S/P/SMP | | | SEND RESULTS THURS/FRIDAY |
| 2012-02-21 | RETS | RETURN HELD SERA | | | JH: SHIP UNUSED TB SERA |
| 2012-02-22 | SHC | SHIPPING DATE | | | SHIP TB SAMPLES WA 616-620 (SEE JH) |
| 2012-02-23 | COM | COMMENTS | | | TLM: CHECK 3RD EIA DATA |

ANIMAL NUMBERS AND STATUSES:

| | | | | | | | |
|---|---|---|---|---|---|---|---|
| A-H 0789 | NA | WA 616 | OK | WA 617 | OK | WA 618 | OK |
| WA 619 | OK | WA 620 | OK | | | | |

---- E N D O F S C H E D U L E ----

## **D** Detailed methodology of mouse polyclonal and monoclonal development.

*Mouse immunization for PAb development*

Immunizing against purified locked-low LD was contracted out to Covance Inc., at their animal facility in Denver, Pennsylvania. A total of 2.15 mgs of pure locked-low LD, or immunogen, was shipped to the facility. Next, a several-month long procedure was followed that consisted of immunization, booster immunization, sera collection, and care of 5 mice (see Appendix B for a "master schedule list" followed by Covance Inc.). Mouse WA 616 through WA 620 received injections of immunogen over 3 months for initial polyclonal antibody development.

*Confirmation of phenotype with PAb sera and selection of 1 mouse for MAb development*

A basic ELISA using provided polyclonal antisera (PAbs) from Covance Inc. was performed by modifying a previous protocol by Tchesnokova et al., (Tchesnokova, Aprikian et al. 2008) for test bleeds done on 1/26/2012 (post 3 injections) and 2/16/2012 (post 4 injections). Each assay followed a similar protocol aside from a few minor changes that will be distinguished in parenthesis to the side of the condition. The condition outside parenthesis will represent the 1/26/2012 bleed, while the one inside of parenthesis will represent the 2/16/2012 test bleed.

In summary, 0.02 (0.05) mg/mL of locked-low LD in 0.02 M $NaHCO_3$ buffer were immobilized in wells of 96-well flat bottom plates at 37 °C for 1 (2) hr(s). Free protein was rinsed off 2x with 1X PBS and then quenched for 30 minutes in 0.2% BSA-PBS. Following these steps, PAb antisera was mixed at 1:200 (1:400) and 1:600 (1:1600) dilution in 0.2% BSA-PBS and added to the wells (For 2/16/2012, PAbs were also mixed with one of three conditions: 0.2% BSA-PBS, 1% αMMP, or 1% αMMP and 1mM DTT.) The mixture was added to designated wells and allowed to incubate 1 (2) hr(s) at 37 °C. Control samples consisted of WT K12 LD without His·Tag and FimC-His·Tag®. FimC- His·Tag® was used to assess cross-reactivity with the immunogen's His·Tag®. Note that FimC, which stands for FimC "chaperone" protein, should not be recognized at all as it does not have the same structure as FimH. In addition, test bleed 1/26/2012 had the additional samples: locked-low pili with WT pilin domain, WT K12 pili (at 1:200 only), and LD with a KB91 background, and pre-immune sera for all 5 mice.

After the incubation, the wells were rinsed 4x with 1X PBS and HRP-conjugated goat-anti-mouse antibodies were added at 1:3000 in 0.2% BSA-PBS followed by an incubation of 1 hour at 37 °C. Free HRP was then rinsed off 6x in 1X PBS and the reaction was visualized with the addition of TMB peroxidase enzyme immunoassay substrate (Bio-Rad). Absorbance was read a few minutes later at 650 nm using Molecular Devices Emaxx microtiter plate reader. All samples were performed in duplicate in the interest of conserving time and reagents.

*Monoclonal development*

Once a particular mouse was selected for monoclonal antibody development, the mouse underwent one last booster immunization several days prior to euthanization. The spleen was then collected from the mouse and *in vitro* hybridoma development began. Briefly, single

spleen cells (containing memory B-cells) were fused to previously prepared myeloma cells by co-centrifugation and incubation with polyethylene glycol. Successfully fused cells were selected by isolating live cells after incubation in hypoxanthine-aminopterin-thymidine (HAT) selection media. The hybridomas were then diluted and separated into 96-well plates in such a way as to secure one clone per well. The supernatants (containing extruded antibody) of each of the 96-wells were then tested for recognition against the immunogen. Successful clones were then harvested and expanded into 24-well plates for enhanced growth. The supernatants from the last round of plating were separated, flash frozen, and shipped to our laboratory for further testing. At Covance Inc., the hybridomas were also harvested, flash frozen, and saved for future sub-clone development of successful clones.

# Curriculum Vitae
# Victoria B. Rodriguez

**Objective –** To engage my scientific knowledge as an advisor/regulator in projects concerning public health.

## SUMMARY of QUALIFICATIONS

- **Leadership:** led the management of a research project that interfaced with a contract company and earned a co-authorship on a recently submitted patent (July 2012) with my co-primary investigators.
- **Interdisciplinary communication:** collaborated between 2 or more laboratories throughout the Ph.D. and M.S. degree programs, often acting as the interpreter for ongoing intellectual and technical processes.
- **Mentorship:** Advised and educated microbiologists, mechanical engineers, and bioengineers on theory and techniques established in each of my co-primary investigator's laboratories during the Ph.D. degree program.

## EDUCATION

*University of Washington, Seattle, WA*

**Ph.D. in Bioengineering, December 2012**

- Focus in Microbiology and Protein Biophysics
- Dissertation title: "*Escherichia coli's* literal link to infection: Exploring mutagenesis of the FimH adhesin to allosterically 'lock' in low-affinity"

**M.S. in Bioengineering, 2007**

- Focus in Molecular Bioengineering and Nanotechnology
- GPA: 3.6/4.0

*Rice University, Houston, TX*

**B.S. in Bioengineering, 2004**

- Focus in Cell/Tissue Engineering
- GPA: 3.9/4.0, *magna cum laude*

## FELLOWSHIPS and AWARDS

- **Molecular Biophysics Training Grant traineeship, 2009-2011,** participating departments, University of Washington
- Article published in *JBO* selected for the **Virtual Journal of Nanoscale Science and Technology issue, February 2008**
  - The online journal posts recently published articles related to the latest research in nanoscale science.

- Selected for **Bioengineering Cardiovascular Training Grant traineeship, August 2007,** Department of Bioengineering, University of Washington
- **Best Student Paper Award, January 24, 2007,** Optical Tomography and Spectroscopy of Tissue VII, BiOS 2007, SPIE's Photonics West Conference
- **The National Academies Ford Foundation Diversity Fellowship, 2004-2007**
  - A nationwide competition awarding 3 years of support to 60 predoctoral students who demonstrate significant academic achievement and impetus in continuing the education of students from all backgrounds.

**RESEARCH**

- **Doctoral Research, 2008 – 2012,** University of Washington, Seattle, WA
  - Collaborated between my primary lab, the Thomas group, in the Department of Bioengineering and the Sokurenko group in the Department of Microbiology.
  - Studied the protein FimH of *E.coli* and its mechanism of adhesion to facilitate a urinary tract infection.
  - Contributed to catch-bond biophysics as well as applications in vaccine development.
  - *Research skills*: microbiology, biophysics, atomic force microscopy, protein structure and design
- **Master's Research, 2004 – 2007,** University of Washington, Seattle, WA
  - Collaborated with the Li, Pun, and Stayton groups in a joint effort to create a novel contrast agent with specific diagnostic and therapeutic applications in near-infrared imaging.
  - *Research skills*: mammalian cell culture, fluorescence/absorbance spectroscopy, basic chemistry

**PUBLICATIONS and PRESENTATIONS**

- Manuscript in preparation: Rodriguez VB, Kidd BA, Sokurenko EV, Thomas WE. "Prevention of type 1 fimbriated *Escherichia coli* adhesion to urothelial cells." 2012.
- Podium presentation: Rodriguez VB, Kidd B, Sokurenko EV, Thomas WE. University of Washington, "Mutating FimH of *E.coli* to allosterically affect catch-bond behavior as a force-activated adhesive." Cell Adhesion – 1, Biomedical Engineering Society Annual Meeting (BMES 2010), Austin, TX. October 6-9, 2010.
- Le Trong I, Aprikian P, Kidd BA, Forero-Shelton M, Tchesnokova V, Rajagopal P, Rodriguez V, Interlandi G, Klevit R, Vogel V, Stenkamp RE, Sokurenko EV, Thomas WE. "Structural basis for mechanical force regulation of the adhesion FimH via finger trap-like beta sheet twisting." *Cell*. **141**(4), 645-655 (2010).
- Rodriguez VB and Henry SM, Hoffman AS, Stayton PS, Li X, Pun SH. "Encapsulation and Stabilization of Indocyanine Green within Poly(styrene-alt-maleic anhydride) block-poly(styrene) Micelles for Near-infrared Imaging". *Journal of Biomedical Optics.* **13**(1), 014025 (2008).

- Podium presentation: Rodriguez VB, MacDonald DJ, Li X, Pun SH. University of Washington, "Enhanced stabilization of indocyanine green in the presence of cyclodextrin." Optical Tomography and Spectroscopy of Tissue VII, Biomedical Optics (BiOS 2007), SPIE Photonics West, San Jose, CA. January 20-25, 2007.
- Liu GL, Rodriguez VB, and Lee LP. "Time-Resolved Optical Sensing of Oligonucleotide Hybridization via Au Colloidal Nanoparticles". *Journal of Nanoscience and Nanotechnology*. **5**(11), 1933–1937 (2005).

**COMMUNICATION and LEADERSHIP EXPERIENCE**

- **PEERs leader, 2011 – 2012**
  - Promoting Equity in Engineering Relationships is an NSF funded grant to promote equity of women, minorities, and people with disabilities within the engineering environment.
  - A PEERs leader is a part of a select group of students who present to the university community on current issues facing inclusion and diversity in engineering.
- **RainyDawg Radio DJ, 2006 – 2012**
  - Student-run radio station at the University of Washington
  - DJ and host of the 2 hour program "Just Enough Education to DJ"
- **Founder/Chair of Minority and Underrepresented Students (MUST) committee, BMES, 2005 – 2006**
  - Established a committee to encourage minority and underrepresented high school students to pursue a career in engineering.
  - Led and participated in multiple planning sessions to lay the foundation for the committee.
- **Team Captain of Rice Lacrosse, 2003 – 2004**
  - Led the university club team in on/off-season practices; coordinated and scheduled fields, tournaments, and games with other Texas teams affiliated with the league; and recorded and balanced team finances.